Study of Anomalous VLF Perturbations in Possible Relation to Seismic Activity

by

Sahil Brijraj

Submitted in fulfilment of the requirements for the degree of Master of Science in the School of Physics, University of KwaZulu-Natal.

As the candidate's Supervisor I have/have not approved this thesis for submission

Signed: .... Name: .... Date: ....

Durban, December 2011.

Abstract

Anomalous perturbations of the ionosphere have been observed either as fluctuations in the critical frequency of the F-region ionosphere, foF2, or as fluctuations in the nighttime VLF signals that propagate through the Earth Ionosphere Waveguide. All anomalies appear from an earliest of three weeks to one day prior to an earthquake occurrence, hence leading to be used as possible presursors and aid in short term earthquake prediction. Earthquakes of magnitude 5.5 and greater have a significant chance of having associated ionospheric anomalies, and anomalies are only detected within a radius of 500km from the epicentre. Solar events, however, greatly affect the ionosphere and make seismogenic ionospheric signals difficult to isolate. This study concentrates on anomalous VLF signal perturbations observed along the propagation path between the NWC transmitter in Australia and narrowband receivers in Budapest and Tihany, Hungary for July 2007 to February 2008. Comparisons of anomaly appearances and seismic activity occurring within the Dobrovolsky area to the propagation path were carried out, with anomalies being observed predominantly prior to major seismic events.

PREFACE

The experimental work presented in this dissertation was carried out in the School of Physics, University of KwaZulu-Natal, Westville Campus from February 2010 to December 2011, under the supervision of Dr. Andrew B. Collier.

These studies represent original work by the author and have not otherwise been submitted in any form for any degree or diploma to any tertiary institution. Where use has been made of the work of others it is duly acknowledged in the text.

DECLARATION 1 - PLAGIARISM

I, ..., declare that

1. The research reported in this thesis, except where otherwise indicated, is my original research.
2. This thesis has not been submitted for any degree or examination at any other university.
3. This thesis does not contain other persons' data, pictures, graphs or other information, unless specifically acknowledged as being sourced from other persons.
4. This thesis does not contain other persons' writing, unless specifically acknowledged as being sourced from other researchers. Where other written sources have been quoted, then:
    (a) Their words have been re-written but the general information attributed to them has been referenced
    (b) Where their exact words have been used, then their writing has been placed in italics and inside quotation marks, and referenced.
5. This thesis does not contain text, graphics or tables copied and pasted from the Internet, unless specifically acknowledged, and the source being detailed in the thesis and in the References sections.

Signed: ....

DECLARATION 2 - PUBLICATIONS

DETAILS OF CONTRIBUTION TO PUBLICATIONS that form part and/or include research presented in this thesis (include publications in preparation, submitted, in press and published and give details of the contributions of each author to the experimental work and writing of each publication)

Signed: ....

Acknowledgement

As this was my first exposure to a study of this gravity it took me longer than expected to adjust to working at such a level. In this regard I would like to extend a very big thank you to my supervisor Dr A.B. Collier for his guidance, constructive comments, his own brand of effective motivation but most of all his tremendous patience with me. I would also like to thank Hermanus Magnetic Observatory (HMO) for funding me through my study. Thank you to my fellow lab colleagues, without whom I would not have been able to complete my work. Thank you to my friends especially, who supported and aided me in any way possible through a very turbulent personal past two years. Finally thank you to my family for pushing me constantly.

Contents

List of Figures

List of Tables

Chapter 1

Introduction

Diurnal VLF fluctuations have been extensively studied previously [*Shvets*, 2004; *Horie et al.*, 2007; *Kasahara et al.*, 2010]. Electromagnetic based earthquake predictions fall into two classifications. Either derived from radio emissions from the earthquake hypocentre or the indirect effect on the atmosphere and ionosphere which are measured by means of radio transmitters. The general consensus is that the ionosphere is drastically influenced by seismic activity [*Hayakawa*, 2008].

The ionosphere is the electrically charged region of the upper atmosphere, reaching up to approximately to an altitude of 500km. The structure of the ionosphere is layered, each with a different electron density. The highest region is the F-region, extending down to an altitude of roughly 150km. Below the F-region lies the E-region, with a lower boundary between 100–90km.

Another region exists closely coupled to the E-region, the D-region, however, it exists only for the sunward-facing ionosphere. This is a narrow band of the atmosphere, with a lower boundary near 50km altitude, as shown in Figure 1.1. The vertical profile of the electron density shows an increase with altitude, until roughly 300km altitude, when the concentration reaches a maximum. The concentration then decreases continuously with altitude. The regions defined by changes in the temperature gradient of the ionosphere with altitude are also shown, along with the D, E and F regions.

Radiation emanating from the Sun incident on the Earth's atmosphere ionise the uncharged atoms or molecules in the daytime hemisphere of the ionosphere, producing free electrons. Non-solar ionisation sources range from precipitating energetic electrons, to meteoric ionisation and cosmic rays. These processess maintain the free electron concentration within the nighttime ionosphere.

The D-region is likely the least studied region of the ionosphere, as it lies too high for balloons to probe and it is too low for in situ satellite measurements. Hence studying subionospheric propagating Very Low Frequency (VLF) radio waves reflecting off the lower ionosphere is the preferred method to probe the D-region [*Cummer*, 2000; *Cheng et al.*, 2006; *Hayakawa*, 2007]. The lower boundary of this region strongly reflects VLF waves. VLF radio waves are electromagnetic waves characterised by frequencies in the range 3–30kHz. The diference between the night and day ionosphere as well as the effect on VLF wave propagation is shown in Figure 1.2.

VLF radio waves experience very little attenuation, about a few dB per Mm, while traversing large distances across the globe [*Kumar et al.*, 2008]. The propagation of such waves are highly sensitive to fluctuations of the lower ionosphere, thus making them ideal probes for identifying local perturbations, as well as detecting the background or ambient state of the lower ionosphere. VLF waves travel within a region bounded below by the ground, and above by the lower ionosphere. This region is called the Earth Ionosphere Waveguide, (EIWG). The electrically conducting region of the upper atmosphere strongly reflects VLF waves.
During the night this upper boundary is the base of the E-region, but during the day it is much lower at the base of the D-region. Localised depressions of the lower ionospheric boundary would alter the propagation characteristics of the EIWG and inevitably lead to distortions in VLF radio waves propagating through the region, between transmitters and receivers on the ground [*Tolstoy et al.*, 1982].

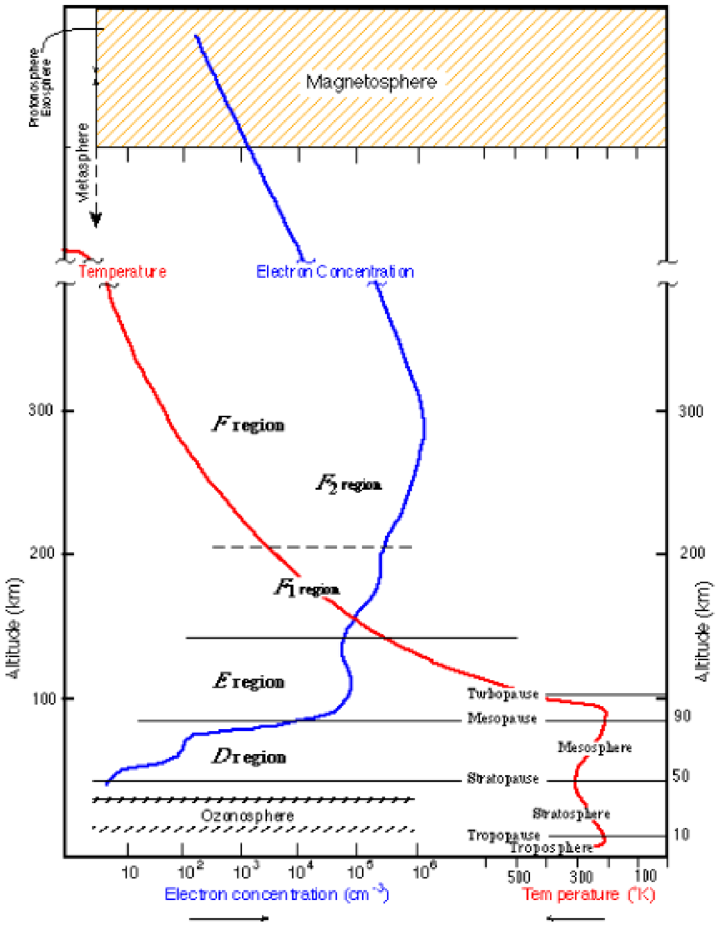

Figure 1.1: Variations of ionospheric electron density and temperature with altitude, taken from http://www.ion.le.ac.uk/images/ionosphere/profile.gif.

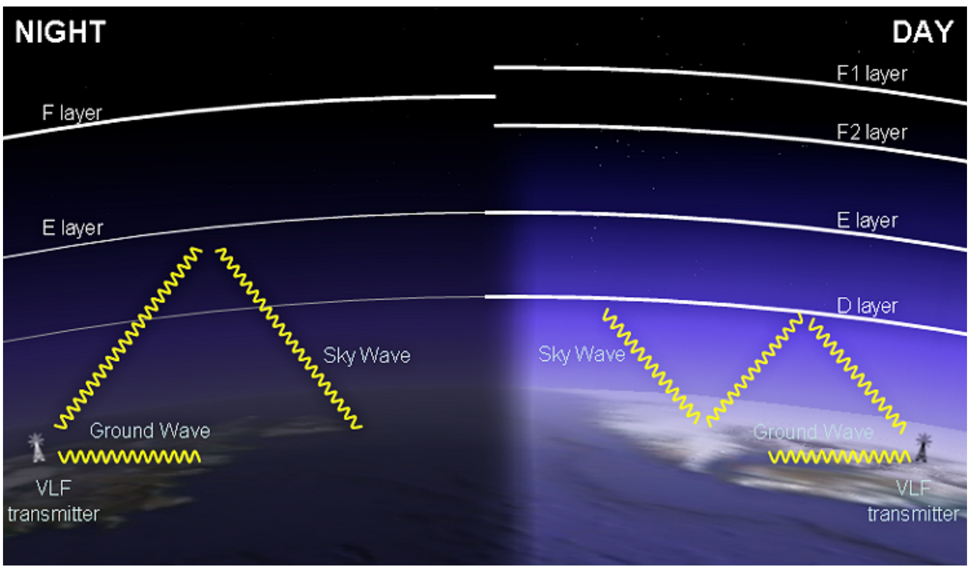

Figure 1.2: Illustration of the differences in ionosphere structure between day and night conditions, as well as the effect on VLF wave propagation between ground-based transmitters and receivers, taken from http://sidstation.loudet.org/04-ionosphere/img/VLF_transmission.png

1.1 The Earth-Ionosphere Waveguide

There are various ways to determine the propagation boundary conditions, with most techniques employing either numerical or approximate analytical formulations based on waveguide mode theory [*Cummer*, 2000]. The ground is homogeneous with permeability μ_0, conductivity σ_g and permittivity ϵ_r. If the medium is vertically homogeneous for atleast a few km then such assumptions are valid for low frequencies. In this case the medium is neutral air. The upper boundary of the EIWG, the lower ionosphere, is obviously treated very differently. This assumption again is valid as long as the wave power is not high enough to modify the medium. It is an inhomogeneous, anisotropic, diffuse and dissipative cold plasma [*Tolstoy et al.*, 1982; *Cummer*, 2000; *Cheng et al.*, 2006].

The electron density of the D-region follows an exponential behaviour as described by

$$N_e = 1.43 \times 10^7 \mathrm{cm}^{-3} \exp(-0.15\mathrm{h}') \cdot \exp[(\beta - 0.15)(\mathrm{h} - \mathrm{h}')], \tag{1.1}$$

with h' representing the height of the D-region in km and β the sharpness of the D-region lower boundary edge in km^{-1} [*Cummer et al.*, 1998]. Higher β values translate into increasing rate of change in the electron density, N_e, with altitude.

A highly simplified but effective method of determining the reflection height of the ionosphere is through studying VLF spectrograms. Spectrograms are useful in identifying and analysing phenomena associated with lightning flashes, such as whistlers, tweeks and sferics.

A lightning discharge is an electrical breakdown current that flows from cloud-to-ground, intra-cloud or the much more rare ground-to-cloud discharge [*Barr et al.*, 2000], occurring from mountain tops and tall buildings. Lightning flashes emit a broadband spectrum of VLF signals.

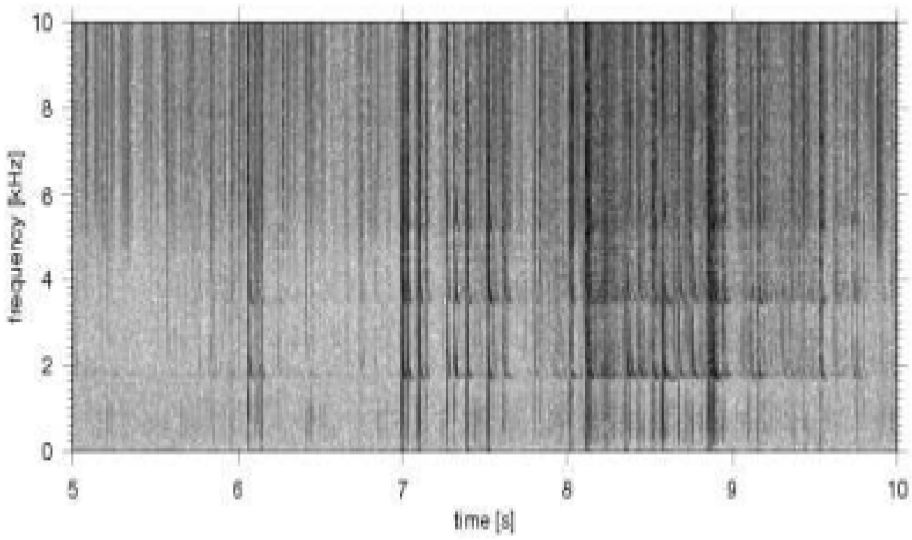

Figure 1.3: Spectrogram showing sferics and tweeks, Recorded on 23 February 2003 at 21:00 UT, at the South African National Antarctic Expedition base, SANAE IV [*Koen*, 2009].

Kumar et al. [2008] collected and showed how various parameters of VLF wave propagation in a waveguide could be calculated. The propagation of VLF radio waves through the EIWG consists of multiple reflections. Electromagnetic waves undergo decomposition in a waveguide, propagating as independent field structures, or modes, with characteristic group velocites, v_{gn}. Each mode has a specific cutoff frequency, f_{cn}. For a waveguide with perfectly conducting boundaries, essentially a parallel plate waveguide, the cutoff frequency of the n^{th} mode is given by

$$f_{cn} = \frac{nc}{2h} \tag{1.2}$$

The effective height of the ionosphere is given by h and c is the velocity of light in free space.

From studying spectrograms, see an example in Figure 1.3, the cutoff frequencies for different modes can be identified. Tweeks are the delay in the sferics caused by dispersion of the sferic along the propagation path. From equation 1.2 it can be seen that the cutoff frequencies are separated by whole integer factors, as is dictated by the mode number of the group. Using this information the reflection height of the ionosphere can be determined, or approximated very well.

On a spectrogram tweek cutoffs form distinctive horizontal lines. For each sferic these cutoff frequencies occur at the same intervals through the full VLF spectrum. *Ohya et al.* [2003] used the frequency dispersion characteristics of tweek atmospherics to estimate electron densities in the low-middle latitude D-region ionosphere. The method employed used accurate readings of the first-order mode cut-off frequency determined by least-mean-square method calculations. Estimated electron densities were found at altitudes equivalent to the reflection height of the first-mode propagation waves of tweeks. Electron densities ranged from 20–28 cm^{-3} at reflection heights of 80–85km. In the study conducted the tweek method had the unique advantage of being capable of estimating electron densities, or reflection heights, in a wide area surrounding Japan.

Thus it was concluded that the tweek method could be used to detect changes in the reflection heights of the D-region ionosphere, eventually leading to identifying abnormal geophysical conditions such as geomagnetic storms. Their findings compared well to rocket-experiment measurements of electron densities in the lower part of the D-region, 80–90km, see papers listed in [*Ohya et al.*, 2003].

The received intensity of the VLF signals depend on various factors, including the excitation of modes, path attenuation, surface conductivity, height of the lower ionosphere and the propagation direction [*Kumar*, 2009].

1.2 Anomalous Ionospheric Perturbations Observed Prior to Seismic Activity

Anomalous ionospheric perturbations observed prior to seismic events have been studied extensively by many authors either as case studies of specific strong earthquakes [*Liu et al.*, 2000; *Rios et al.*, 2004; *Hobara and Parrot*, 2005] or as extensive investigations based on a number of earthquakes within a certain region [*Fujiwara*, 2004; *Popov*, 2004; *Liu et al.*, 2006]. However, it should be kept in mind that even though the literature reviewed does show high correlation between seismic activity and ionospheric perturbations, the existence of definitive ionospheric precursors to seismic events is still very difficult to verify due to a lack of reproducibility and definitive criteria [*Fujiwara*, 2004]. The term precursor throughout this thesis will be used to describe anomalous ionospheric signals observed prior to seismic events.

1.2.1 Variations of F-region Critical Frequency Prior to Earthquakes

One type of anomaly is the dramatic depression in the maximum plasma frequency, in the ionosphere, also called the critical frequency of the F-region, $foF2 = 9 \times 10^{-3}\sqrt{N}$, where N is the electron density per cm^{-3}, observed in the week leading up to a strong earthquake [*Liu et al.*, 2000, 2006]. The anomalous decrease has been comprehensively investigated [*Liu et al.*, 2001; *Fujiwara*, 2004; *Rios et al.*, 2004].

Liu et al. [2000] studied ionospheric signatures related to seismicity prior to earthquakes of magnitude $M \geq 6$ between 1994–1999. The foF2 readings for the 20 days leading up to the earthquakes were recorded and used to construct the lower and upper bounds of the interquartile range. Anomalies were defined as when the value of foF2 observed on a particular day exceded either the lower or upper bounds of the previous 15-day running interquartile ranges [*Fujiwara*, 2004]. The strength of the anomaly was given by the value in excess of the lower or upper bounds. However, it was observed that the lower bound anomalous excursions, which were during the afternoon hours, 12h00–18h00LT, were greater than the highest value of the upper anomaly leading to the decision to rather use the lower anomalous signals during the afternoon as possible precursor indicators.

Clear excursions of foF2 below the lower bound of the monthly median between 1200-1800LT are given in *Liu et al.* [2006] as well. Studying twenty $M \geq 6$ earthquakes from September 1999 to December 2002, *Liu et al.* [2000] reaffirms the decision to use the lower anomalies as the indicators rather than the upper anomalies.

It was also observed that the primary factor in determining the presence of an anomaly was the magnitude of the seismic event. Earthquakes of $M \geq 5$ had a 73.8% chance of having associated anomalies with 1 anomaly per shock or earthquake within 5 days prior to the shock, whereas, earthquakes of $M \geq 6$ had a 85% chance of having an anomaly observed within 3 days prior *Liu et al.* [2000]. The strongest seismic event studied was the ChiChi earthquake of $M = 7.3$. This particular shock had 3 associated precursory signals 1, 3 and 4 days prior to the shock. Thus it was concluded that the stronger the earthquake, both the chance of observing a possible precursory signal as well as the magnitude of such signals would be greater.

Pulinets [2003] found similar readings in their analysis of 10 years of ionospheric foF2 perturbation data recorded over seismically active regions. They observed that 73% of $M = 5$ earthquakes were preceded by at least one ionospheric precursor and 100% of $M = 6$ earthquakes had associated precursors, again emphasizing the dependence on earthquake magnitude above a certain threshold as a key factor in producing significant ionospheric deviations, which they gave as $M = 5$. Studies of 184 $M > 5$ earthquakes in Taiwan over 6 years showed earthquakes of $M > 5.4$ have a greater chance of having observed ionospheric deviations within a radius of 150km [*Liu et al.*, 2006]. The magnitude dependence on ionospheric precursor generation lends itself to the idea that the energy released during the preparation stage of earthquakes is the prime generator of the fluctuations experienced by the ionosphere.

Recently scientists have started to use total electron content, TEC, readings derived from the GPS (Global Positioning System) network as an alternative probe into the electron density fluctuations in the ionosphere [*Liu et al.*, 2006].

In the investigation of the strong 1999 Chi-Chi earthquake results show that there are significant drops in TEC and peak F region electron density, NmF2, simultaneously within 6 days prior to the shock. In fact both sets of data decreased by almost 50% 4 and 3 days prior and a decrease to a lesser degree 1 day before the shock, with a correlation coefficient of 0.953 [*Liu et al.*, 2001]. This data compares well with *Liu et al.* [2000], where precursors were observed 4, 3 and 1 days prior to the earthquake, see Figure 1.4.

1.2.2 Unexpected VLF wave Perturbations Observed Prior to Seismic Activity

The previous section described a well documented and extensively studied ionospheric phenomenon observed prior to seismic activity. The parameters in question were different to the topic of this thesis but nonetheless showed definite and well defined deviations from quiet conditions that were concluded to be caused by impending seismic events. Also the methodology for comparing ambient conditions to perturbed periods can be adapted for VLF data. It would be ideal to conduct both types of investigations simultaneously to get an understanding of the effect of seismicity on the ionosphere, as foF2 readings are taken at high altitudes in the F-region and the observations studied in this thesis are of VLF signal perturbation propagating below the lower ionosphere.

This section and the focus of this thesis concentrates on the distortion of VLF waves observed prior to seismic activity.

VLF waves serve as an efficient probe into the dynamics of the ionosphere. The waves propagate between transmitter and receiver, echoing off the atmosphere-ionosphere boundary. Very little attenuation occurs through the EIWG. Thus if any abnormal fluctuations are observed, the state of the lower ionosphere will be responsible. Only sufficiently large irregularities in the ionosphere will cause signal fluctuation. Diurnal VLF fluctuations have been extensively studied previously [*Shvets*, 2004; *Horie et al.*, 2007; *Kasahara et al.*, 2010].

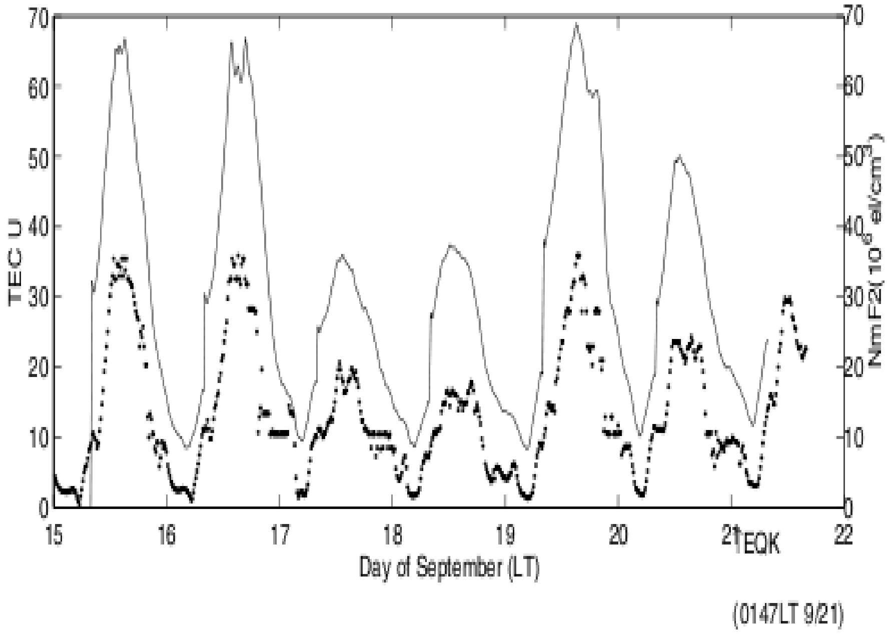

Figure 1.4: TEC and NmF2 variations at Chung-Li observed within 6 days before the Chi-Chi earthquake [*Liu et al.*, 2001].

An example of the general diurnal trend of VLF waves propagating through the EIWG is shown in Figure 1.5. There is a very distinctive shape to VLF waves propagating within the EIWG. An initial period of relatively higher amplitudes is followed by a sharp drop. The amplitude fluctuates around the lower amplitudes before rising again at a later time, where it reverts back to the another higher amplitude period. The sharp drops and rises are due to the effects imposed by the sunrise and sunset on the ionosphere. Frames from an animation done by *Koen* [2009], shown in Figure 1.5, illustrate the change in the amplitude as the sun terminator crosses the transmitter-receiver path. The shaded areas reflect the nighttime portion of the Earth. Figure 1.5(a) shows the sunrise at the receiver in Hungary. Reflected by the sharp drop in the accompanying VLF profile. As the sunrise moves West and eventually passes the transmitter at the Western end of the propagation path the VLF profile is seen to remain at the lower amplitude. However, it will revert back to the higher amplitudes when the sunset passes across the propagation path.

There is an increase observed just after the terminator drop. As *Koen* [2009] explains there was interference between the first-order mode excited at the transmitter and the converted first-order mode that was originally excited as the second-order mode at the transmitter. The magnitude of the converted mode became comparable with the original first-order mode, which contributed to the amplitude of the signal. After the terminator passed over the transmitter (Figure 1.5(c)), the first-order mode became predominant and was the main source contributing to the amplitude signal.

When a receiver is placed near an interference minimum point, the amplitude decreases at night due to multimode interaction and the sensitivity of VLF propagation to irregularities in the lower ionosphere increases, which leads to increased signal fluctuations. Thus certain receivers are chosen over others based on their relative position to a minimum interference point, to increase the sensitivity of the VLF perturbation observations [*Shvets*, 2004]. *Shvets* [2004] considered nighttime fluctuations in VLF signals simultaneously received by only two (Omega and NWC) out of four VLF stations because of their proximity to the interference minimum and expected increased sensitivity to ionospheric perturbations, see Figure 1.6.

The VLF profiles follow a general well-shaped structure, with initial and final periods of relatively higher amplitudes, separated by a period of much lower amplitudes. The transition from high to low and back

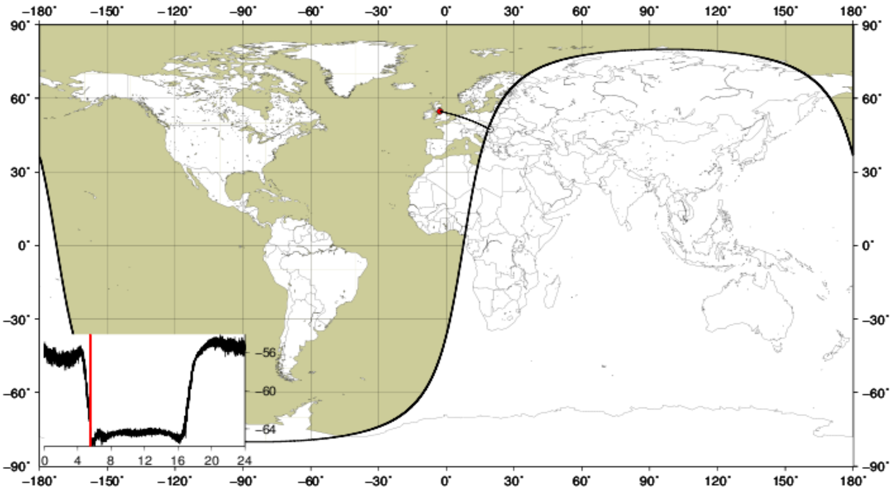

(a)

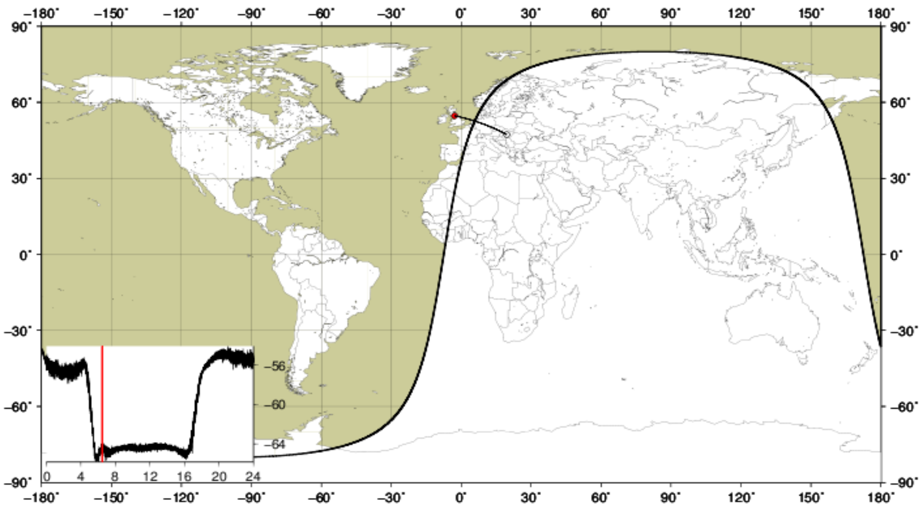

(b)

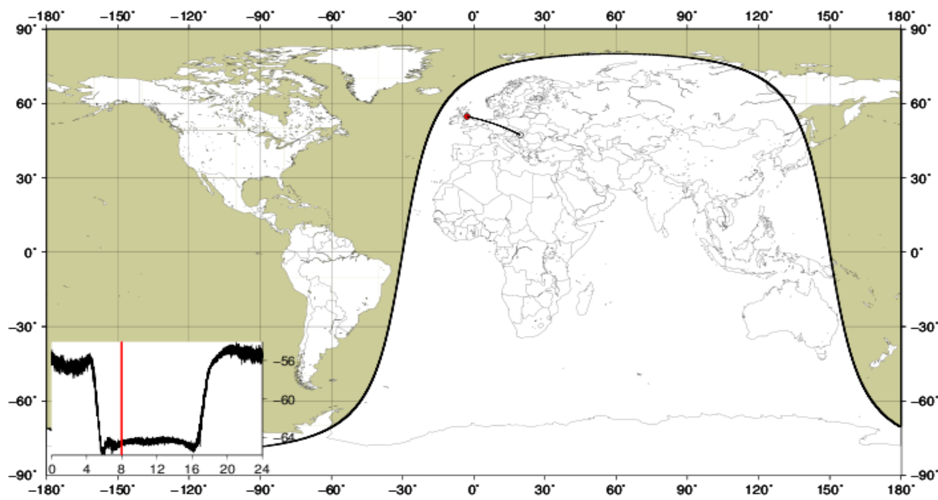

(c)

Figure 1.5: Frames captured from an animation illustrating the terminator effect on the VLF diurnal profile. The VLF waves propagated between a European transmitter and receiver located in Budapest, Hungary. (a) Sunrise occurring at the receiver. (b) Terminator lying between transmitter and receiver. Interference taking place between different modes modifying the amplitude profile. (c) Corresponding amplitude profile after terminator has crossed both the receiver and transmitter [*Koen*, 2009].

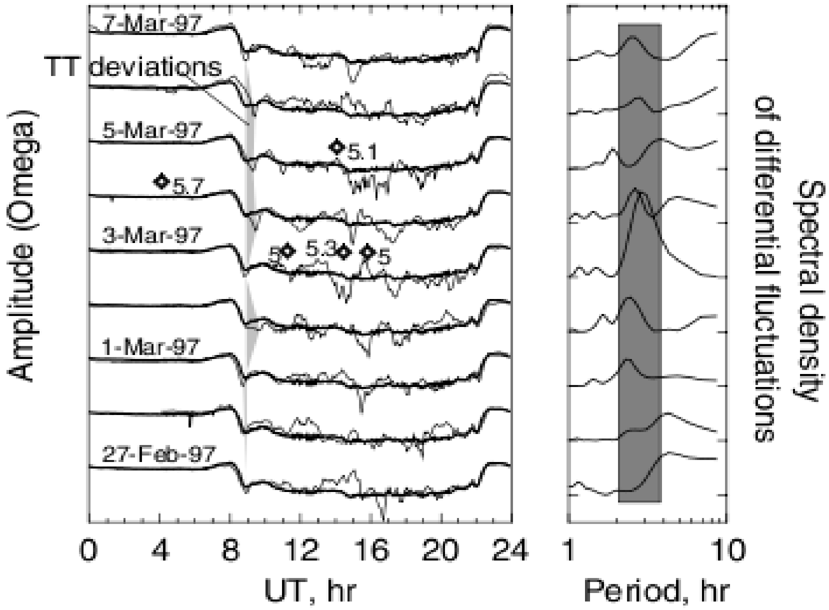

Figure 1.6: Daily VLF amplitudes for the propagation path between the Chofu receiver and Omega transmitter stations, located at longitudes 139°32' E and 129°E respectively, with anomalous terminator time fluctuations shown by shaded areas (left graph) and corresponding spectral analysis contents of nighttime fluctuations (right graph) for period leading up to and including Izu peninsula earthquake swarm starting on 3 March 1997 [*Shvets*, 2004].

to high amplitudes are well defined drops and rises called the Terminator Times (TT) [*Shvets*, 2004], and it indicates the ionosphere reacting to the influence of the sunrise as the atoms and molecules in the lower ionosphere start to become ionised by solar radiation. Analysis of this feature of a VLF profile is also a diagnostic tool studied when investigating seismic influences on the ionosphere. However, the terminator time method is best used for East-West orientated propagation paths.

Anomalous perturbations in VLF signals observed prior to seismic activity in the absence of geomagnetic influences range from a day to over two weeks before the onset of an earthquake [*Singh et al.*, 2001; *Shvets*, 2004; *Maekawa et al.*, 2006; *Molchanov et al.*, 2006; *Horie et al.*, 2007; *Singh et al.*, 2009].

Spectral analysis of nighttime fluctuations revealed wave-like anomalies or oscillations with periods of about 3 h, that occurred on the night that a moderately strong earthquake swarm, $5 \leq M \leq 6.1$, began [*Shvets*, 2004]. The nighttime amplitudes showed unexpected deviations from the contemporary average diurnal runs. The anomalies were found to lead the earthquake occurrences by 1-3 days, preceding the largest earthquake of $M = 7.1$ by two days. Correlation between regional seismicity and fluctuations along the studied propagation paths yielded a correlation coefficient of 0.5, with maximum correlation occurring 1-2 days prior to a shock[*Shvets*, 2004].

Shvets [2004] also employed using the differential amplitude, dA ,in analysing the VLF signals observed. An example of a dA plot is given in Figure 1.7. The amplitude on a single day was subtracted from the average signal taken over the previous 17 days. This is expressed in equation 1.3, where dA represents the differential diurnal amplitude, $A_k(t)$ is the amplitude of the current day amplitudes and $< A(t) >_k$ is the average amplitude.

$$dA = A_k(t) - < A(t) >_k \tag{1.3}$$

Studying $M \geq 5.5$ earthquakes around Japan over a five year period it was found that nighttime average amplitude signals decreased 2–5 days before earthquakes of $M \geq 6$ beyond the 2σ level, where σ is standard deviation used as a statistical reference level for identification of anomalies. The nighttime fluctuations were enhanced above the 2σ level for the same period 2–5 days prior to an earthquake

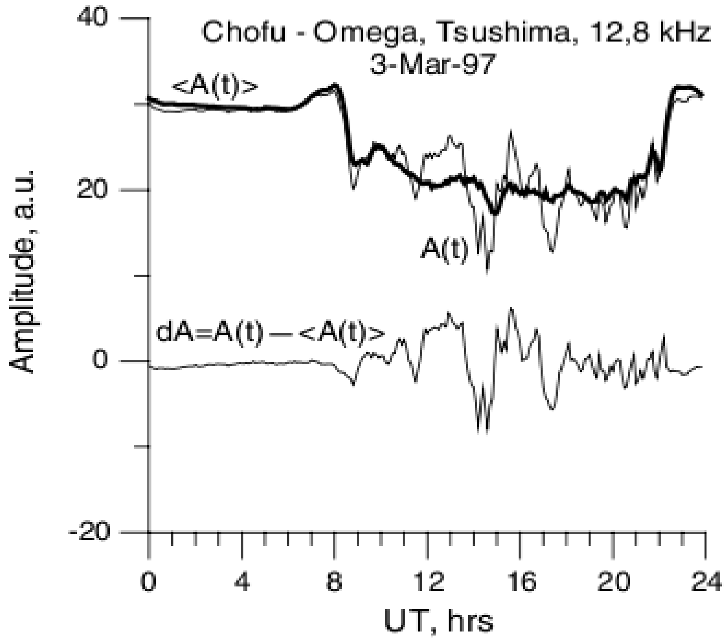

Figure 1.7: An example of diurnal runs of amplitude variations in VLF amplitudes for the propagation path between the Chofu receiver and Omega transmitter stations, located at longitudes 139°32' E and 129°E respectively [*Shvets*, 2004].

[*Maekawa et al.*, 2006].

Singh et al. [2001] observed VLF noise-bursts up to 16 days prior to the onset of the 29 March 1999 $M = 6.6$ Chamoli earthquake. A VLF noise-burst is a rapid variation in a signal amplitude for brief durations ranging from a few mins to 2–3 hours. Their results showed that there were two types of VLF noise-burst activity. Either as isolated activities that correlated positively with isolated earthquakes, or as periods of prolonged perturbation that also correlated positively with prolonged periods of seismic activity.

Significant irregular perturbations of the lower ionosphere can be expected only for strong $M \geq 6$ and shallow earthquakes, but the threshold for seismic-related signatures to be observed in comparison to other sources of ionospheric disturbance is $M = 5.5$ [*Horie et al.*, 2007; *Kasahara et al.*, 2010]. The boundary given by *Kasahara et al.* [2010] was $M = 6.6$ and depth 96km for a VLF anomaly to be produced.

Two methods for VLF wave analysis were considered, being either the terminator-time method or night-time fluctuation analysis. The night-time fluctuation method was used because the propagation paths studied between Japan and NW Australia lay in a N-S orientation, and the terminator-time method is only effective for E-W propagation paths. The earthquake investigated was the devastating $M = 9$ Sumatra earthquake on 26 December 2004. The preparation area, which is the circular area of the ground effected by the earthquake with central point at the epicenter, is determined using the Dobrovolsky formula

$$R = 10^{0.43M} \tag{1.4}$$

where M is the magnitude of the earthquake and R the radius of the preparation zone. This formula is shown in Figure 1.8.

Figure 1.8 shows the increase in preparation zone area size by virtue of its radius with increasing earthquake magnitude. It is clear that the small scale seismic events, $5.5 < M < 6$, would not have a significant effect on the immediate environment as the dimensions of their preparation zones are of the order of a few hundreds of km, whereas there is a substantial jump in the size of the affected area of the

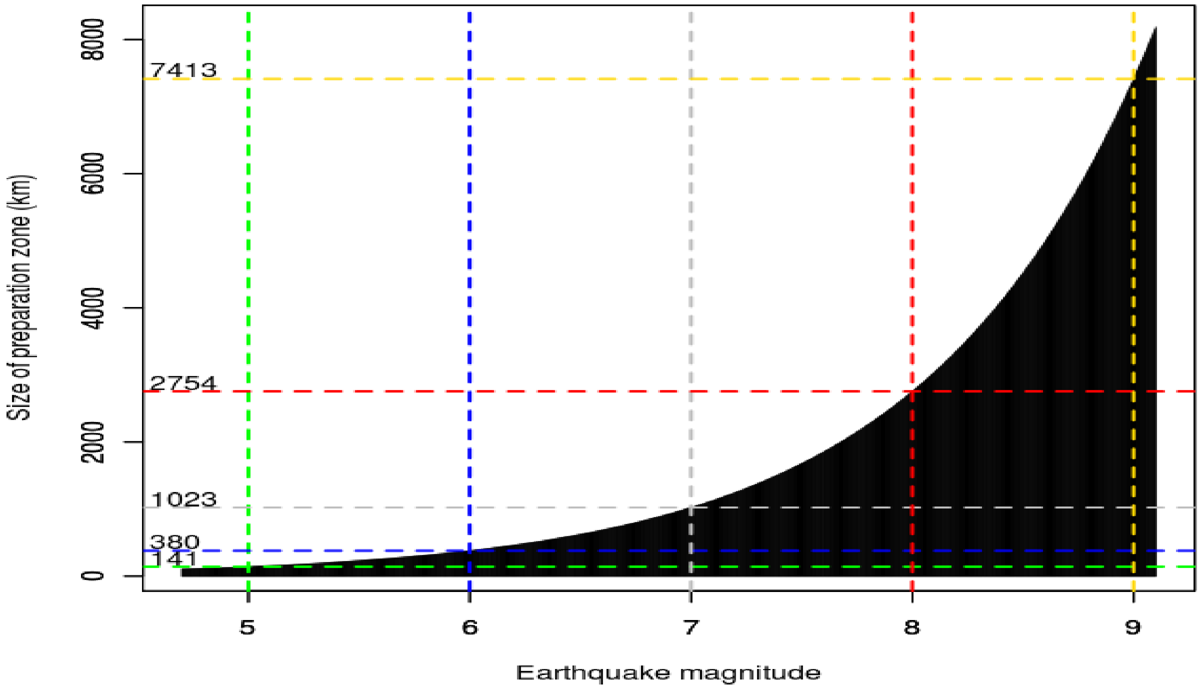

Figure 1.8: Dobrovolsky formula plotted for $M \geq 5$, showing calculated earthquake preparation zone radii for increasing magnitudes.

surface from medium to large earthquakes, $6 < M < 9$. As can be seen the rate of increase in radius of the preparation zone increases rapidly from about $M = 6$.

Horie et al. [2007] found that for the extremely strong magnitude 9 2004 Sumatra earthquake, there were abnormal VLF perturbations observed on a propagation path passing 2000km from the epicentre. This was later explained by the fact that the calculated preparation zone radius was between 7000–8000km. In fact a $M = 9$, corresponds to a preparation zone radius of 7413km. For a clearer image, the preparation zone for such an earthquake occurring at 0°N 0°E would cover the entire African continent, the eastern half of South America, Europe south of Scandinavia as well as Iran and Oman in the East.
The Sumatra earthquake had a calculated preparation area with radius 7000–8000km. Even though the propagation paths were 2000km away from the epicentre, they clearly fell within a highly affected zone. Prolonged periods of VLF fluctuations were recorded simultaneously with a period of high seismic activity starting a few days before the main shock and continuing into the beginning of the next month, due to the numerous and sizeable, M = 6.1–6.7, aftershocks.

Using data retrieved off the DEMETER satellite *Molchanov et al.* [2006] recorded periods of ionospheric drops in received VLF signals over areas of Europe and Indonesia prior to the onset of a series of earthquakes, Figure 1.9. The blue circles represent the strength of the signal-to-noise ratio. The largest circles represent a ratio of 56 − 112. Areas of decreased VLF activity within the ionosphere were termed 'scattering spots'. From the observations it was deduced that the magnitude of the earthquakes had a great influence on the spatial dimensions of the scattering spots. For the European earthquake series between 23 November to 5 December 2004 four earthquakes ranging from $5.4 < M < 5.5$ were selected, the resulting scattering spot diameter was found to be about 1000km. Figure 1.9a shows the signal-to-noise ratio distribution, SNR, (a) for the 18.3kHz FTU transmitter, located in Western Europe, during about a month (from 25 October to 22 November 2004) before the earthquakes series. (b) During and just after the earthquakes series (from 23 November to 12 December 2004). (c) During the period from 26 December 2004 to 31 January 2005, which was after the series of earthquakes. The red circled area approximately indicates the possible area of the "scattering spot".
Figure 1.9b shows the SNR distribution for the 16.56kHz DFY transmitter for the same earthquake series as Figure 1.9a. The frames for Figure 1.9b show the SNR distributions during/just after, 23 November to 12 December 2004 (left frame), and after the seismic period, 26 December 2004 to 31 January

2005, (right frame). The first frame shows a scattering spot (red circled area) formed over the central seismically active zone, whereas the second frame, recorded just after the earthquake activity shows no decrease in SNR distribution for the same area.
The left frame of Figure 1.9c shows SNR distribution for the North West Cape (NWC) 19.8kHz transmitter from 1 November to 15 December 2004, i.e. before the large Sumatra earthquake on 26 December 2004. The right frame shows the same area but from 6 January to 15 February 2005. The scattering spot diameter for the Indonesian earthquakes in November 2004, Figure 1.9c, was larger, 2000–3000km. The area enlargement was attributed to the fact that the earthquakes were much more powerful, $7 < M < 7.5$. Working up through earthquake magnitudes, the $M = 9$ 2004 Sumatra Earthquake showed a VLF drop for a diameter of roughly 5000km around its epicentre.

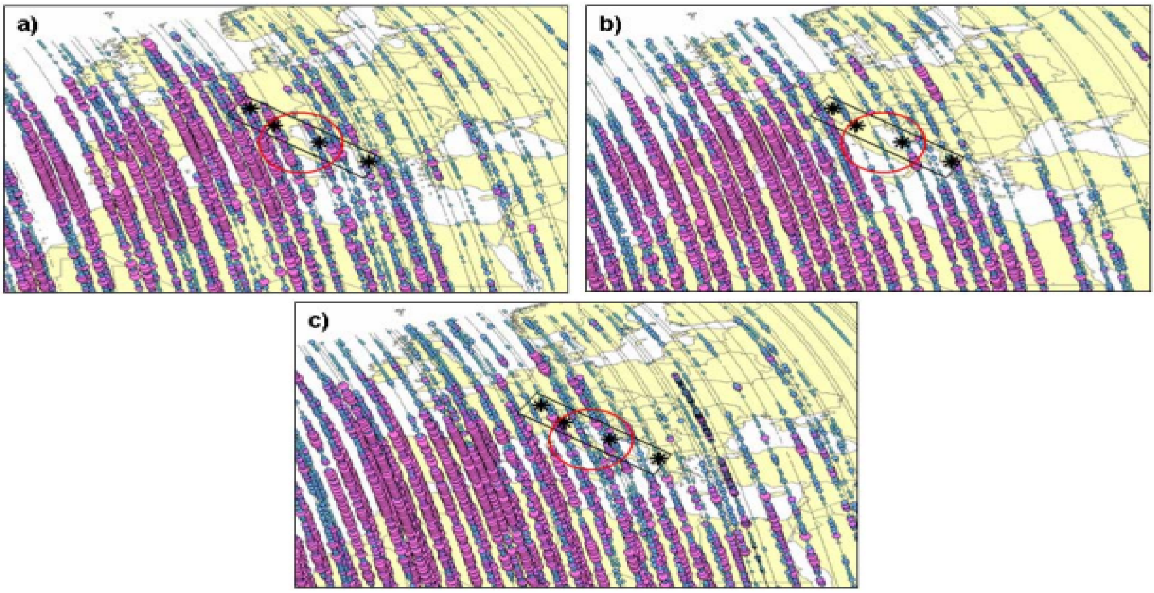

(a) Western Europe(FTU 18.3kHz)

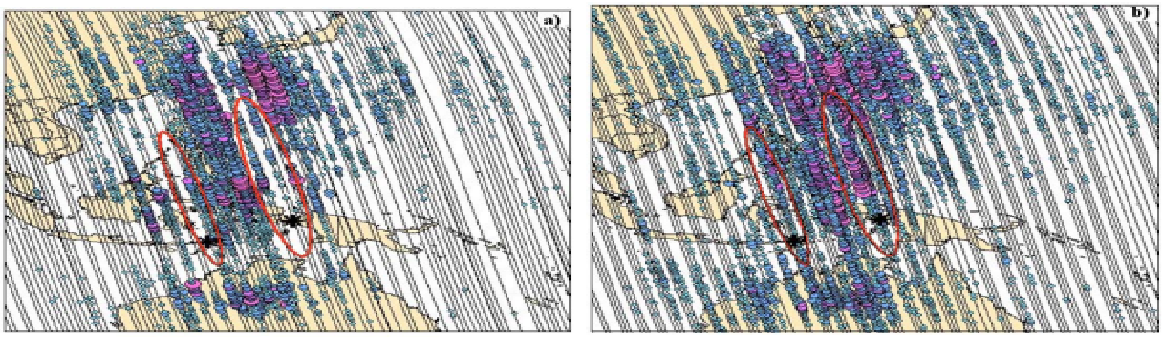

(b) Western Europe(FTU 16.56kHz)

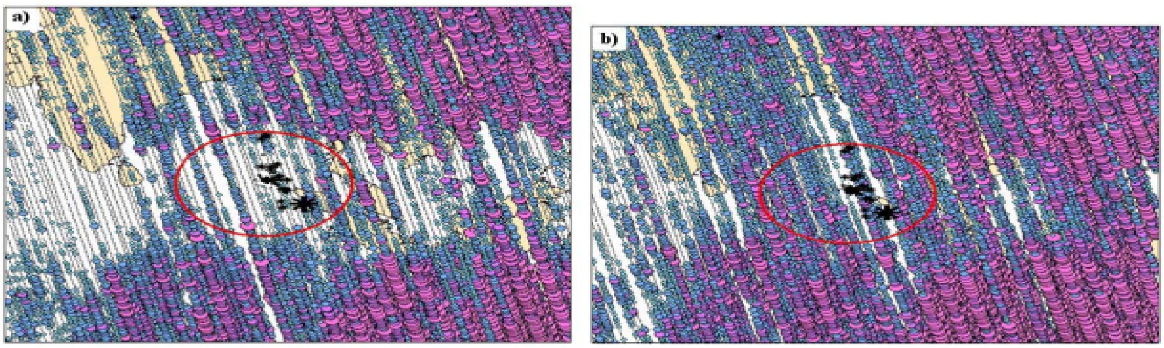

(c) Indonesia

Figure 1.9: The averaged SNR distribution (circles) showing VLF scattering spots (area within red curves) associated with the a) Western European earthquakes during October to November 2004 for the FTU 18.3kHz transmitter, b) Western European earthquakes during November to December 2004 for the DFY 16.56kHz transmitter c) Indonesian earthquakes for the period 30 October 2004 to 7 February 2005 (Sumatra earthquake, 26 December 2004, shown by largest asterix)[*Molchanov et al.*, 2006].

1.2.3 Possible Mechanisms for Anomaly Generation

The preparation stage of a forthcoming earthquake consists of dilation and relaxation of the lithosphere within the future epicentral zone [*Liu et al.*, 2000]. This causes rock fragments to become loosened and move around between the underlying rock formations, or lithologies, as well as causing fractures to be formed. The movement of loosened fragments can create electric charges that affect currents in the near-surface atmosphere [*Hobara and Parrot*, 2005]. An enhanced atmospheric vertical electric field can penetrate the lower ionosphere to be transported along highly conductive geomagnetic field lines to the F-region.

Effective penetration of an enhanced electric field occurs for an earthquake preparation zone on the surface of an area of 200km in diameter. The magnitude of an earthquake and the size of the preparation zone are related by the Dobrovolsky formula, 1.4, Using this formula, for an area of diameter 200km, the corresponding threshold magnitude would have to be 4.3 [*Pulinets*, 2003].

Once at the F-region altitudes the enhanced electric field can cause ionospheric irregularities [*Rios et al.*, 2004]. *Rios et al.* [2004] studied variations in the critical frequency of the F-region looking for any correlation with an earthquake, $M = 7.4$, near San Juan city, Argentina 1977. The geomagnetic field lines that originate around San Juan propagate over the observatory at Tucuman, which made readings far more accurate.

The generation of the near-ground atmospheric electric field enhancements is attributed to the emanation of Radon, light gases (H and He) as well as highly metallic submicron aerosols. Observations of Radon concentration and foF2 readings before the 1980 Tashkent earthquake showed a very high anti-correlation between the two datasets However, it was concluded that Radon concentration increase is not sufficiently large enough to be responsible for the generation of large scale electric fields that could propagate to and affect the ionosphere. Supplementary to Radon were other metallic aerosols emanating from the future epicentre. These combined with the Radon can greatly increase the atmospheric conductivity thus enhancing the atmospheric electric field from 200mV/m to 500mV/m up to several kV/m. The local ambient atmospheric electric field also decreases due to the increase in radioactive emissions. Thus the enhanced electric fields then propagate to the lower ionosphere, where due to anisotropic conductivity the field lines transform from vertical to horizontal. The greatest penetration being during the night, as the D-region disappears at night. An electric field of 1000Mv/m translates to 1mV/m once in the ionosphere. The presence of the surplus electric field modifies the electron density distribution both horizontally and vertically. [*Pulinets*, 1997, 1998; *Popov*, 2004].

The problem with this hypothesis is that radon is highly soluble, and there have been observations of ionospheric anomalies of the same nature over sea-based earthquakes [*Shvets*, 2004]. *Shvets* [2004] rather uses the affect of acoustic-gravity waves on the lower ionosphere as a possible mechanism for the generation of ionospheric anomalies. Studying VLF perturbations on the Omega-Chofu and NWC-Chofu propagation paths, fluctuations with periods of 1-4h were observed in the received signals. Acoustic-gravity wave periods range from 10minutes to a few hours, the relation holds. Acoustic-gravity waves amplify and dissipate at the mesopause heights, 80-90km, which is the reflection height of VLF signals. However, another study showed that the energy dissipate at a much higher latitude between 150-200km and again the generation of an electric field at the surface was a preferred option [*Hobara and Parrot*, 2005].

Pulses of electric fields of 2-3h duration is another considered possibility for causing enough of an effect to modify the electron density distribution in the ionosphere. Acoustic-gravity waves of periods of 2h propagate horizontally and, according to the dispersion relation, are observed 1500km away from the point of generation. Thus if acoustic-gravity waves are responsible for ionospheric perturbations, then anomalous fluctuations should be observed at large distances away. However, bay-formed disturbances at an altitude of 300km and less than 500km from the region of a future epicentre were observed [*Popov*, 2004]. Acoustic-gravity waves could not explain the observations. To explain such phenomena it was conceived that during the preparation stage of an earthquake the area and underlying lithologies undergoes dilation, expansion and relaxation. Radon, other radioactive gases and metallic aerosols may be released between the expansion and relaxation periods with durations of 2-3h. Hence causing electric field enhancements with the same time scales to propagate up to the ionosphere and effect the ionosphere electron density distribution with disturbances of 2-3h.

Rai et al. [1998] also confidently reports that gravity waves cannot substantially effect the ionosphere as they propagate horizontally and will not reach ionospheric F-region heights to influence the electron density distribution. Rather the perturbations are attributed to the quasistatic electric fields and electromagnetic waves penetrating the F-region at VLF frequencies.

Clearly the generation process of the ionospheric anomalies is still very far from being fully understood, and the parameters change from study to study, based on many factors including time of day, location, land- or sea-based, distance between epicentre region and observation point.

Hayakawa [2008] presented a summary of all the processes mentioned that may cause ionospheric perturbations in relation to seismic activity, shown in Figure 1.10.

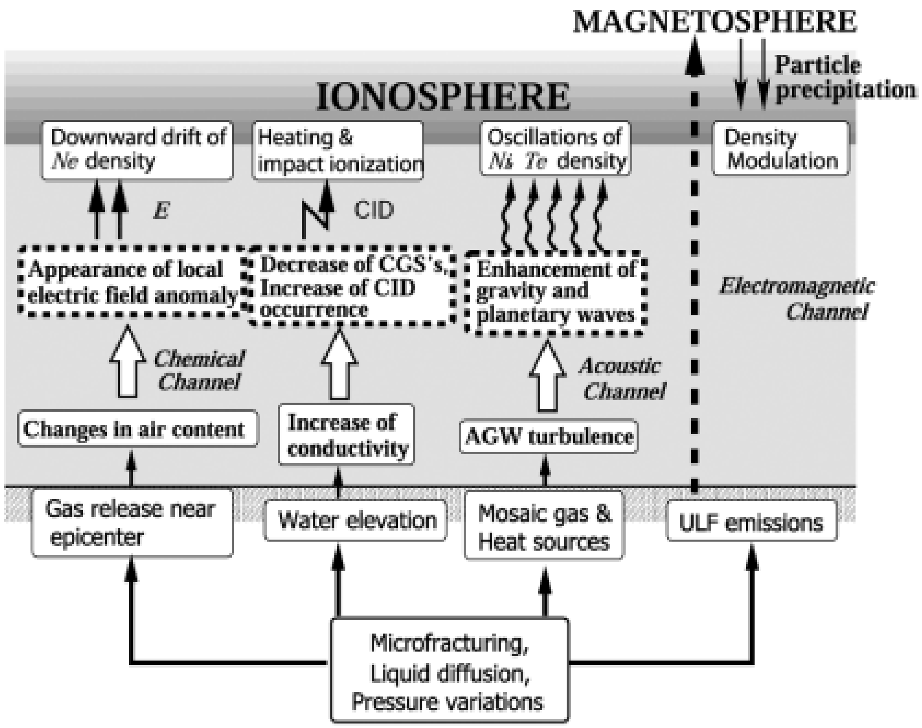

Figure 1.10: Schematic representation of the electromagnetic effects associated with EQs and lithosphere-atmosphere-ionosphere coupling [*Hayakawa*, 2008].

1.2.4 Solar Influences on the Ionosphere

The ionosphere is primarily influenced on large-scales by the solar wind, thus any perturbation of the ionosphere originating from the Earth would be very difficult to isolate and analyze [*Hobara and Parrot*, 2005]. Large fluctuations in the solar wind are of main concern in terms of contaminating ionospheric data when trying to isolate seismogenic responses of the ionosphere. Any perturbation that may possibly be effected by any other source other than a seismic event is disregarded immediately [*Liu et al.*, 2000]. Such fluctuations are solar flares or sudden storm commencements (SSC). Storms that originate from the Sun modify the ionosphere, and in particular, depress the critical frequency of the F-region, foF2, for periods from a few hours to two days. A major storm day is defined as a day with a SSC and Kp and Dst indices of > 6 and $> 60nT$ respectively [*Liu et al.*, 2006].

The Kp index monitors the planetary geomagnetic activity on a global scale, whereas the Dst index records fluctuations in the equatorial ring current indicating geomagnetic storms [*Liu et al.*, 2000; *Rios et al.*, 2004].

Authors studying seismo-ionospheric signatures state clearly that the study period, especially around the earthquake under study was done under geomagnetic quiet conditions, so as to isolate any perturbations observed in the ionosphere as highly probably seismogenic [*Liu et al.*, 2001; *Rios et al.*, 2004; *Dutta et al.*, 2007]
Investigating a storm event during 11-13 April 2001, using the same ionosonde station that recorded the foF2 readings for the Bhuj earthquake, yielded that foF2 deceased by 40% during the main phase of the storm. The depression of foF2 was close to the 50% drop reported by *Liu et al.* [2000] and could then be classified as a possible seismic related anomaly. Hence the ionospheric reaction to solar effects must be well understood to ensure no false truths are entered into seismo-ionospheric signal analysis.

Ho et al. [1998] found that ionospheric TEC signatures were greatly influenced by a solar storm. Studying a solar storm during 10 January 1997 it was found that ionospheric TEC readings varied drastically with latitude for a specific longitude, shown in Figure 1.11. The Figure displays the percentage changes of ionospheric TEC relative to quiet times at different latitude bands. The vertical solid line marks the start time of the storm main phase (06h00 UT, Jan 10), while the dashed lines gives the local noons. The main phase lasted from 06–10h00 UT, reaching a minimum Dst index of -81nT. The positive phase started three hours after the begining of the geomagnetic storm. Within the 60°–80°N geomagnetic latitude band, the first peak was observed during the day, while the second one appeared as a pre-midnight enhancement, whose rate exceded 100% of the quiet levels. At most latitudes, enhancements in TEC signatures reached their maximum between 12–16 UT. In the southern hemisphere high latitudes (60°–8O°S), however, there was a clear negative phase, which started after 16 UT. At higher geomagnetic latitudes, smaller extended negative phases occurred during the next two days.

Other main differences between storm-originated and seismogenic signals in the ionosphere are that anomalies associated with seismic events stay fixed to the ionosphere above the earthquake preparation region, whereas disturbances related to solar activity travel through the ionosphere and are able to be monitored globally. Seismic signatures in the ionosphere are very much a localized phenomenon, observed by stations less than 200km away from the anticipated epicentre [*Pulinets*, 2000]. Storms have a general duration of 8–48h, but seismogenic signatures last from 2-3h and appear at the same local time from 5 days prior to the shock [*Pulinets*, 1998].

An example of the effect of geomagnetic storms on VLF profiles is shown in Figure 1.12. The profiles for 20 and 21 November 2007 are shown, as well as the Dst and ΣKp indices for the month. A large storm occurred on these days. The Dst index drops to a minimum of close to -60nT, with the ΣKp rising to almost 30. Both profiles are seen to have a drastic variation just after the morning terminator time. The second drop in amplitude in these profiles are missing during the non-perturbed days during November 2007.

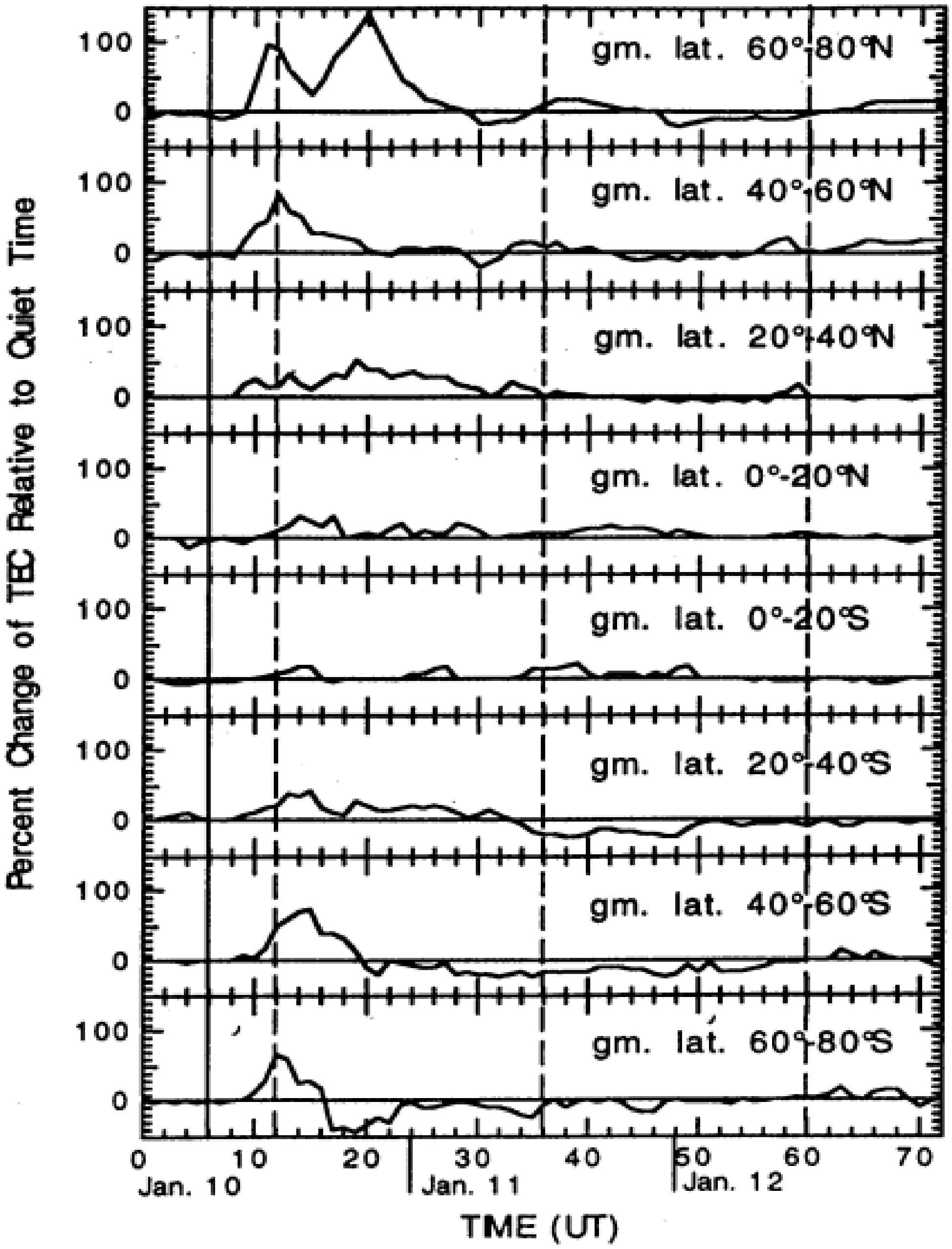

Figure 1.11: Latitudinal variation in percent changes of ionospheric TEC signatures relative to quiet times for 10, 11 and 12 January 1997. The vertical solid line marks the onset of the solar storm main phase at 06h00 UT during 10 January 1997, while the dashed lines gives the local noons. The positive and negative phases of the storm appear clearly at higher latitudes (N or S). At lower latitudes (20°), the storm effect is less obvious [*Ho et al.*, 1998].

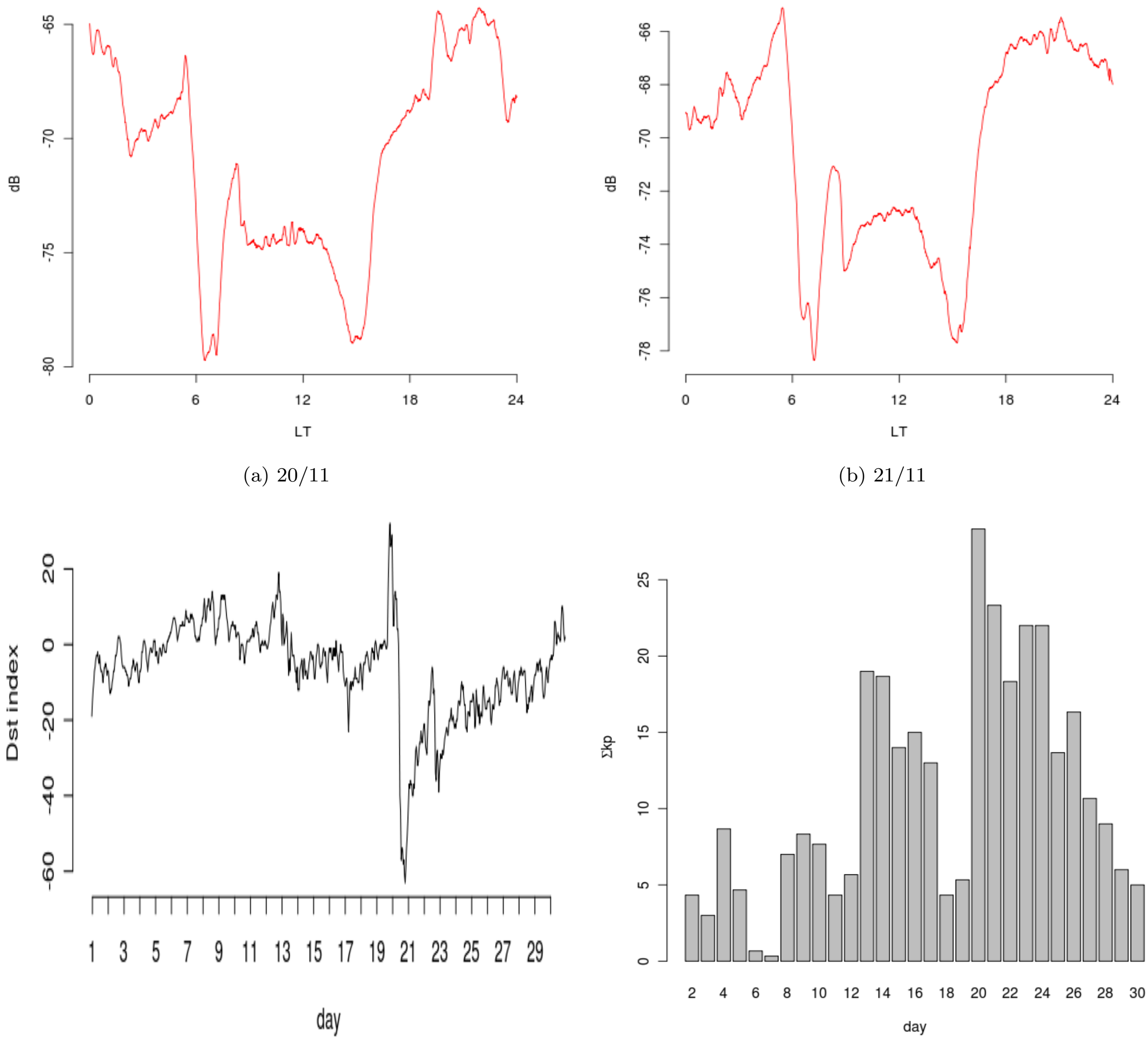

(a) 20/11

(b) 21/11

(c) Dst

(d) ΣKp

Figure 1.12: VLF signals observed for 20 and 21 November 2007, recorded along the propagation path between the North West Cape (NWC), Australia VLF 19.8kHz transmitter and the Budapest, Hungary receiver, showing effect of geomagnetic storm during 20 November on VLF profiles with Dst and ΣKp indices reaching -60nT and 30 respectively during 20 Novmber 2007.

Chapter 2

Results

2.1 Data

The research of this thesis concentrates on earthquakes occurring from 25/07/2007 to 28/02/2008 along two propagation paths from the Australian North West Cape (NWC) 19.8kHz transmitter (21.810° S, 114.166° E) to the VLF narrowband receivers in Budapest (47.472°N, 19.050°E) and Tihany(46.908° N, 17.879° E). The earthquake data were collected from the USGS website. Details such as the longitude, latitude, time, depth and magnitude of the earthquakes were given. The set of data for earthquakes that occurred within an area in close enough proximity to the propagation paths during the study period is shown in Table 2.1. Clusters of earthquakes that occurred within a few degrees of each other were treated as a single extended seismic period, such as the group of earthquakes that occurred during 12 September 2007. The table is sectioned off by earthquakes that are relevant to the each specific case study

Figure 2.1 shows the global distribution of earthquakes in relation to propagation paths between transmitters and the receivers in Hungary. There were predominantly low to medium magnitude earthquakes ($5 < M < 6$) that occurred, generally limited to tectonic plate boundaries. The lower limit of the earthquake magnitudes was taken as 5.5 as has been the consensus as the threshold for VLF ionospheric anomaly generation [*Pulinets*, 2003; *Shvets*, 2004; *Hobara and Parrot*, 2005; *Liu et al.*, 2006; *Molchanov et al.*, 2006]. This helped to simplify the number of earthquakes to take into consideration. It can be noticed that the majority of the transmission paths are limited to the Northern Hemisphere with little to none seismic activity occurring within the Dobrovolsky area to any. The three transmission paths that extend further to the South and East traverse far more seismically active areas. Unfortunately for the JJI transmitter path the dates of the two relevant earthquakes occurred before the dataset dates. Hence only the NAU and NWC transmitters could be used. For the NAU transmission path, an earthquake of $M = 7.4$ occurred just South-East of the transmitter, thus it would seem to be an ideal event to study, as no other earthquakes occurred near the transmission path. However, the depth of the earthquakes epicenter occurred at 156km. This makes the earthquake ineligible to be considered as it is to deep to effect the ionosphere sufficiently enough so as to generate anomalies, based on the literature. In summation the lack of seismic activity in the areas covered by transmission paths, the great depth of possible earthquakes to be studied and broken data aided in finally isolating the 19.8kHz NWC transmitter as the propagation path to be studied.

Another method of data elimination was the actual spacial distribution of the earthquake epicentres from the surface projection of the propagation paths. This was accomplished by using the Dobrovolsky formula given in equation (1.4).
Using the Dobrovolsky formula to calculate the radius of the preparation zones of the earthquakes, earthquakes that would have a significant chance of affecting readings along a particular transmission path were identified. Thus studying all the transmitter-receiver paths, it was possible to eliminate earthquakes that would not have an effect on the nearest propagation path based on their magnitudes. This in turn helped to choose specific propagation paths that were highly affected by seismic activity and would give the best chance of having perturbations being observed in the signals propagating along.

Due to the strictly regional area of the ionosphere that is influenced by an impending earthquake, only the area of the ionosphere above the preparation zone would have a significant chance of being perturbed.

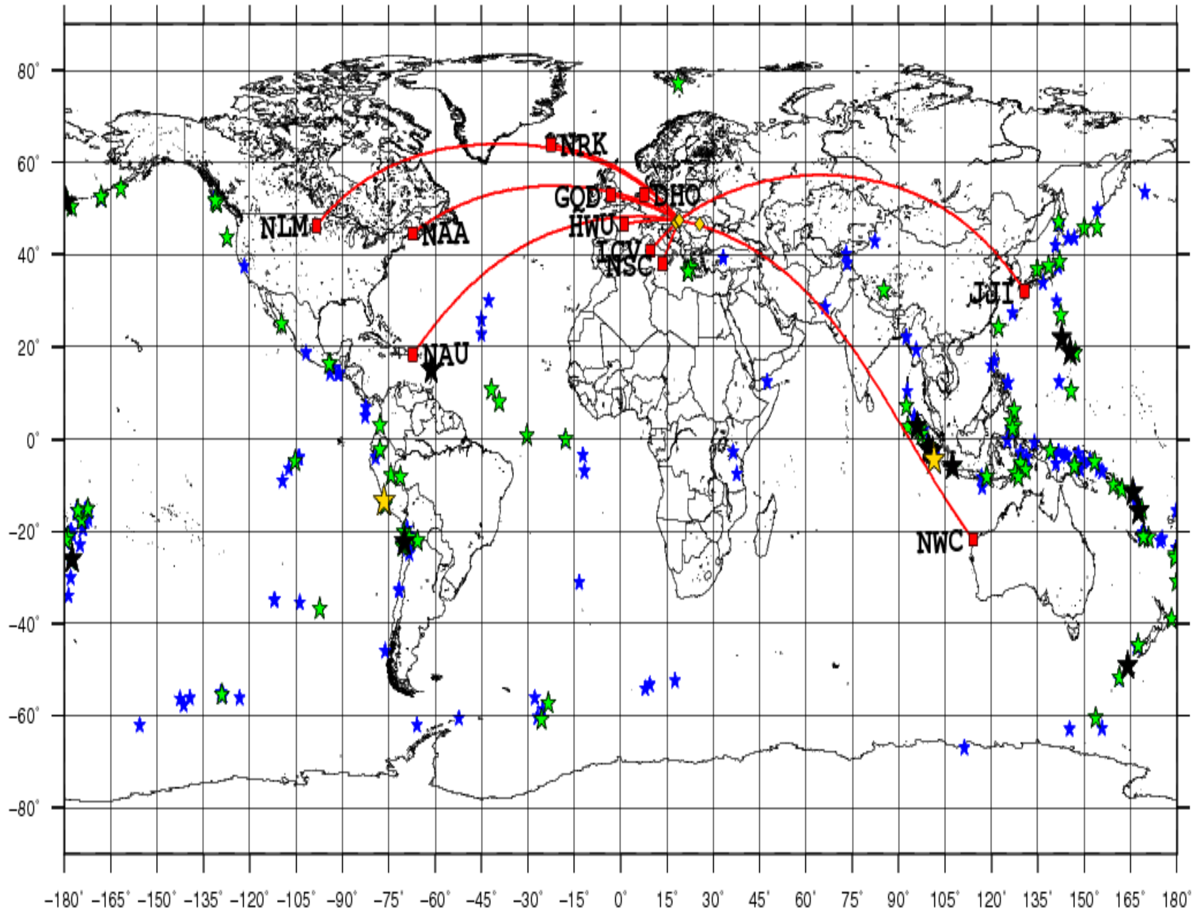

Figure 2.1: Locations of VLF receivers (diamonds) and transmitters (squares); propagation paths (red lines); Earthquakes (stars): 5.5< M <5.9 - blue, 6< M <6.9 - green, 7< M <7.9 - black, 8< M <9 - yellow.

VLF wave data obtained from narrowband receivers situated in Hungary were analyzed. The propagation paths from the 19.8kHz NWC transmitter to the receivers in Hungary were investigated in detail. The path passes over a region of a high density of earthquake activity off the West coast of Indonesia.

The daily VLF profiles throughout the study period were investigated for anomalous perturbations. Deviations were observed around the dates of certain periods of seismic and geomagnetic activity. The quiet-day curves were constructed by using the VLF amplitudes for at least a seven day period leading up to the perturbed periods. Somewhat similar to that employed by *Shvets* [2004], where the 17 day running mean was used. Smoothing the data to eliminate noise, gave the quiet-day curves used in this work.

Table 2.1: Earthquakes for study period 25 July to 31 December 2007

Year	Month	Day	Longitude(^{o})	Latitude(^{o})	Magnitude	Depth(km)
2007	7	25	92.518	7.157	6.1	15
2007	8	8	107.681	-5.926	6.1	291
2007	8	8	107.419	-5.859	7.5	280
2007	9	12	100.221	-2.840	5.5	35
2007	9	12	101.379	-2.930	5.6	35
2007	9	12	101.396	-3.145	5.8	35
2007	9	12	101.463	-3.158	5.9	35
2007	9	12	100.841	-2.625	7.9	35
2007	9	12	101.367	-4.438	8.5	34
2007	9	13	99.635	-1.724	5.5	32
2007	9	13	99.947	-2.234	5.5	30
2007	9	13	100.974	-2.749	5.5	17
2007	9	13	99.816	-1.900	5.7	16
2007	9	13	101.524	-3.172	6.0	53
2007	9	13	99.668	-1.689	6.5	28
2007	9	13	99.627	-2.130	7.0	22
2007	9	14	100.953	-4.416	5.8	25
2007	9	14	101.169	-4.074	6.4	23
2007	9	15	101.190	-2.788	5.5	35
2007	9	18	101.348	-3.259	5.6	35
2007	9	20	100.141	-1.999	6.7	30
2007	9	23	99.935	-2.135	5.5	28
2007	9	24	100.362	-3.155	5.7	18
2007	9	26	99.488	-1.787	6.1	26
2007	9	29	95.533	2.915	5.7	20
2007	9	29	95.523	2.900	6.0	35
2007	10	19	66.290	28.650	5.5	35
2007	10	21	100.803	-3.591	5.5	35
2007	10	21	100.859	-3.592	5.6	27
2007	10	23	99.896	-1.996	5.8	30
2007	10	24	101.020	-3.899	6.8	21
2007	10	25	100.794	-3.541	5.5	29
2007	12	20	33.212	39.417	5.7	10
2007	12	22	96.806	2.087	6.1	23
2007	12	26	33.162	39.446	5.6	8

2.2 Budapest Observations

Once the 19.8kHz propagation path was chosen the dates of earthquakes to be investigated, based on their Dobrovolsky preparation zones, were determined, given in Figure 2.2. This means that based on their magnitudes earthquakes with preparation zone areas that were traversed by the propagation path were considered as significant. The size of the preparation zones were calculated by the Dobrovolsky formula (1.4).

Figure 2.2 shows a more detailed image of the earthquake epicenter distribution in relation to the 19.8kHz transmitter-receiver propagation path. There was one low magnitude earthquake just north of India near enough to the path to affect signals propagating along, further south occurred a high density series of shocks with much greater magnitudes between latitudes 7°N to 10°S and longitudes 92°to 107°E.

The VLF profiles for each case study as well as their corresponding amplitude differential plots, dA, are shown for each. The VLF signals were observed at the Budapest receiving station from 22 July to 31 December 2007. The black curves represent the quiet-day curves. The red curves are the VLF signals received on the particular day. The figures can be analysed for daytime and nighttime fluctuations. The following section shows the results of isolating days which were observed to display specific shaped perturbations. Such perturbations were step-down and step-up changes in the amplitudes of the signals.

These can be described as sudden appreciable increases or decreases in the signal in a very short period of time, less than an hour. As well as anomalous enhancements or depressions of the signals for longer periods through the day, called bay-shaped disturbances.

It must be stated that only days that showed anomalous VLF behaviour as already described were analysed. Other days were not included in dicussions as the profiles either followed their respective quiet-day curves showing no substantial amounts of fluctuation or the data for such days were broken and could not be analysed.

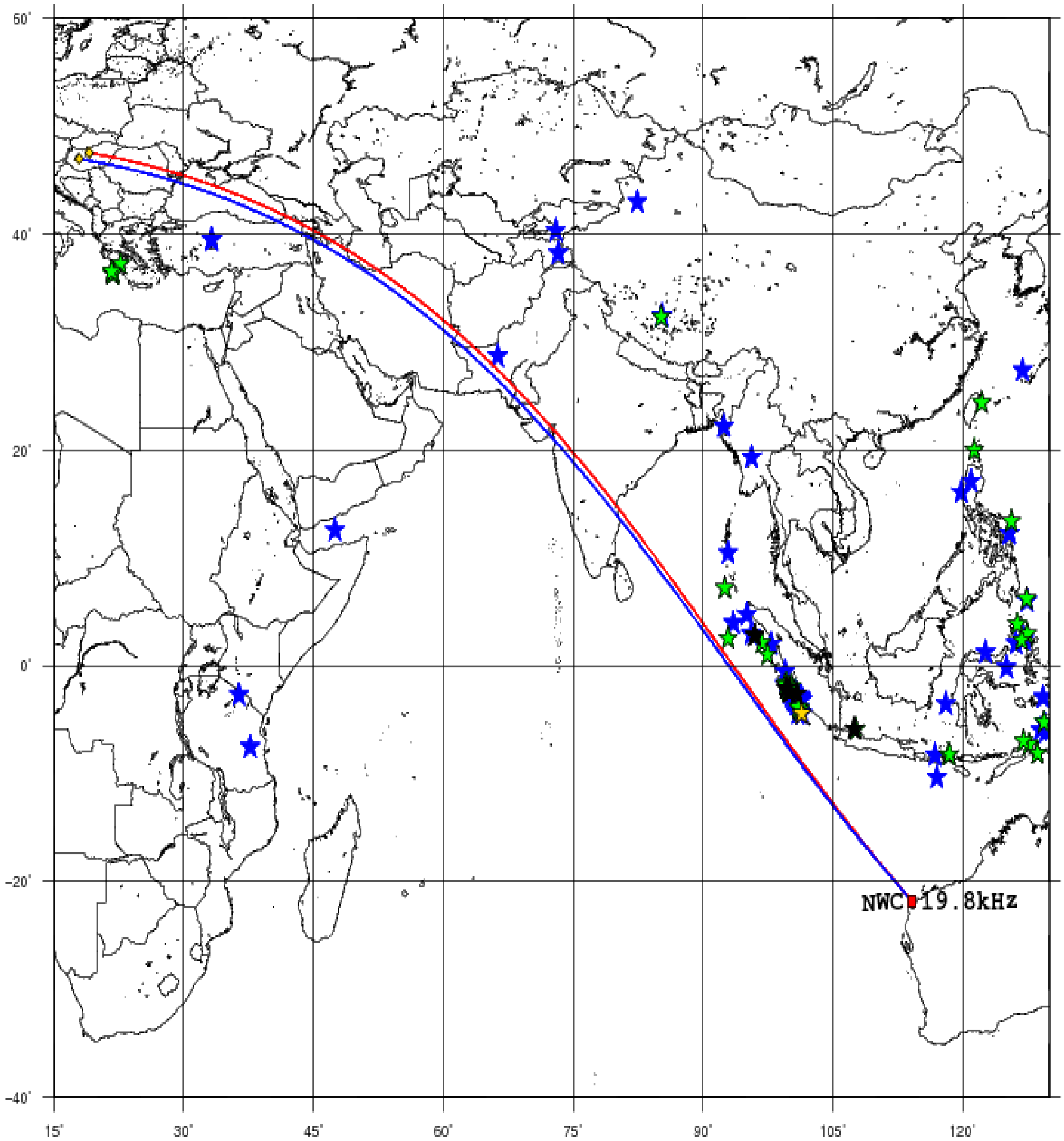

Figure 2.2: Locations of European VLF receivers (diamonds) and 19.8kHz NWC transmitter (square); propagation paths: NWC-Budapest (red), NWC-Tihany (blue); Earthquakes (stars): 5.5< M <5.9 - blue, 6< M <6.9 - green, 7< M <7.9 - black, 8< M <9 - yellow.

2.2.1 Diurnal Anomaly Analysis

This section identifies specific days during which anomalous VLF signal behaviours were observed. An anomalous day is defined in this work as any day in which the VLF profile deviates substantially from the quiet-day curve, This is determined using the differential amplitude, dA, plots. If the dA value extends further than either the 2σ and -2σ during the night hours, or deviating by more than 2σ during the daytime hours the perturbation is considered as anomalous. This distinction in day/nighttime anomaly criteria was made as it was observed there was relativley little fluctuation through the daytime hours compared to the nighttime fluctuations.

As the comparison of the individual day VLF amplitudes to the quiet-day curves is the main diagnostic tool for anomaly identification in this study, each month's quiet-day curve is given a brief description first. The VLF profiles for individual days around seismic activity were superimposed on the quiet-day curves, making any significant deviations easier to identify. The structures of the deviations were found to be either short lived drops or rises (less than 30 mins) during the day or night respectively. Or as broader periods of enhancement and depressions in the signal amplitude. One general anomaly form observed was an extended period of anomalous amplitude depressions (or enhancements), in relation to the corresponding quiet-day curve, observed during the nighttime (or daytime hours). The other more interesting type of anomaly seen were short-lived drops or rises in the signal amplitudes. Such deviations were seen during the post-terminatortime periods.

Once a set of dates of anomalous VLF perturbations were collected, the dates were then compared to seismic activty as well as other geomagnetic influences. The aim is to identify VLF anomalies observed prior to seismic events, ideally within two weeks of an earthquake, but also in the absence of large geomagnetic storms. The effect of large geomagnetic storms on the ionosphere would bias any perturbations observed, thus making it very diffcult to determine that an anomaly presence is due solely to the impending seismic event.

2.2.2 Case study 1: 12 September 2007 Earthquake swarm

On 12 September 2007 an earthquake swarm started that lasted until 15 September. The swarm was characterised by a magnitude 8.5 earthquake (4.438° S, 101.367° E), at a depth of 34km.

Investigating the VLF profiles preceding and during the swarm revealed anomalous VLF behaviour being observed from the end of August 2007 to the day before the swarm began on. The days of interest for August are 24, 25, 29 and 30 August, as shown in Figure 2.3.

Figure 2.3 shows the pre-terminator time periods displaying different behaviours for 24, 25, 29 and 30 August. The August 24 VLF profile displayed quiet behaviour, however, the VLF amplitudes for the following day were noticed to be much lower. There were enhancements noticed in the midday readings for 24 and 25 August between 12h00 to 16h00LT. The former had a noticeable drop, initially rising at 13h00LT then sharply dropping below quiet conditions at 15h00LT, whereas the latter shows a period of enhanced VLF readings for 11h00 to 16h00LT. For the evening period (18h00 - 00h00LT) the profiles either decrease with the quiet curve, as for 24 August, or continue to rise, as for 25 August.

Irregular decreases in the VLF profiles were noticed for 29 and 30 August. At 02h00LT on 29 August there was a sharp drop from -63 to -67dB. During the afternoon the signal suddenly dropped by a few dB. During the evening the signal did not rise as high as the quiet-day curve, but rather rose from -77 to -67dB, with a local minimum in the nighttime signal at 22h00LT. The 30 August profile had far more structured deviations. The morning pre-terminator time VLF amplitudes were highly depressed compared to the quiet conditions, but in terms of fluctuations was very quiet. The terminator minimum was also lower. The signal deviated at 11h00LT, rising above quiesence, then dropped back to the same amplitude between 17h00 and 18h00LT. The signal then immediately rose at 18h00LT, but again only to a much lower amplitude than the quiet curve, then staying level until 00h00LT.

Figure 2.4 shows the differential amplitude (dA) plots for August 2007. These show the difference in amplitudes between the current day amplitude and the quiet-day curve as calculated by equation (1.3). The dashed lines represent the standard deviations $2\sigma = 2.2$,$\sigma = 1.1$, -$\sigma = -1.1$, -$2\sigma = -2.2$, The daytime amplitudes are seen to fluctuate between 2σ and -2σ. However for the night of 24 July as well as for 29 July the dA values fall below -σ and continues through to the next mornings.

The VLF profiles for September can be seen in Figures 2.5 and 2.7. The quiet-day curve for September fluctuated around -63dB until 04h00LT. The terminator time commenced at 04h00LT, as seen from the dramatic drop in signal amplitude. The curve amplitude dropped to -76dB by 05h00LT. The amplitude then gradually fluctuated between -76 and -75dB until 18h00LT when it increased to -62dB, similar to the amplitude at the morning terminator time.

The behaviour on certain days after the evening rise in amplitude varied dramatically. The profiles reached a maximum peak between 20h00LT - 21h00LT, and then either tapered off as shown in the profiles for 1, 8 and 9 September, or tapered off to begin with, but reached another minimum (between 22h00 - 23h00LT) and rose again, such as for the 6, 11 and 12 September. The is a clear break in the evening terminator rise for September 9. The signal for 7 September, very contrastingly, continued to rise after 20h00LT.

The most striking features were sudden well defined anomalous decreases in the signal amplitudes. Figure 2.5 shows two such drops for 1 September. One at roughly 10h00LT and a later one in the afternoon at 15h00LT, where the signal amplitude decreased decreased rapidly twice at 10h00LT and 15h00LT. This occurred 11 days prior to the start of a very strong series of earthquakes ranging in magnitude from 5.5–8.5. A very similar drop occurred on 6 September,Figure 2.5, but only in the afternoon at 15h00LT. For 11 September, Figure 2.7 the daytime amplitudes seem to be consistently higher than the quiet-day curve, whereas the other days roughly followed the quiet-day curve well.

The dA plots are shown in Figures 2.6 and 2.8. The dashed lines represent the standard deviations $\sigma = 2.2$,$\sigma = 1.1$, $-\sigma = -1.1$, $-2\sigma = -2.2$. Clear nighttime deviations below $-\sigma$ are seen for the nights between 1-2, 6-7, 8-9 and 11-12 September. Sharp peaks around the terminator times are interpreted as a shift in the terminator time for that day.

Literature states that anomalous ionospheric readings have a higher chance of being observed during the day, normally occurring within a week of the impending earthquake [*Shvets*, 2004; *Liu et al.*, 2006]. But on 1 September there is another distinctive, well defined drop observed in the mid-morning hours (10h00LT) 11 days prior to the earthquakes.

The 11 September anomaly, on the day prior to the earthquake, only showed nighttime fluctuations far below the quiet-day curve, but only for the morning hours for 00h00LT - 04h00LT, as compared to the daytime deviations for 1 and 6 September. The daytime signal was stable, enhanced slightly higher than the quiet-day curve with no major perturbations for the evening hours.

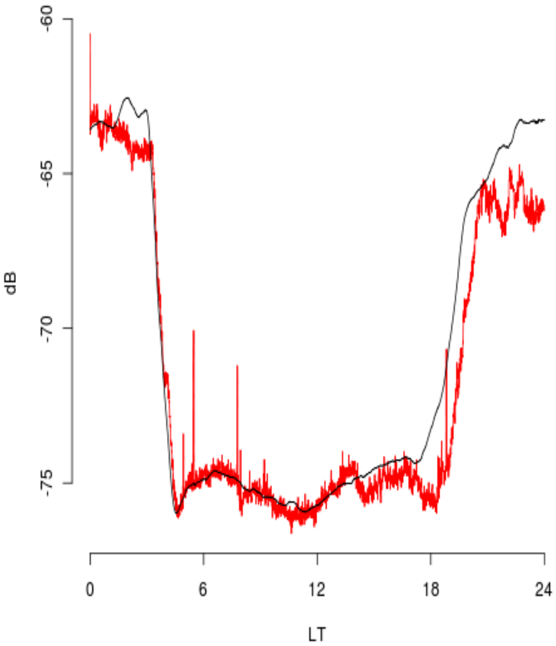

(a) 24/08

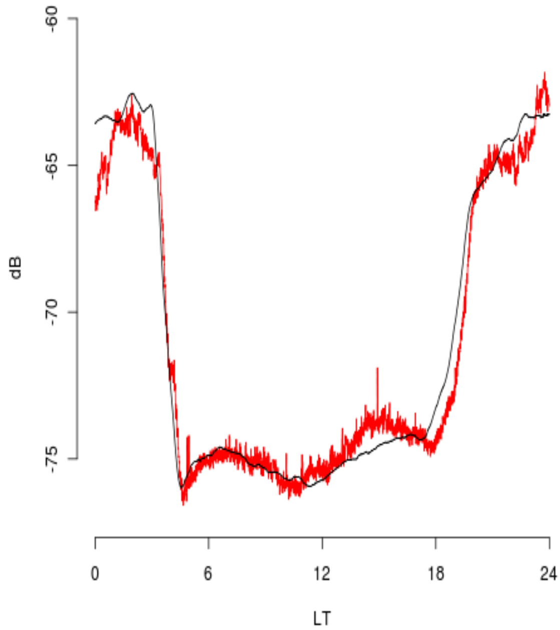

(b) 25/08

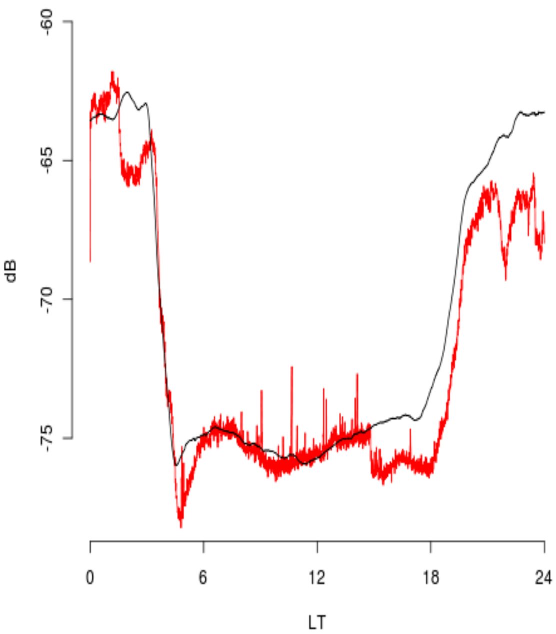

(c) 29/08

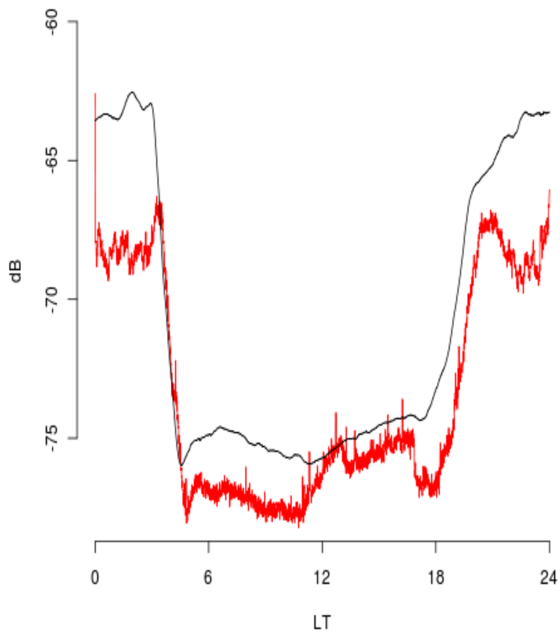

(d) 30/08

Figure 2.3: VLF signals observed on particular days (red) compared to quiet-day curves (black) showing anomalous drops for 24, 25, 29 and 30 August 2007.

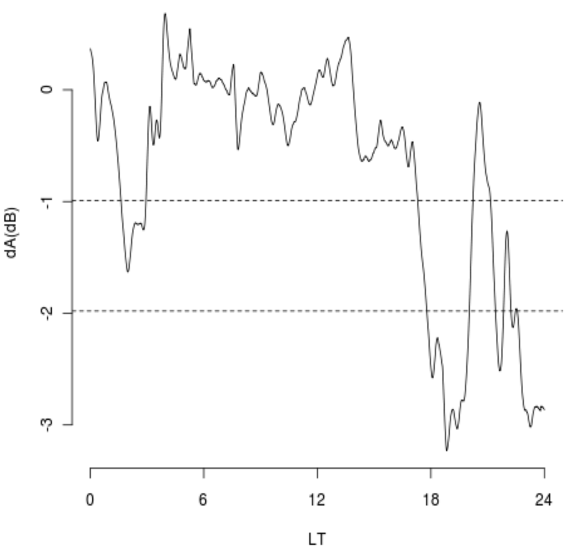

(a) 24/08

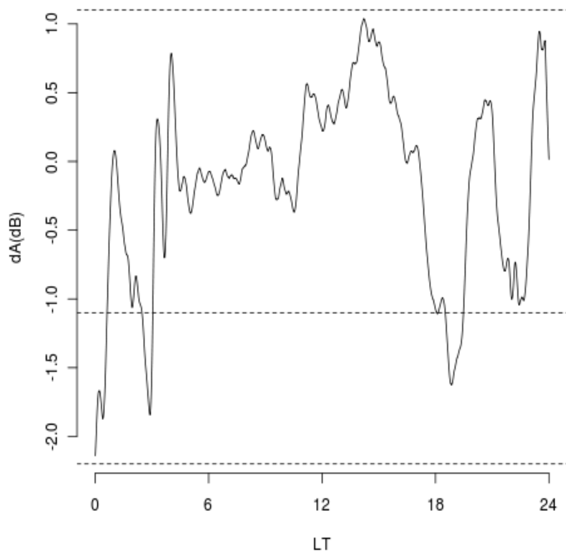

(b) 25/08

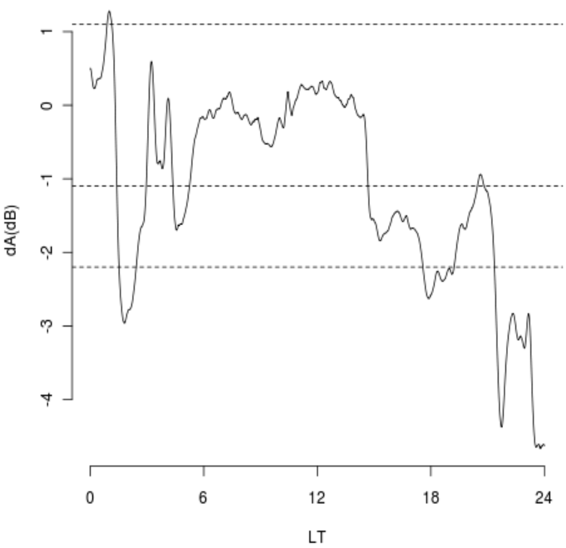

(c) 29/08

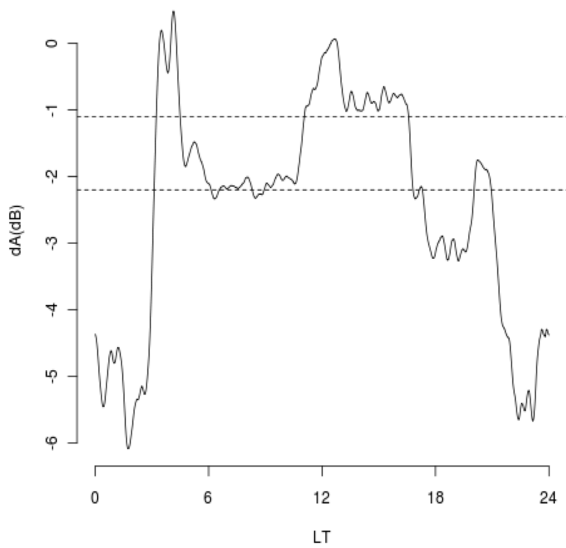

(d) 30/08

Figure 2.4: dA plots for 24, 25, 29 and 30 August 2007. Large drops in dA seen for 24, 29 and 30 August at terminator times. Strong nighttime fluctuations well below -σ observed, with relatively low fluctuation during daytime hours. $\sigma = 2.2$,$\sigma = 1.1$, -$\sigma = -1.1$, -2$\sigma = -2.2$

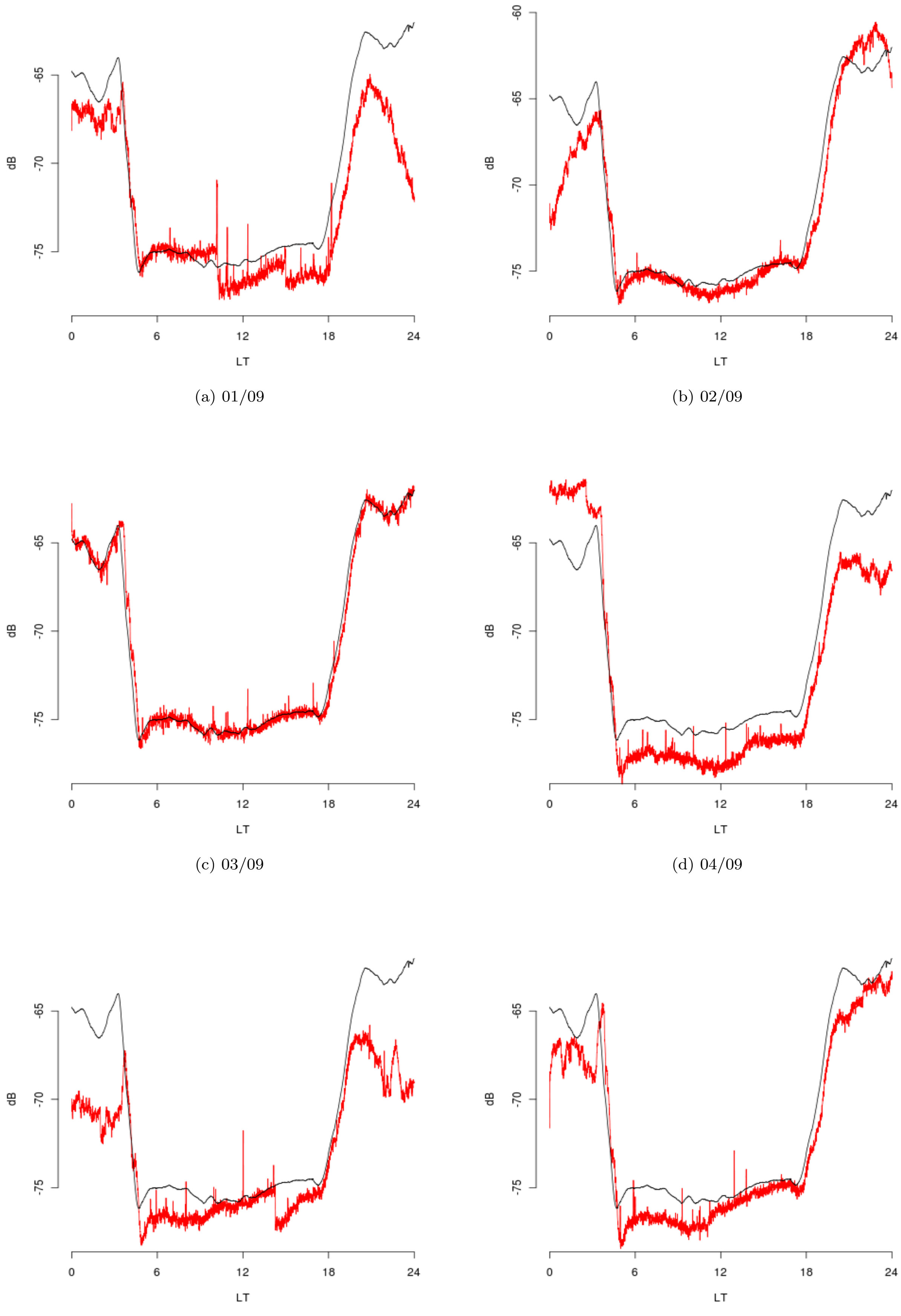

(a) 01/09

(b) 02/09

(c) 03/09

(d) 04/09

(e) 06/09

(f) 07/09

Figure 2.5: Behaviour of VLF signals observed (red) for 1-4 September 2007 superimposed on the quiet-day curve (black), showing strong nighttime deviations as well as well defined drops in the daytime signals for 1 and 6 September.

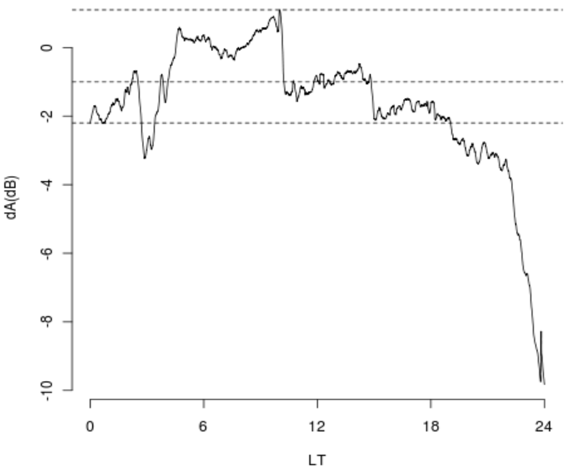

(a) 01/09

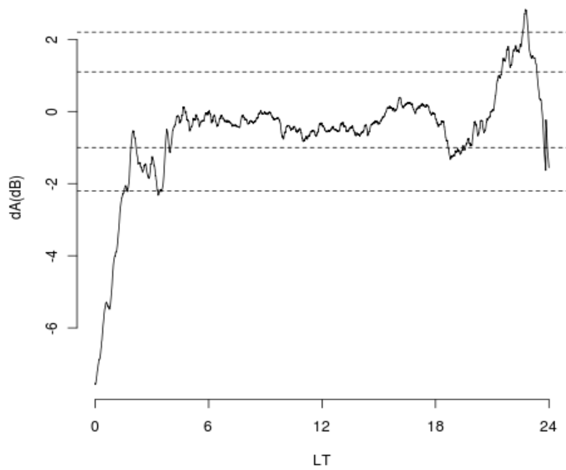

(b) 02/09

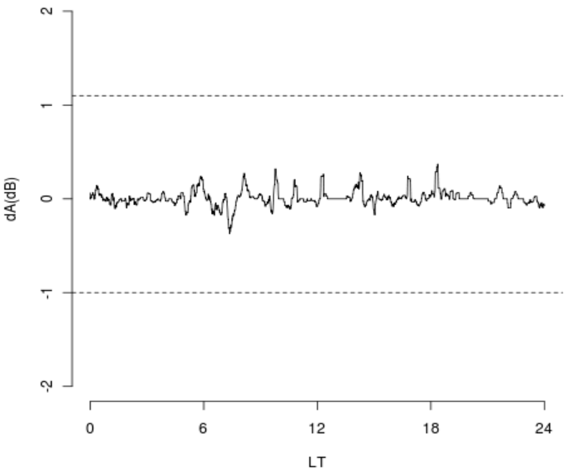

(c) 03/09

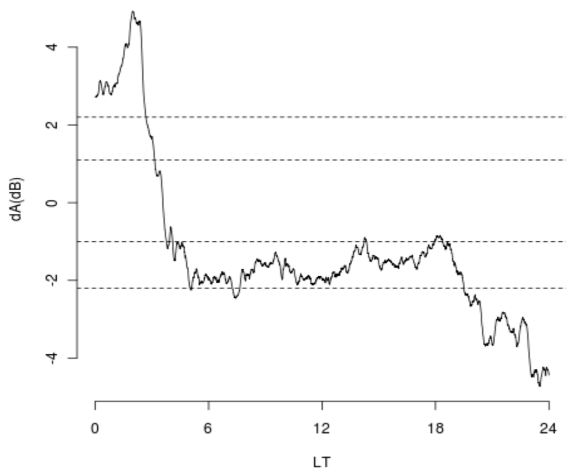

(d) 04/09

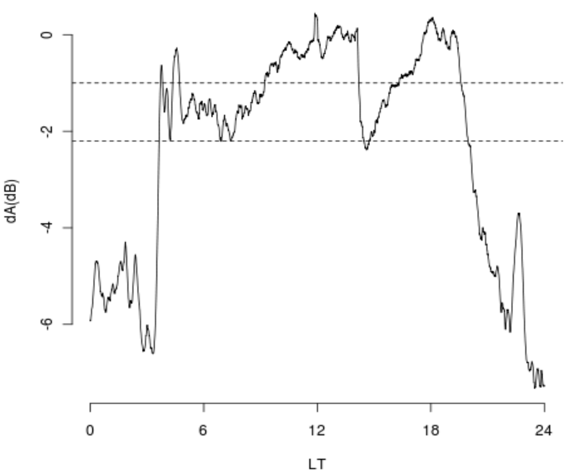

(e) 06/09

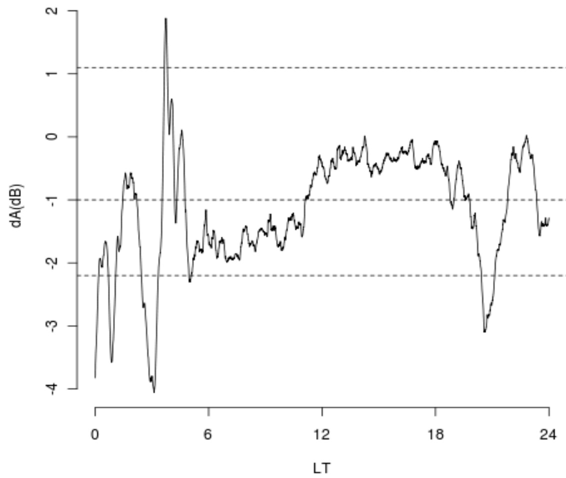

(f) 07/09

Figure 2.6: dA plots for 1-7 September 2007. Dashed lines represent the standard deviations ($2\sigma = 2.2$,$\sigma = 1.1$, $-\sigma = -1.1$, $-2\sigma = -2.2$). Large drop in amplitude seen over night between 1 and 2 September, as well as large sudden rise for 4 Septmeber. The daytime amplitudes are seen to keeping well within the standard deviation. Sharp drop during 6 September midday

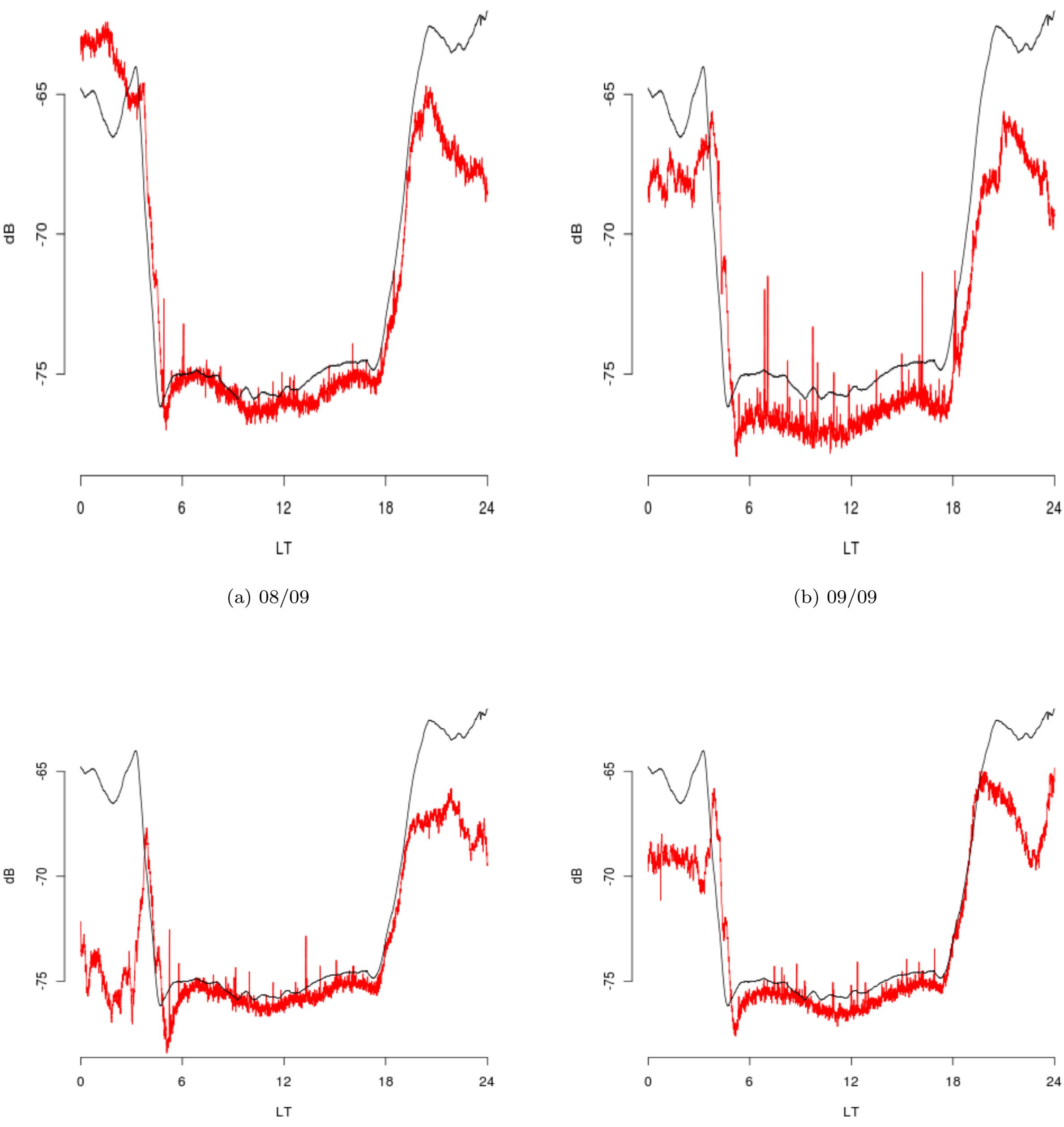

(a) 08/09

(b) 09/09

(c) 11/09

(d) 12/09

Figure 2.7: Behaviour of VLF signals observed (red) for 8–12 September 2007, with the quiet-day curve (black) superimposed. Strong nighttime deviations in both the morning and evening hours are seen, but with little fluctuation during the daytime hours. Nighttime amplitudes are suppressed, with a large disturbance in the early morning of 11 September, the day before the onset of the earthquake swarm.

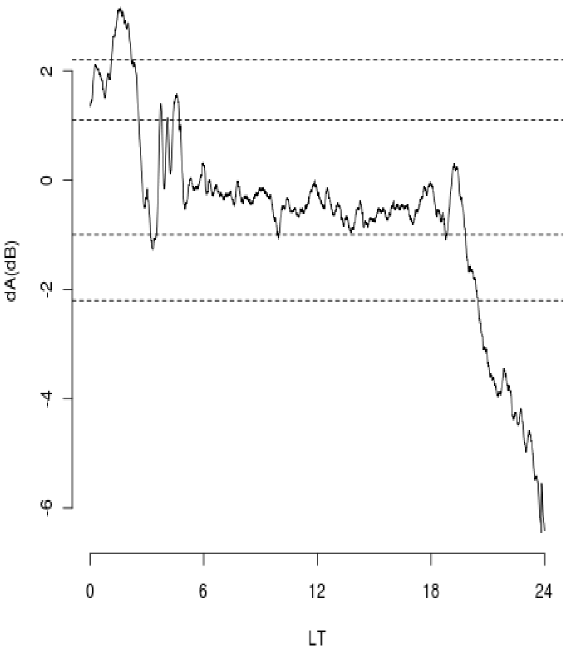

(a) 08/09

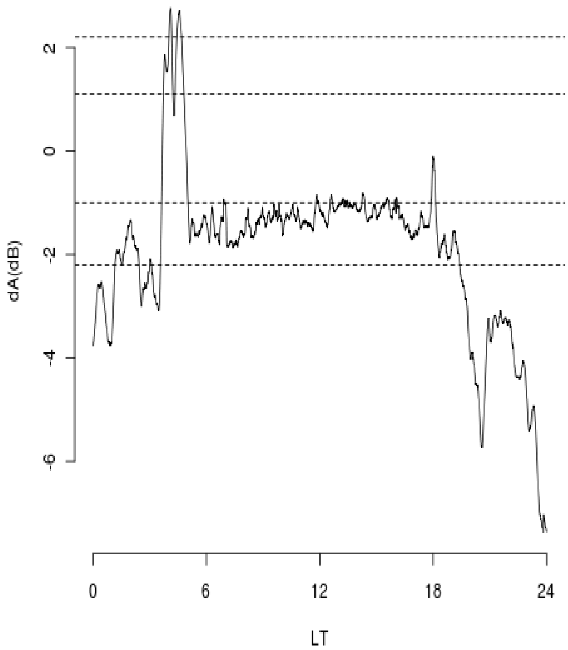

(b) 09/09

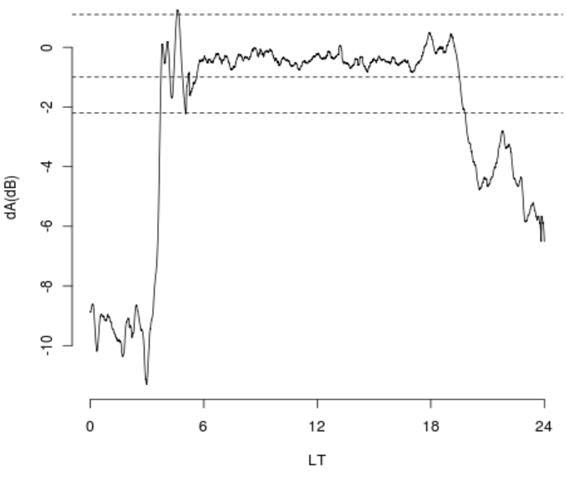

(c) 11/09

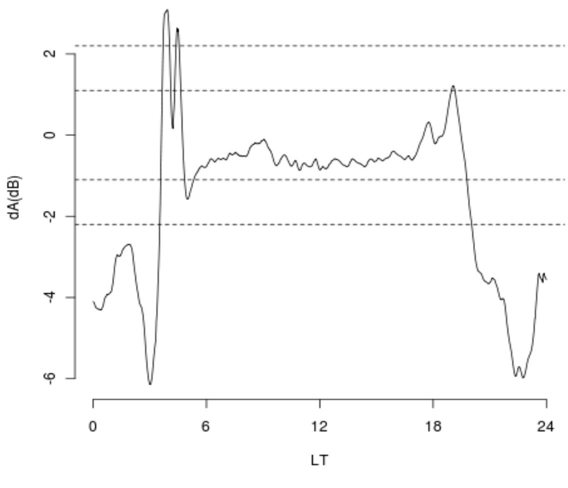

(d) 12/09

Figure 2.8: dA plots for 8–12 September 2007. Strong terminator deviations are seen as well as late night amplitude depressions below $-2\sigma = -2.2$. Sharp drop during 6 September midday. Strong activity seen before and after terminator times. Little variation observed during daytime hours $.2\sigma = 2.2$,$\sigma = 1.1$, $-\sigma = -1.1$, $-2\sigma = -2.2$

VLF anomaly relation to seismic activity

The month of September 2007 was characterised by a large series of earthquakes in a short period of time, an earthquake swarm, that began on the twelfth, ended on the fifteenth, with single-quake days that continued through to the end of the month. On the first day of the swarm (12 September) six earthquakes occurred within a limited region. Four were relatively low magnitude (5.5 - 5.9), one was much stronger, magnitude 7 and the largest of the swarm had a magnitude of 8.5. On the second day 7 more earthquakes occurred; four low, two of medium $6 < M < 6.9$ and one large $M > 7$. The next day experienced two smaller quakes and one shock the following day to end the swarm. The month then tapered off with one low magnitude earthquake almost everyday on 17, 20, 23, 24, 26 and two on the 30th.

It must be said that all the earthquakes had shallow epicentres, less than 40km depth. For the spatial distribution and details of individual earthquakes please see Figure 2.2 and table 2.1 respectively.

Figure 2.9 shows the temporal distribution of the VLF anomaly days and earthquake activity. The earthquakes have been distinguished by magnitude, as described by the plot legend. It is well worth noting that the periods of anomaly appearance and earthquake occurrence did not overlap. The anomalies appeared 11, 6 and 1 day prior to the onset of the earthquake swarm.

The deviations observed at the end of August 2007, see Figure 2.3 cannot be attributed to geomagnetic influences. The Dst and ΣKp indices are shown in Figure 2.10. There are two earthquakes that occurred at the beginning of August, but these occurred almost three weeks prior to the anomaly appearances. The anomalous perturbations can thus be possibly linked with the earthquake swarm in the next month, commencing on September 12. As the swarm consisted of 16 earthquakes ranging in magnitude from 5.5–8.5 occurring in four days the region would be experiencing a substantially high amount of processes during the earthquake preparation stage.

As stated before, anomalous VLF signal perturbations have been observed from a day to over two weeks before the onset of an earthquake in the absence of geomagnetic influences [*Singh et al.*, 2001; *Shvets*, 2004; *Molchanov et al.*, 2006; *Maekawa et al.*, 2006; *Horie et al.*, 2007; *Singh et al.*, 2009]. The perturbations for the four days at the end of August could very well be the first days indicating the ionosphere starting to be influenced by processes within the impending earthquake zone.
The geomagnetic influence on the ionosphere has been ruled out as possible causes for the anomlies observed. As can be seen in Figure 2.10, it is clear that the Dst(2.10a and 2.10b) and ΣKp(2.10c and 2.10d) indices did not exceed the minimum levels required for a geomagnetic storm to be held responsible for the anomalous deviations recorded. The Dst index reached a minimum of -22nT during 27 and 28 August, which was also reflected by the rise in the ΣKp index around the same dates. From the beginning of September it is clear that both indices showed very low degrees of fluctuation. The ΣKp index reached a maximum of 28 on 1 September decreasing to near zero on the twelfth. The Dst index greatest deviation, during the period of anomaly observation, reached a minimum of -28 during 6 September and stabilised to around zero again by 12 September. From these readings any geomagnetic influences can be ruled out and thus the possibility that the anomalous VLF perturbations are infact seismogenic is of a much greater probability.

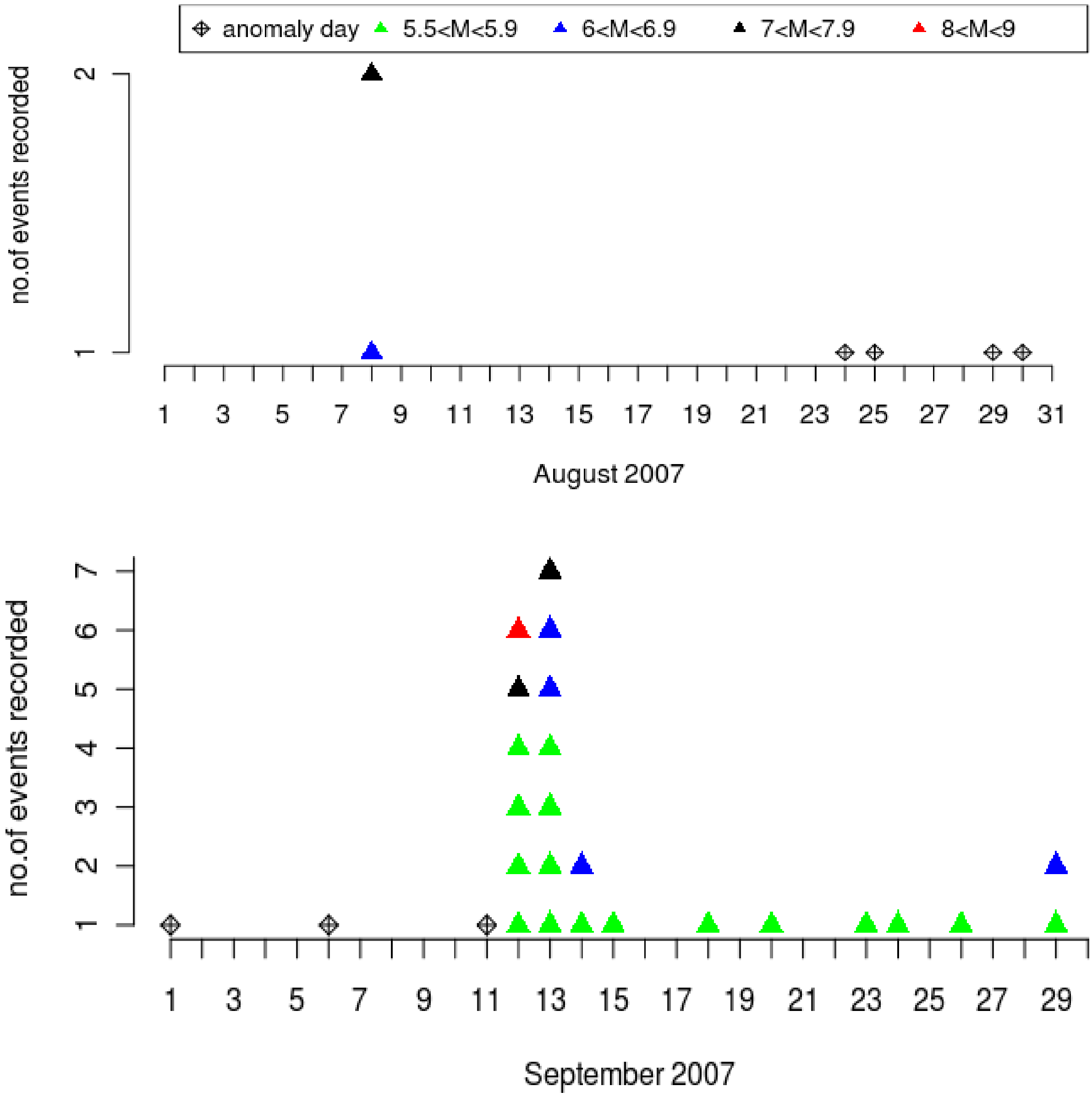

Figure 2.9: Temporal distribution of observed VLF anomalies (◇) in relation to seismic activity for August and September 2007 (triangles). Anomalies are seen at the end of August as well as 11, 6 and 1 day prior to the start of the earthquake swarm on 12 September, but none after or during the swarm.

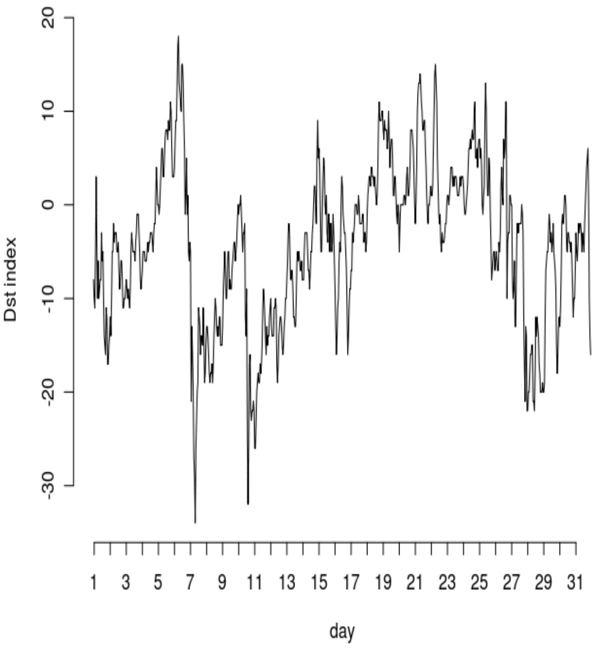

(a) August 2007

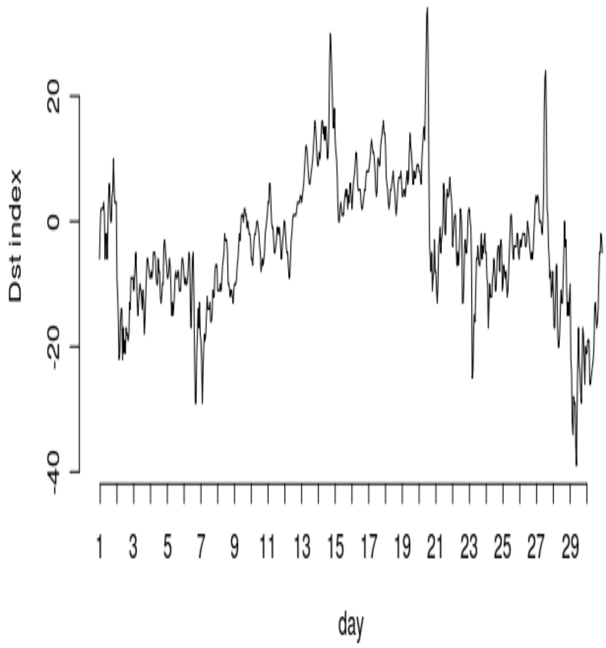

(b) September 2007

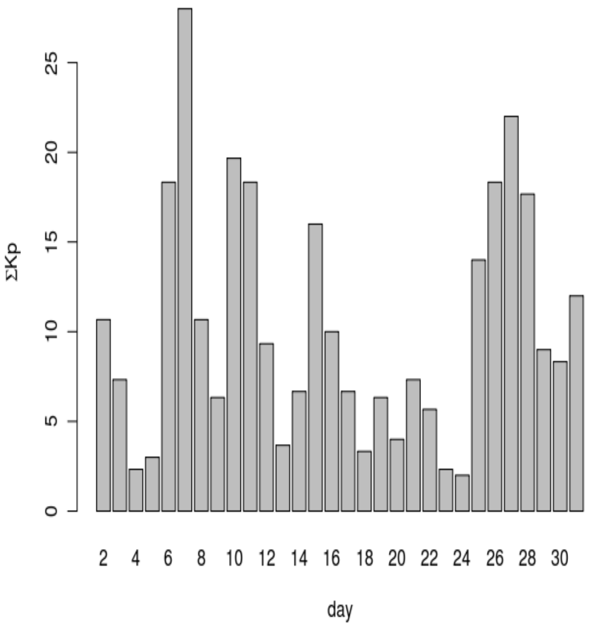

(c) August 2007

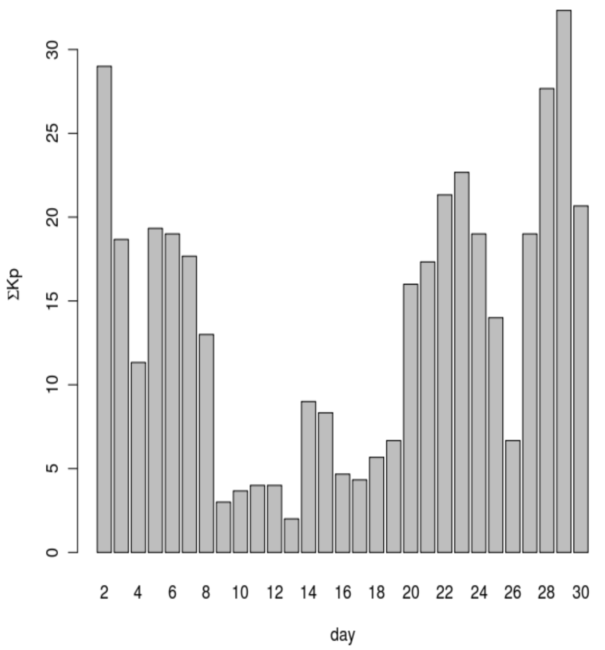

(d) September 2007

Figure 2.10: Dst and ΣKp indices for August and September 2007.

2.2.3 Case study 2: 25 July 2007 Earthquake

Unfortunately the data set for July started from 22 July, so the quiet-day curve, does consist of a rather high amount of fluctuation due to the lack of data available. Thus the quiet-day curve was constructed from days of low VLF fluctuations before and after the period of seismicity. This was not ideal, however, the strong anomalous VLF deviations observed for this period, which were very similar to the other perturbations studied in the previous case study, compelled me to investigate as best I could. Even so, significant deviations in the VLF profiles were observed. Figures 2.11 and 2.13 show the VLF profiles for the period leading up to the earthquake on 25 July (black curve - quiet-day, red curve - diurnal VLF profile).

The general VLF diurnal trends were, an initial period that fluctuated around -40dB, from 00h00LT through to 03h00LT, followed by a sudden sharp drop in about an hour to around -50dB.

The morning hours were noticed to follow distinctive variations, namely, starting off at higher amplitudes than the quiet conditions and decreasing until the terminator time such as for 22, 23, 25 and 27 July, or decreasing to a local minimum of -41dB at 02h00 then rising back to the quiet amplitudes at the terminator time as for 24 July, July 28 followed the quiet conditions well.

From 04h00LT onwards the signals increased gradually until 20h00LT. The signals for 23, 24, 25 and 27 July showed very well defined unusual structures in their profiles. The profiles for 23 and 24 July did not immediately reach the quiet-day curve but rather fell to higher amplitudes, rose due to multimode interactions but then fell sharply by 10h00LT. July 27 has a similar smaller amplitude feature but at 14h30LT. It is a very similar structure to those seen at the end of August 2007, and could be the first perturbations in relation to the two earthquakes on 8 August 2007.

The step-down deviations observed on 23 and 24 July 2007 are very similar to that seen during 1 and 6 September 2007, see Figures 2.5 and 2.7. Figures 2.12 and 2.14 represent the difference in amplitudes between the current and quiet-day amplitudes. The dashed lines represent the standard deviations $2\sigma = 2.2$,$\sigma = 1.1$, -$\sigma = -1.1$, -$2\sigma = -2.2$. The two daytime drops recorded for 23 and 24 July have a dA magnitude of almost 3σ, thus considered significant variations.

On the day of the earthquake, 25 July, there is a deviation in the VLF profile during the afternoon and at 23h00LT. From 10h00LT to 18h00LT the signal deviated from the quiet amplitude of -53dB to a peak of -49 dB. This can be possibly attributed to the effect of the earthquake on the ionosphere as it occurred.

For the evening hours in a period of an hour the signals elevated back to higher amplitudes around -40dB. The late night amplitudes, 20h00–24h00LT, were observed to be higher than that before the terminator times. No dramatic deviations were observed in the VLF profiles, except for 22, 23, 24 and 26 July. Between 20h00 and 23h00LT each day showed an increase in amplitude, not seen in the other profiles. On 25 July the late night amplitudes are highly suppressed but again, it is possible that the direct effect of the earthquake may be the cause.

The dA plots for 22-25 July 2007, showing sharp deviations seen around both terminator times indicating slight terminator time shifts. Clear sharp amplitude drops for 24 and 25 July at similar times reaching a maximum $2\sigma = 2.05$. The overnight amplitudes were enhanced above 2σ for 22-23 July as well as 24-25 July.

The dA plots for 26-28 July 2007 show the difference in amplitudes rise above 2σ during nighttime between 26 and 27 July. There are terminator dA peaks seen for 28 July, again showing a temporal shift in the profile in relation to the quiet conditions.

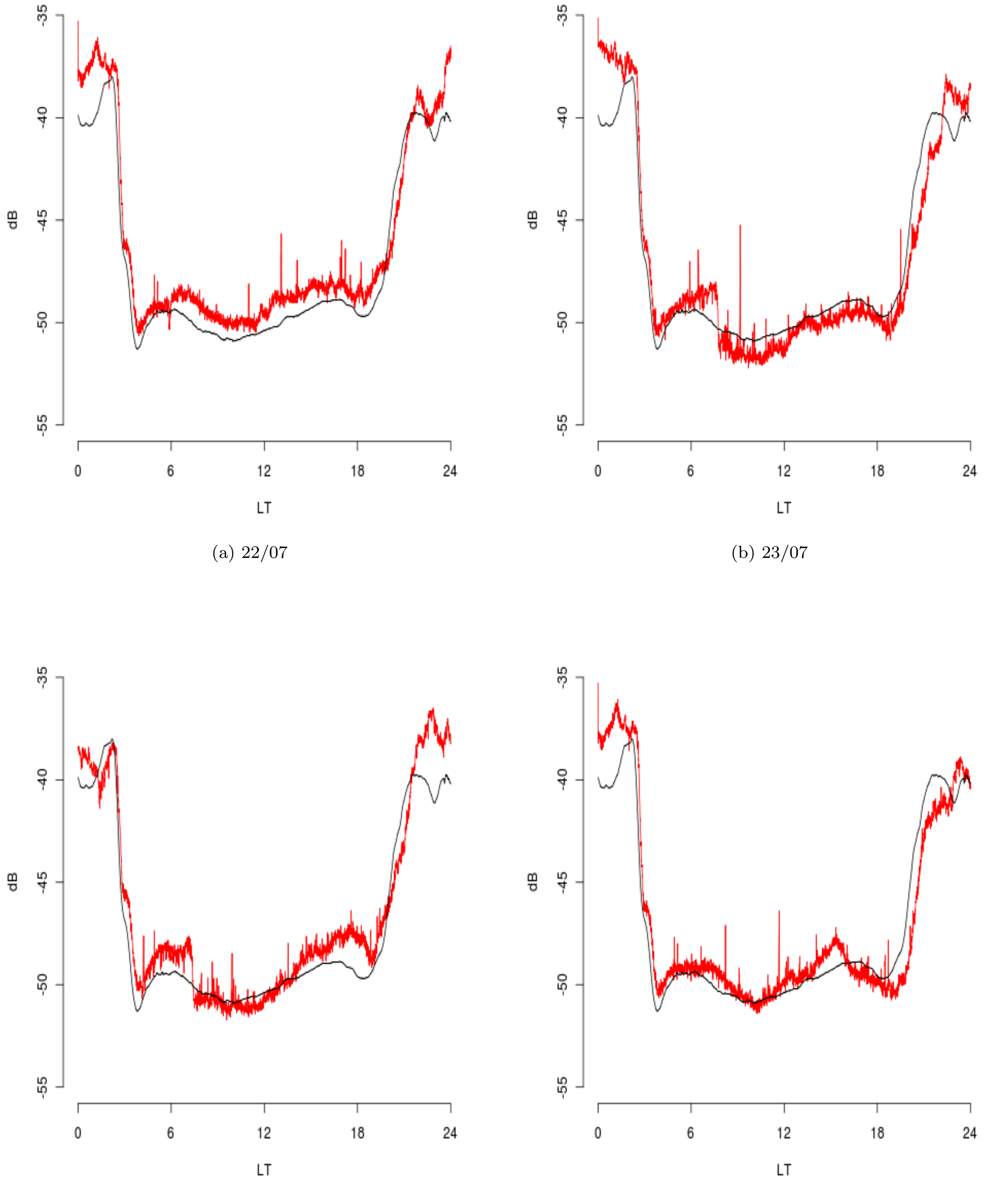

Figure 2.11: VLF signals observed on 22-25 July 2007 (red) compared to the quiet-day curve (black). Anomalous drops seen during daytime hours for 23 and 24 July 2007.

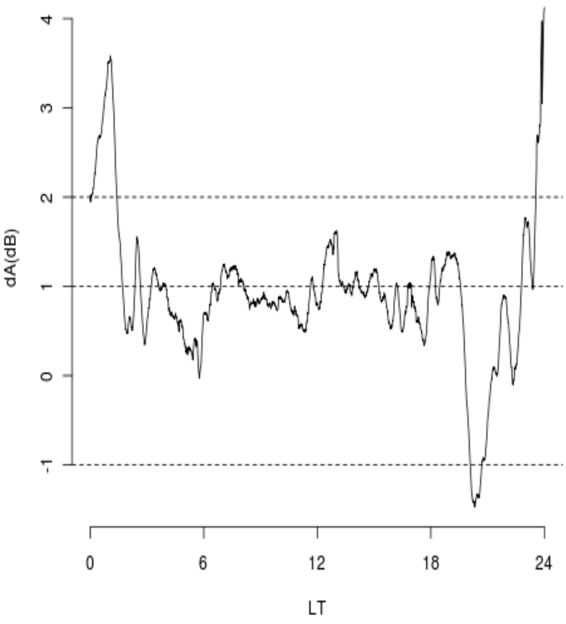

(a) 22/07

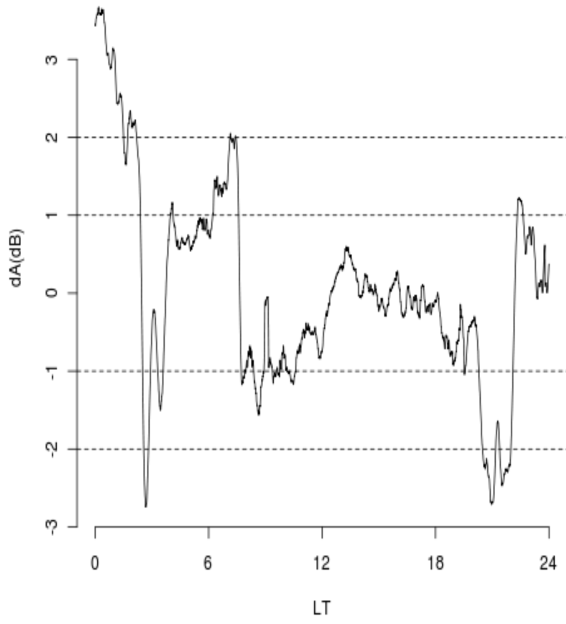

(b) 23/07

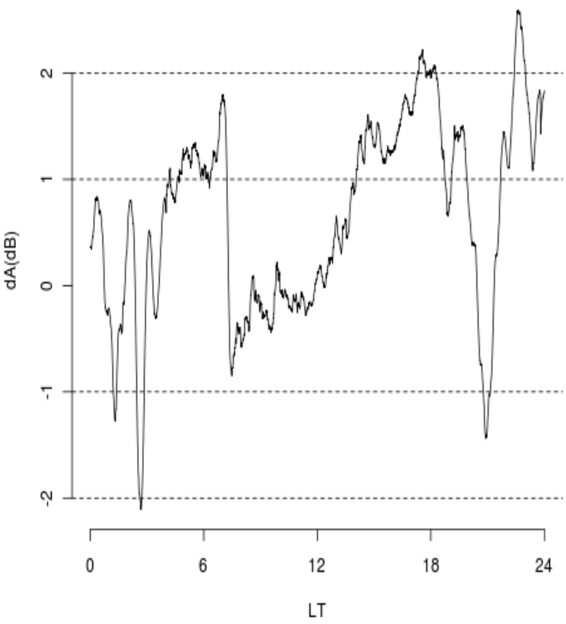

(c) 24/07

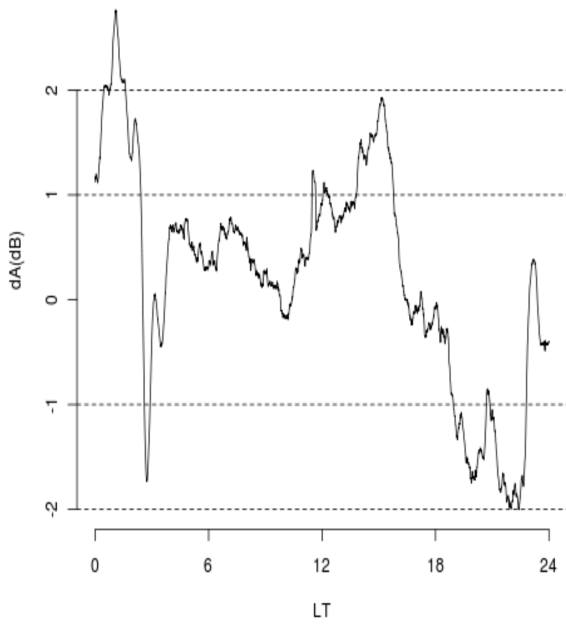

(d) 25/07

Figure 2.12: dA plots for 22-25 July 2007, showing sharp deviations seen around both terminator times. Overnight amplitudes enhanced above $2\sigma = 2.05$ for 22-23 July. Clear sharp amplitude drops for 24 and 25 July at similar times reaching a mniimum -$2\sigma = -2.05$.

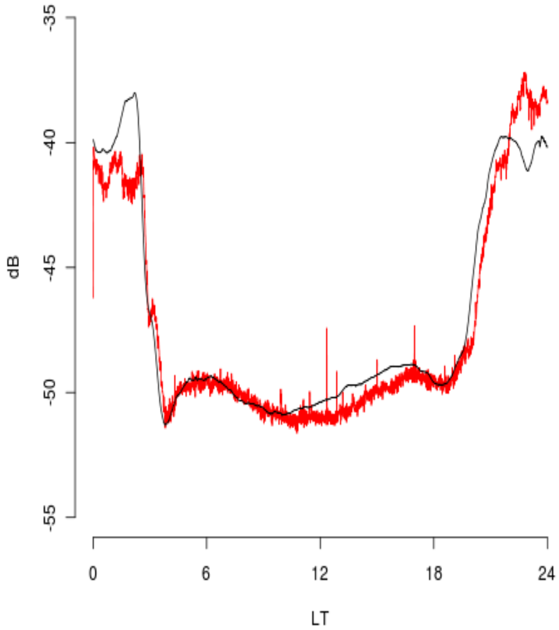

(a) 26/07

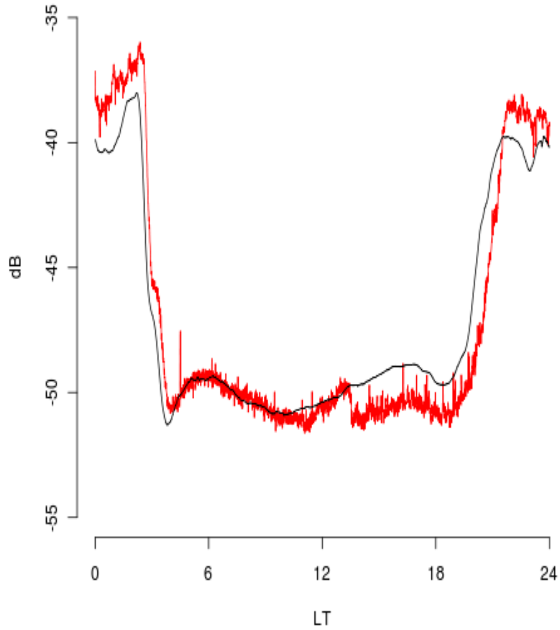

(b) 27/07

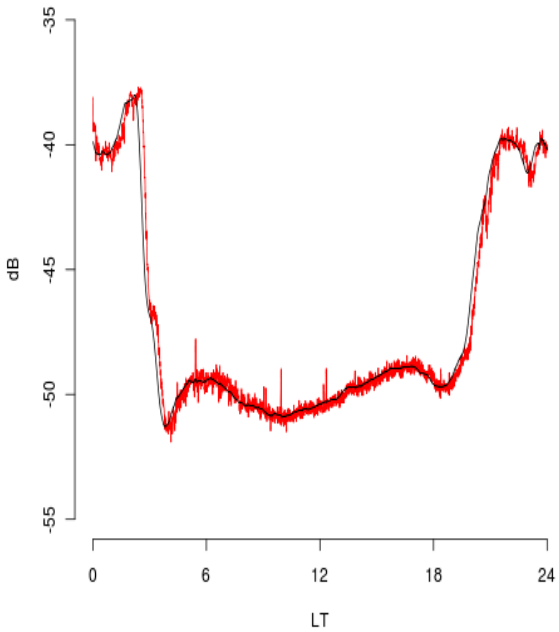

(c) 28/07

Figure 2.13: VLF signals observed on 26-28 July 2007 (red) compared to quiet-day curves (black). Relatively quiet period but small deviation similar to 23 and 24 July on 27 July, but at a later time (12h00LT).

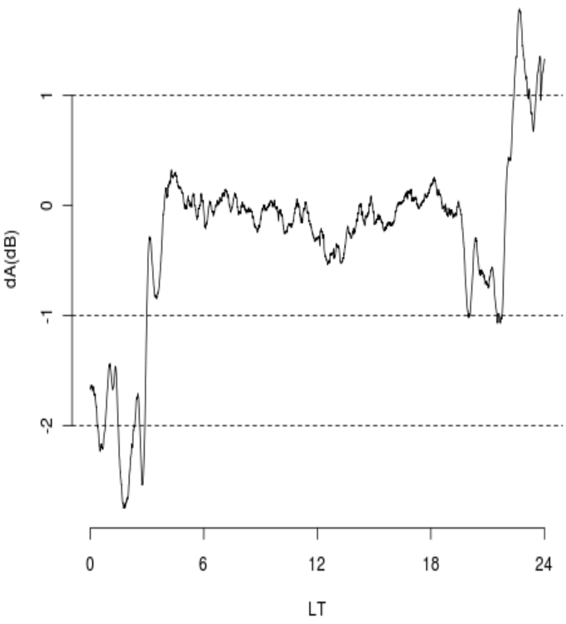

(a) 26/07

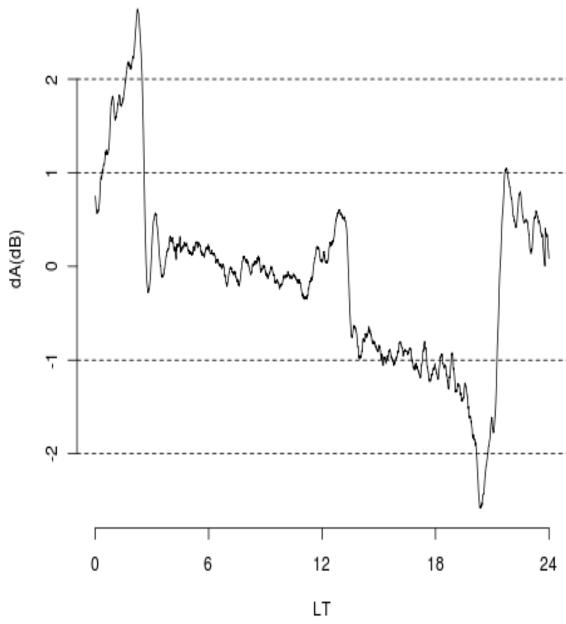

(b) 27/07

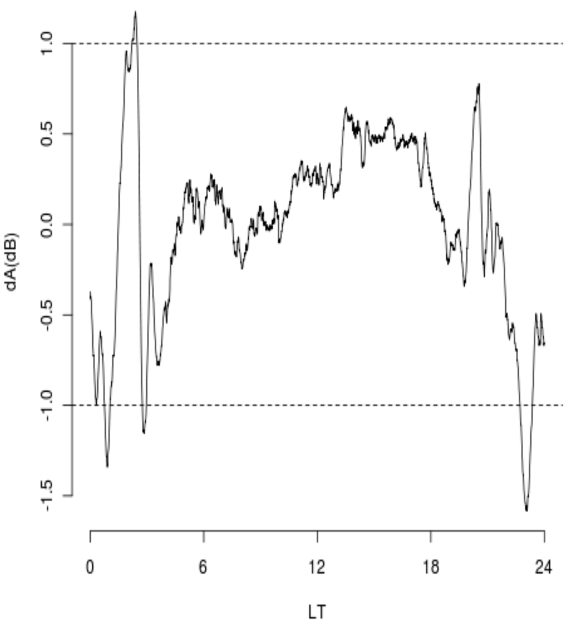

(c) 28/07

Figure 2.14: dA plots for 26-28 July 2007. Amplitudes rise above $2\sigma = 2.05$ during nighttime bewteen 26 and 27 July. Terminator dA peaks seen for 28 July.

Seismic activity

There was only one significant earthquake on July 25 of magnitude 6.1 located at 7.157°N, 92.518°E and a depth of 15km. These parameters fit within the boundary condition of 96km depth for an earthquake to be an ionospheric anomaly generating source [*Kasahara et al.*, 2010]. Anomalies were recorded for July 23, 24, 25 and 27. The VLF perturbations are discussed in detail in the previous section, shown in Figures 2.11 and 2.13 but to re-state, each anomaly day showed a sharp, well defined and short-lived drop either between 07h00 - 08h00LT as for July 23 and 24, or in the afternoon at 14h00 and 13h00LT for July 25 and 27 respectively.

Worth noting is that the former two drops occurred 1 and 2 days prior to the onset of the earthquake, whereas the latter two occurred on the day of and 2 days after the earthquake. The anomalous signal fluctuations for these two days have been explained as due to the direct effect of the earthquake and the seismic activity in the following month, respectively. This could explain the difference in the times of the presence of the anomalous drops.

Taking geomagnetic influences into consideration, the Dst index shows a series of minor events for July 09 - 20. ranging between 30 and -40nT, see Figure 2.16a. The ΣKp index reached 26 on 11 July,Figure 2.16c, indicating a possibly geomagnetic influenced day, but no anomaly was observed. Therefore, any substantial effect on the ionosphere caused by geomagnetic influences can be ruled out, making the perturbations recorded highly likely to be seismogenic.

The distribution of the observed VLF anomalies as well as the relevant seismic activity discussed are shown in 2.15. It would have been ideal to observe the VLF behaviour for atleast the full week preceding the earthquake on 25 July 2007, however, the anomalous deviations seen on the days leading up to the earthquake compare well to those seen prior to the earthquake swarm that commenced on 12 September 2007.

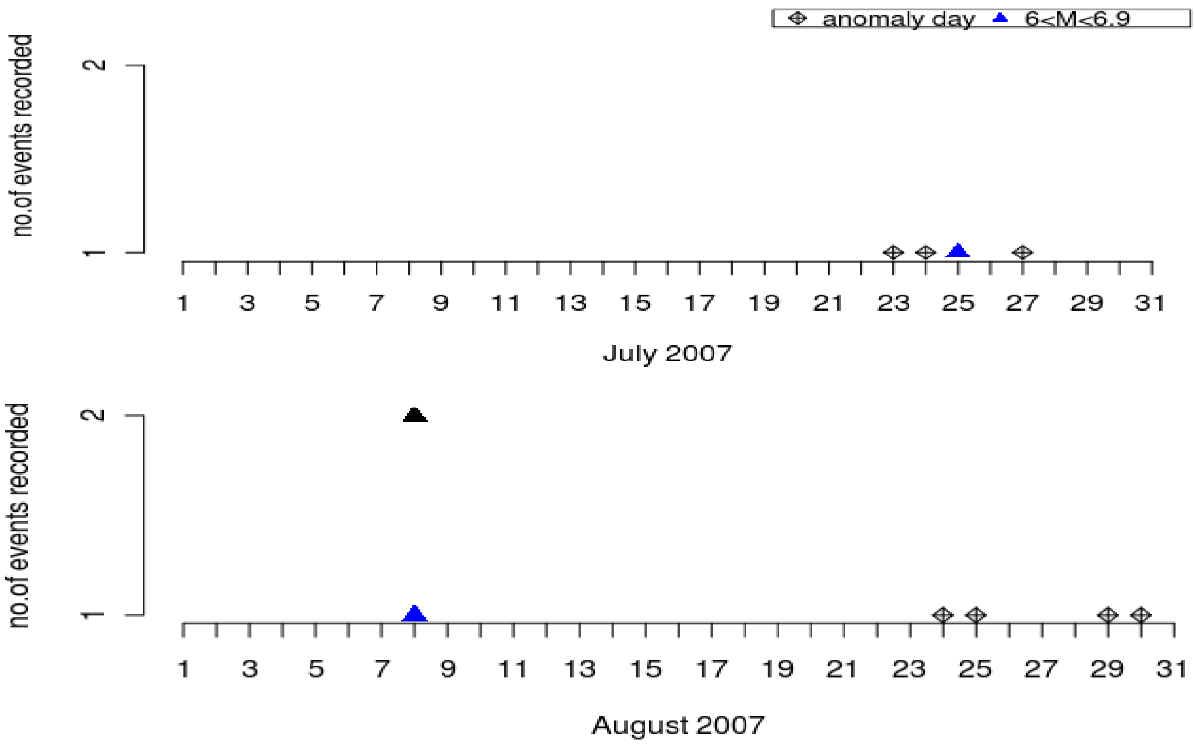

Figure 2.15: Temporal distribution of observed VLF anomalies (◇) in relation to seismic activity for end of July to August 2007 (triangles).

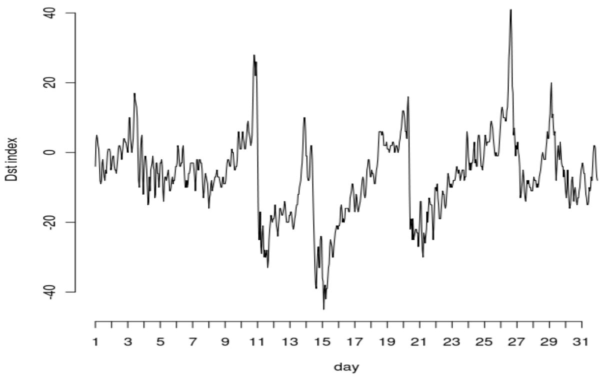

(a) July 2007

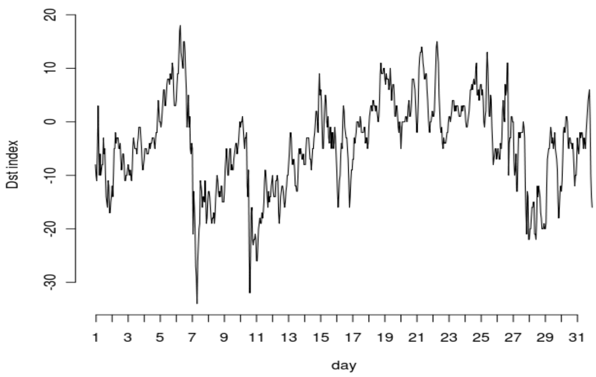

(b) August 2007

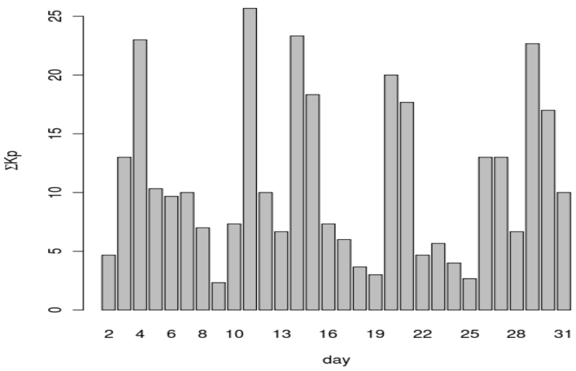

(c) July 2007

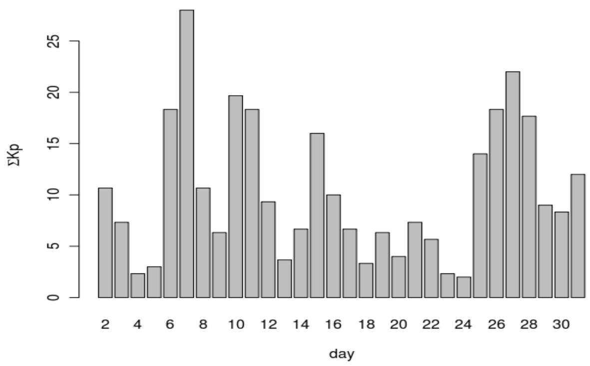

(d) August 2007

Figure 2.16: Dst and ΣKp indices for July and August 2007.

2.2.4 Case study 3: Nighttime anomalous signals recorded between 12–23 October 2007

A short period of seismic activity was observed from 19–25 October 2007. Six earthquakes occurred within a few geomagnetic degrees of each other with magnitudes reaching from a minimum of 5.5 to a maximum of 6.8. The largest earthquake occurred during 24 October at a depth of 21km.

Studying the VLF profiles for October 2007 a period of anomalous latenight deviations was observed from 12–23 October 2007. These VLF profiles can be seen in Figures 2.17, 2.19 and 2.21. The corresponding dA plots are shown in Figures 2.18, 2.20 and 2.22. The standard deviation for this set of data is $\sigma = 0.75$. Perturbations exceding 2σ or -2σ are considered anomalous. However, large perturbations around the terminator times, just before 06h00 and 18h00LT, are considered as terminator shifts.

Latenight sharp drops in amplitude are seen for 12–14 October, Figure 2.17. There are large fluctuations during the morning hours for each day, however, the latenight drops are far mor structured and of similar shape. They are step-down perturbations. The profiles for 12 and 14 have similar features in the evening. An initial large drop at around 19h00LT is then followed by another a few hours later. The profiles for 13 and 16 have the second drop missing. The dA plots for these days, seen in Figure 2.18, show large terminator drops before 18h00LT. These indicate terminator shifts in the profiles. However, after 18h00LT, the deviations have magnitudes that range from a maximum above 2σ (13–16/10) to a minimum well below -2σ (12 and 13/10). These deviations were observed in the period leading up to the period of seimicity that started on 19 October 2007.

Figure 2.19 shows the VLF profiles for 17–21 October 2007. Quiet conditions are seen to have prevailed for 17 and 21 October. For 19 and 20 October there were very distinctive deviations observed both commencing between 19h00 and 23h00LT. A Depression in the amplitudes is seen for 19 October, whereas, a sharp drop in the amplitude is seen for 20 October. The magnitudes of these drops are evident in their dA plots, Figure 2.20. As can be seen, the diurnal dA values for 17 and 21 October fluctuated between 2σ and -2σ. Thus no significant perturbations were present. The morning of 19 and 20 October fell below -2σ, as did the values during the evenings between 19h00 and 23h00LT.

The VLF profiles for the final two days of anomalous VLF perturbations for this case study are seen in Figure 2.21. The profile for 22 October is seen to have a sharp latenight amplitude increase after 22h00LT. The morning hours for 23 October show a sudden rise and fall in the amplitudes around 03h00LT. The rest of the day fluctuates below the queit-day curve except for a rise around local noon. The dA plots, Figure 2.22 show terminator shifts just before 06h00Lt, but also two large increases above $2\sigma = 1.5$ a few hours before. The latenight amplitudes fluctuate below -2σ, with the distinctive lower peak for 22 October observed just before 23h00LT.

It was observed that on the days of earthquakes (19, 21 and 23/10) there were only major fluctuations in the signal for 19 October. It may be possible that the other earthquakes in this period were overshadowed by the earthquake during 24 October 2007. This earthquake occurred at the shallowest depth of 21km and was by far the strongest with $M = 6.8$ compared to the next srongest of $M = 5.8$ the day before. The earthquake on 23 October could explain the highly depressed amplitudes seen throughout the day.

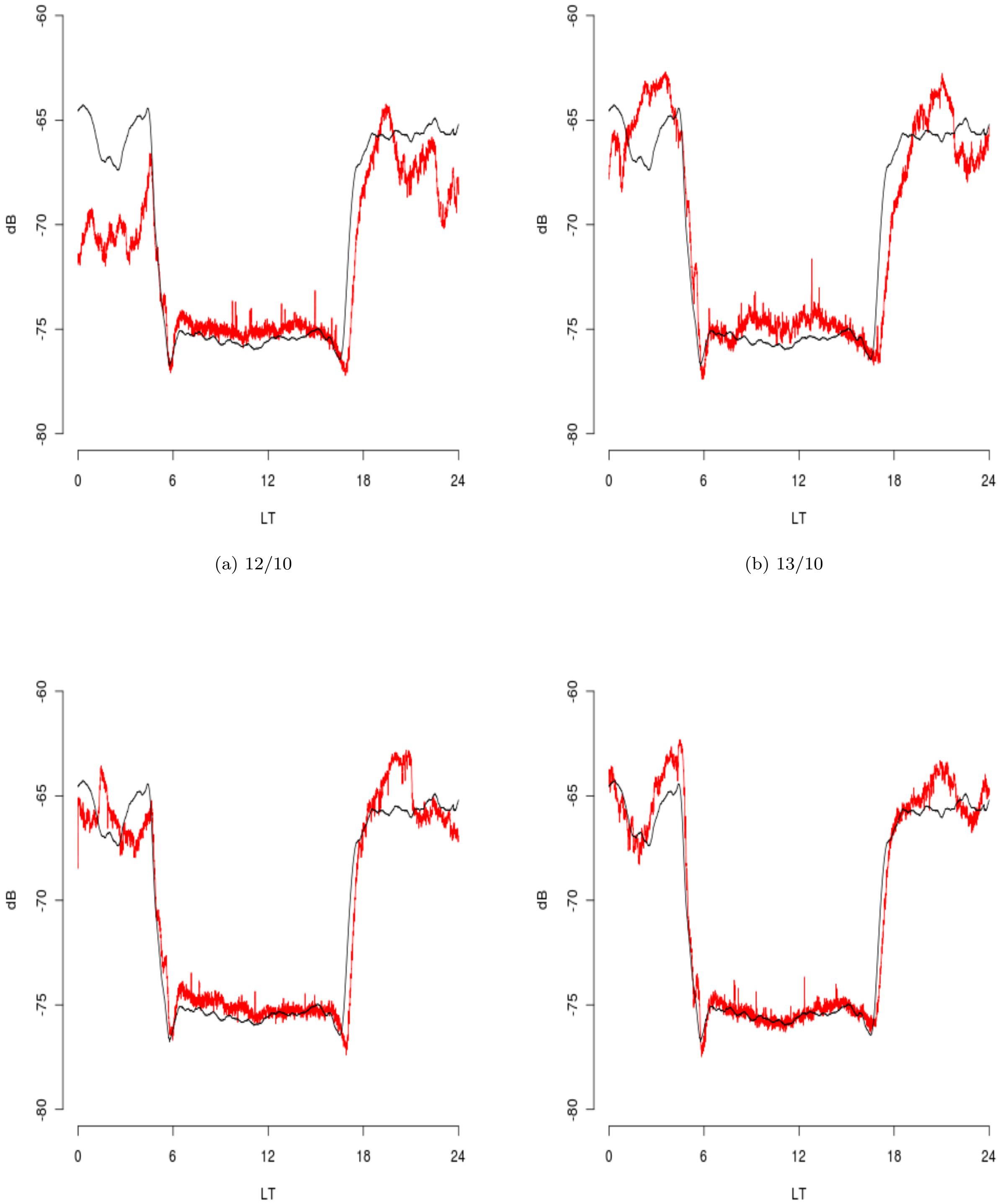

(a) 12/10

(b) 13/10

(c) 14/10

(d) 16/10

Figure 2.17: Anomalous nighttime VLF step-like perturbations (red) above the quiet-day curve (black) for 12–16 October 2007, with the well defined step-like perturbations seen in the late hours.

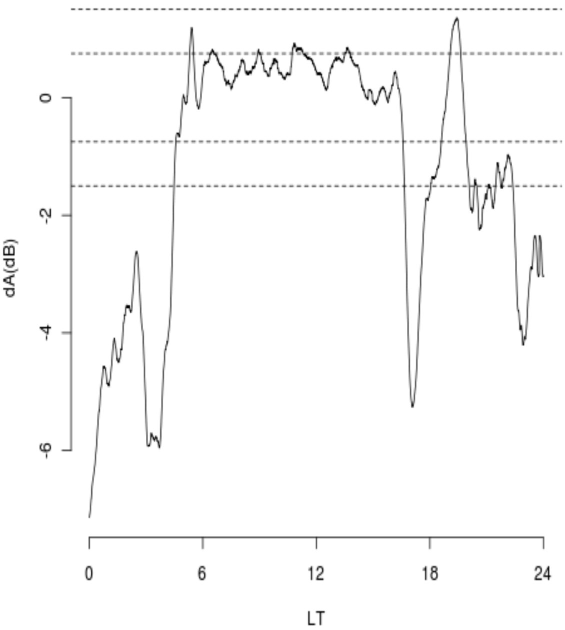

(a) 12/10

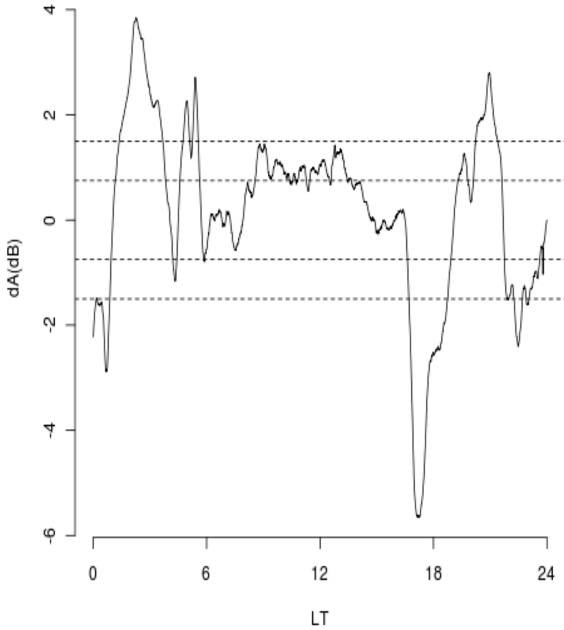

(b) 13/10

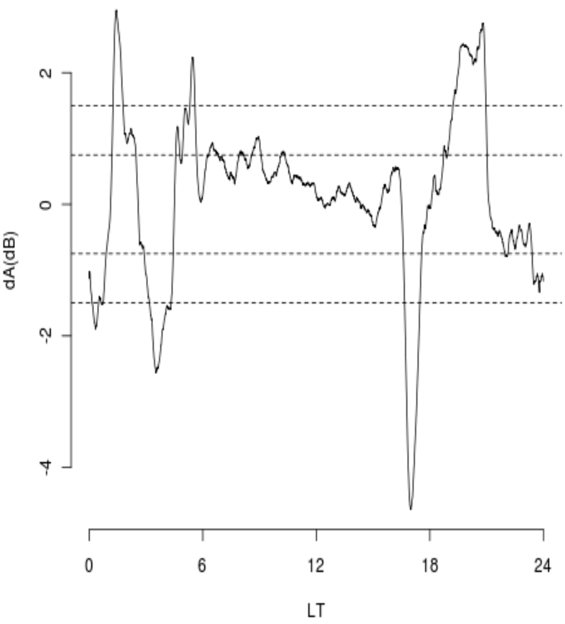

(c) 14/10

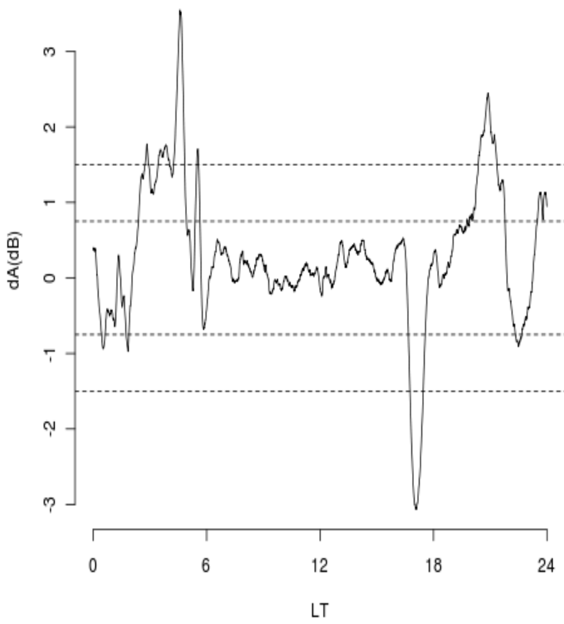

(d) 16/10

Figure 2.18: dA plots for 12–16 October 2007. Large deviations below $-2\sigma = -1.5$ seen at terminator times indicating terminator shifts. with large daytime deviations seen from 20h00LT near and below $2\sigma = 1.5$ and -2σ, respectively.

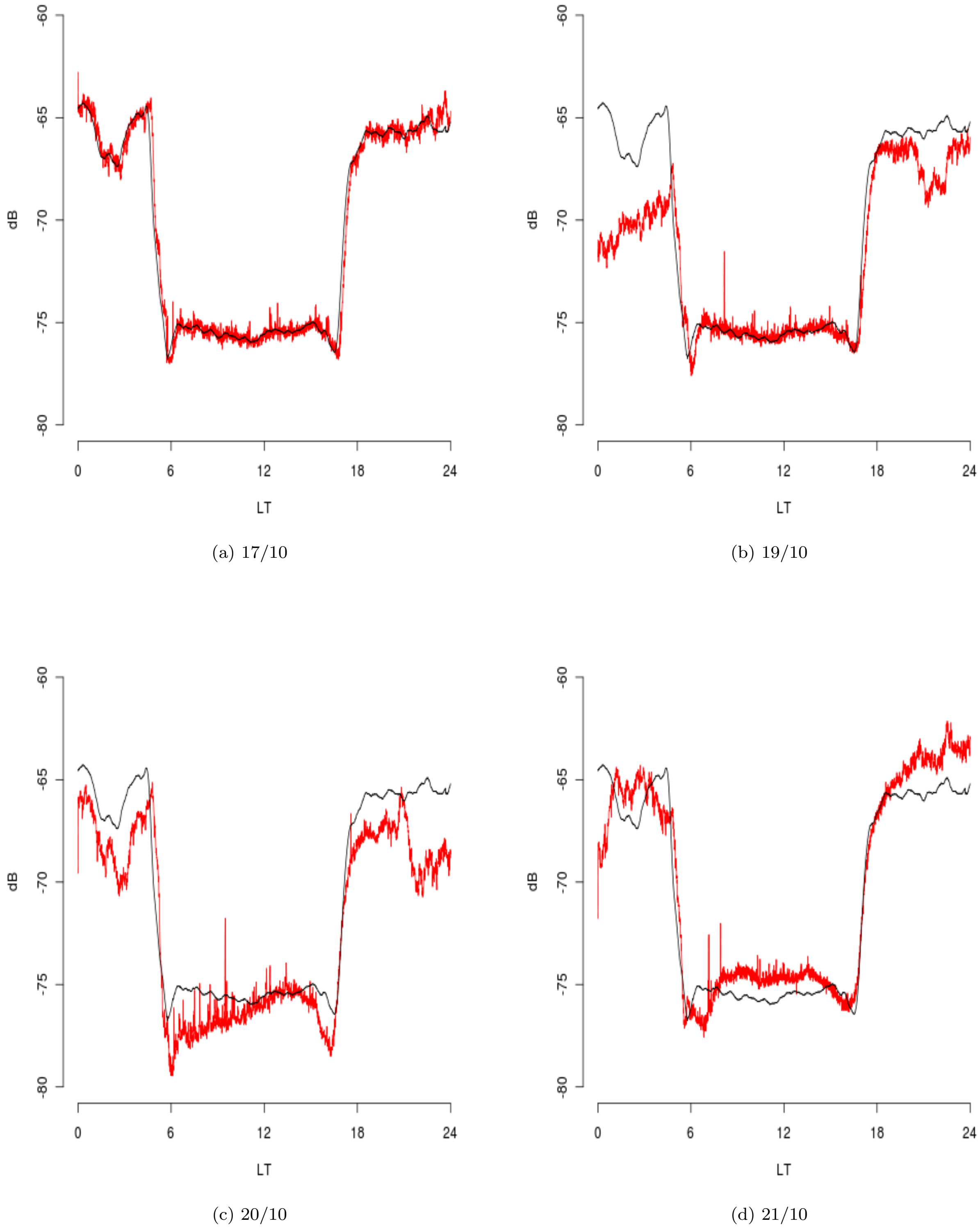

(a) 17/10

(b) 19/10

(c) 20/10

(d) 21/10

Figure 2.19: Anomalous VLF step-like perturbations (red) observed for 17–21 October 2007, with well defined step-like perturbations seen during the late hours for 19 and 20 October.

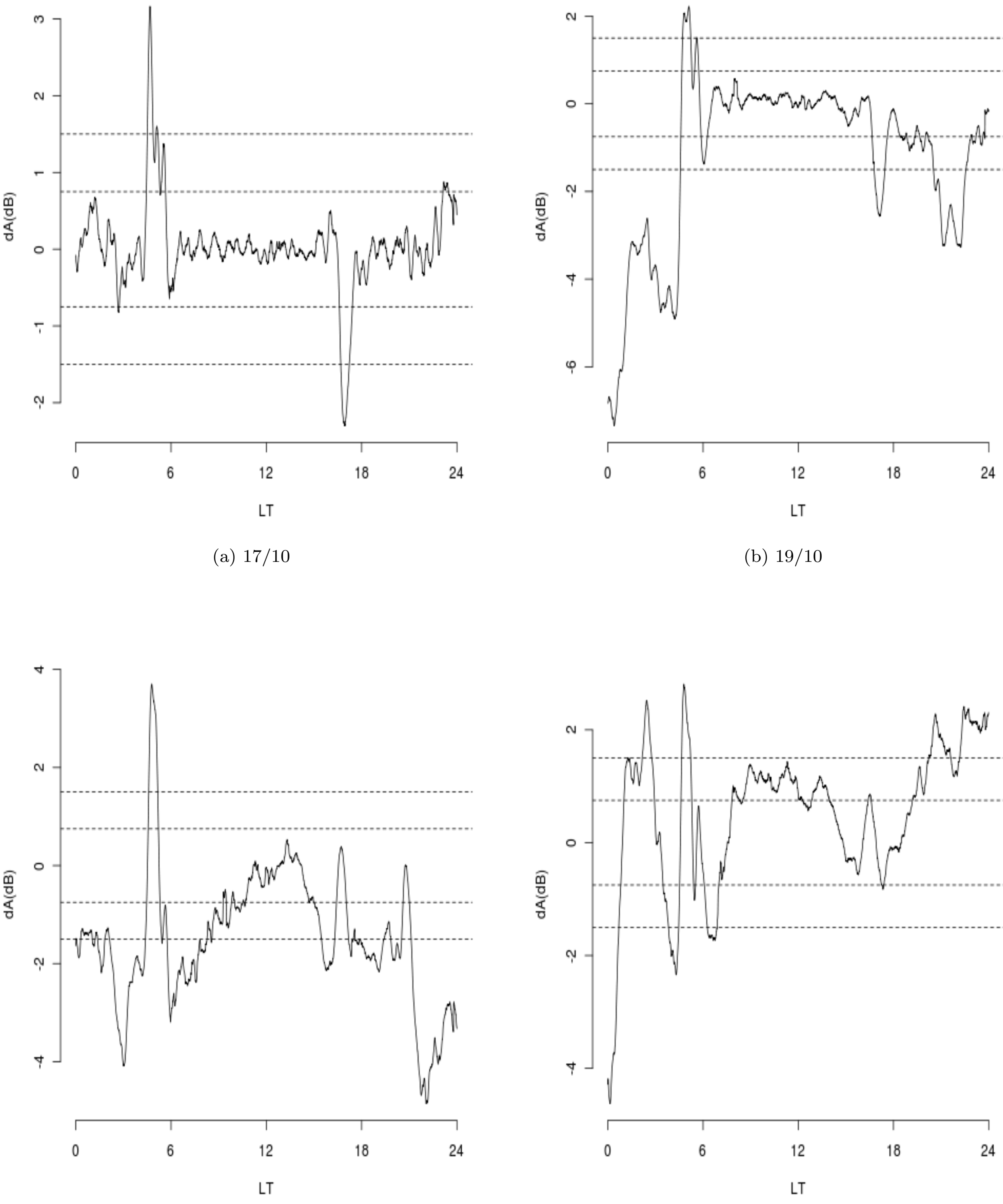

(a) 17/10

(b) 19/10

(c) 20/10

(d) 21/10

Figure 2.20: dA plots for 17–21 October 2007. Large deviations above $2\sigma = 1.5$ seen for all four days showing terminator shifts. Deviations below $-2\sigma = -1.5$ seen only during evening hours for 19 and 20 October.

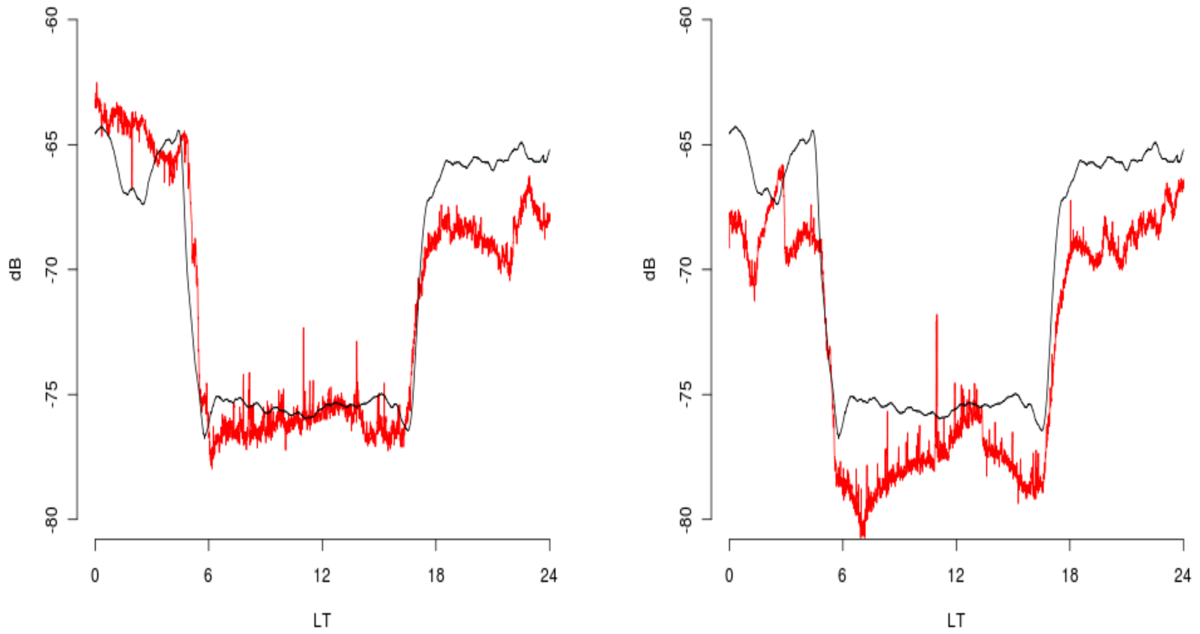

(a) 22/10

(b) 23/10

Figure 2.21: VLF profiles (red) for 22 and 23 October 2007, Large nighttime anomalous behaviour seen for overnight period.

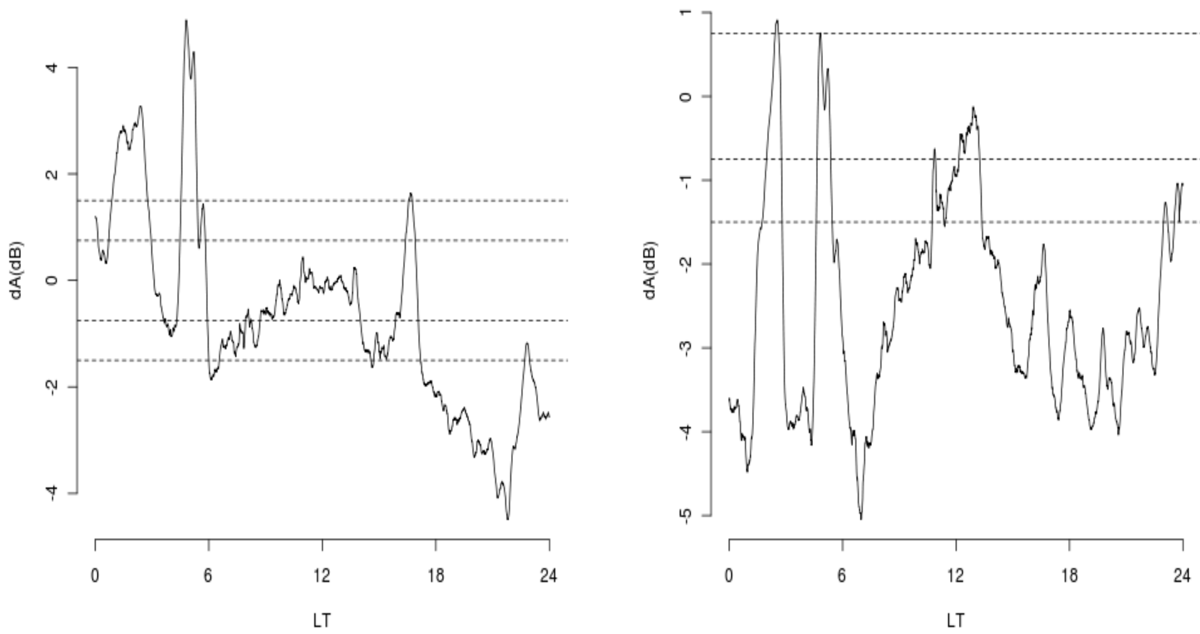

(a) 22/10

(b) 23/10

Figure 2.22: dA plots for 22 and 23 October 2007. Large deviations above $2\sigma = 1.5$ seen before morning terminator times. Deviations below $-2\sigma = -1.5$ seen during latenight hours for both days.

Possible associated seismic activity

The seismic activity for this case study occurred during 19–25 October 2007. There were six earthquakes that occurred within the Dobrovolsky area so as to be considered as possibly anomaly causative. The earthquake days were 19, 21, 23, 24 and 25 October. Four were of $M = 5.5 - 5.6$, but the two that occurred on 23 and 24 October were $M = 5.8$ and 6.8, respectively. These occurred at relatively shallow depths of 30 and 21km respectively. The details of these earthquakes are summarised in Table 2.1 and are plotted in Figure 2.2.

Comparing the VLF anomaly days to the seismic activity, it is clearly seen, from Figure 2.23 that the anomaly dys appear from seven days prior to the onset of the earthquakes occurrences. In general the days of anomaly apperance did not overlap with that of an earthquake day. However, it is seen that there are two days, 19 and 23 October, that counter this statement. When looking at the actual form of the anomalies in Figures 2.19 and 2.21, respectively it is seen that they have very different anomlaous deviations as opposed to the other days. This could be in part to the effect of the earthquake on the day that may be directly effecting the ionosphere. The rest of the anomalies are seen to be of the sam form, a step-down perturbation during the latenight hours. The anomalies do not appear after 23 October 2007. Thus it may be reasonable to assume that the shallowest, strongest earthquake on 24 October may be the prime genrator of the ionospheric anomalies.

Looking at the geomagnetic influences expressed by the Dst and ΣKp indices, Figure 2.24, it is seen that there was a large geomagnetic storm that occurred on 25 October, where the Dst index fell to a minimum of -50nT and the ΣKp index reached a maximum of 22 during 25–27 October. It was becuase of these parameters that indicate a geomagnetic storm imposing on The Earth that the VLF profiles for these days were not studied, as the data would have a good chance of being biased by the geomagnetic storm. In this way the anomaly day on 19 October can be ruled out as the ΣKp index peaks on this day close to 25. The days at the beginning of the anomlay period are seen to fall within a geomagnetically very quiet period. Thus these anomaly days can at least be possibly concluded to have been in association with the seismic activity discussed.

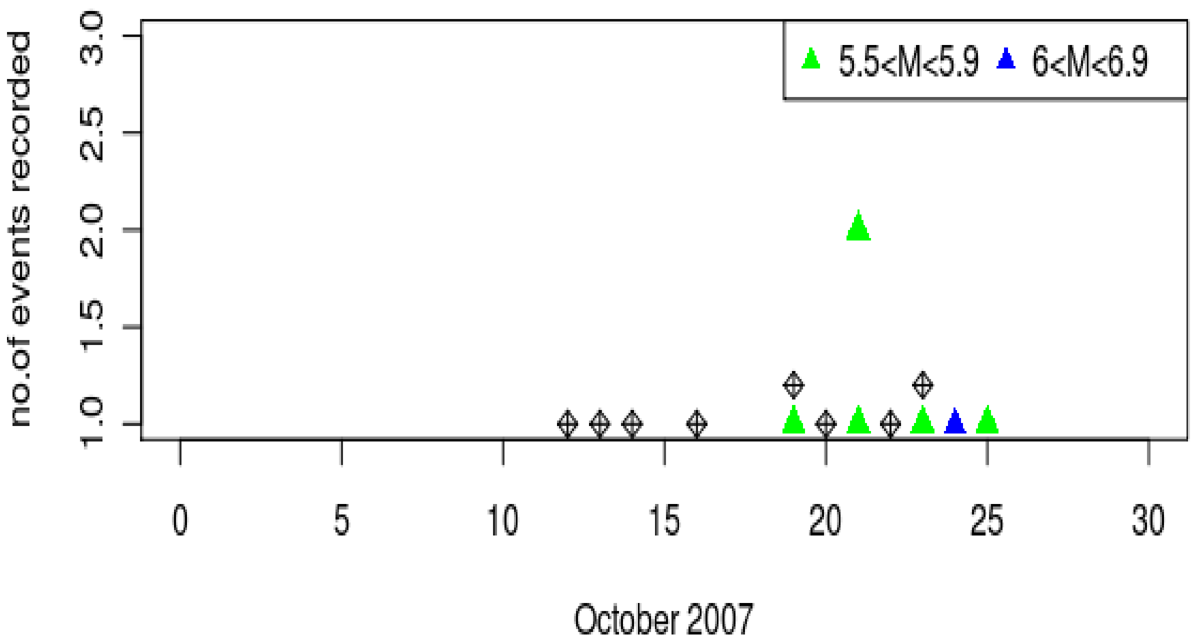

Figure 2.23: Temporal distribution of observed VLF anomalies (◇) in relation to seismic activity for October 2007(triangles). VLF anomaly period seen to lead earthquake days by 7 days, then occuring on days with no earthquake activity, except for 19 and 23 October, which were seen of different forms compared to the other anomalies.

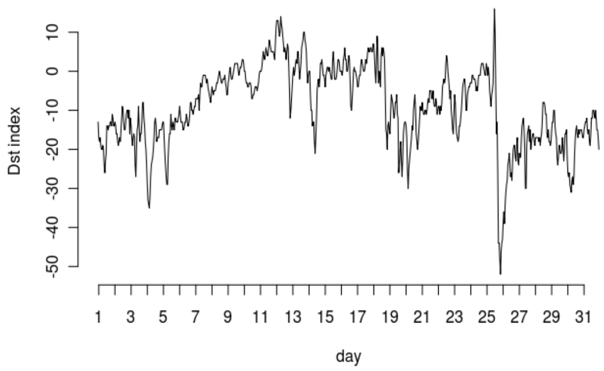

(a) Dst

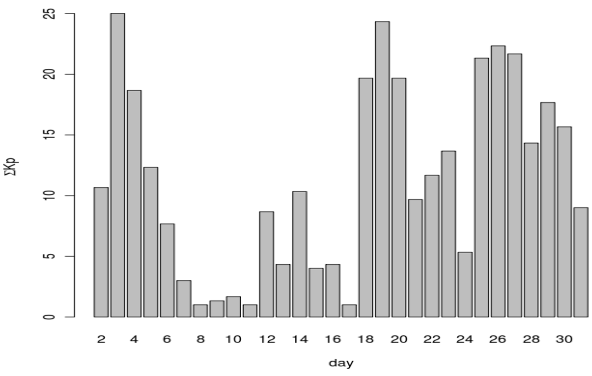

(b) ΣKp

Figure 2.24: Dst and ΣKp indices for October 2007.

2.2.5 Case study 4: Nighttime anomalous signals recorded between 20–26 December 2007

There were seven days in December 2007 with deviations from the corresponding quiet-day curve over the perturbed period, as shown in Figures 2.25 and 2.27.

The quiet-day curve is described by a constant amplitude of -67dB from 00h00 to 06h00LT, then falling to -85dB at 08h00LT, rising to a mid-day peak of -77dB at 12h00, before decreasing again to -75dB at 15h00LT. Then steadily increasing to -67dB by 18h00LT and staying level till 24h00LT. The anomlous signals for December 2007 were observed as sharp rises in the signal rcorded during the late night hours from 19h00LT to 24h00LT.

There were five consecutive days, 21 - 25 December, toward the end of the month that showed step-like deviations from the quiet conditions during the mid-day and late night periods.

The standard deviations for the December dA plots are $2\sigma = 2$,$\sigma = 1$, -$\sigma = -1$, -$2\sigma = -2$. From 00h00 to 06h00LT on the first three days the signals started and persisted below, until meeting the quiet-day curve at or just before 06h00LT. Thereafter the signals show very different behaviours. Between 11h00 and 12h00LT there was a step-down in the signal amplitude for December 21, then followed by a steady decrease far below -σ by 16h00LT.

The signal on 22 December showed a large enhancement in the daytime amplitudes between terminators for the same respective time period as for the step-down perturbations on 21 December. Both days are shown to have terminator drops at the same time in their respective dA plots in Figure 2.26. Step-up perturbations occurred during the evening hours after 18h00LT for 23, 24 and 25 December. The step-up deviation was observed for 23 December between 19h00 and 20h00LT. This deviations had values of 4σ.

November 25 showed an enhancement of the daytime signal above the quiet-day curve between 08h00 and 15h00LT, with a peak of -78dB at 12h00LT. The 26 December showed no significant fluctuations, except an extended suppressed period around -72 to -73dB from 17h00 to 24h00LT.

It should be noticed that the quiet-day curves for 26, 27 and 28 December are different to the quiet-day curve used for the earlier dates in December. This is due to the observation that there seemed to be a seasonal change in the VLF profiles, that began on 26 December, hence a new quiet-day curve had to be constructed for dates from 24 December onward to keep the comparisons realistic.

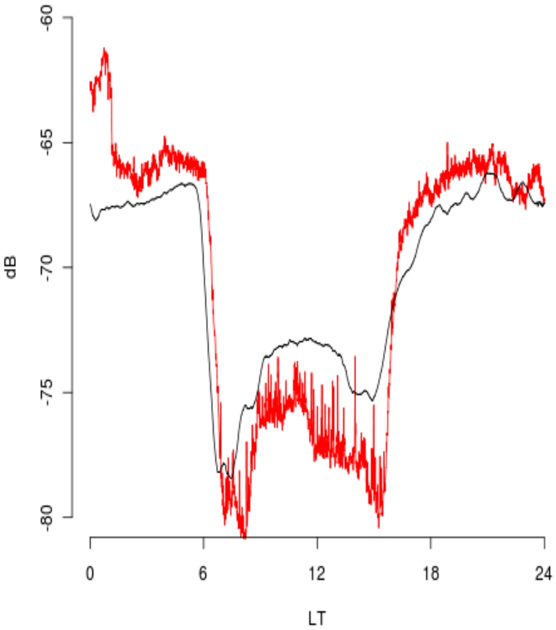

(a) 21/12

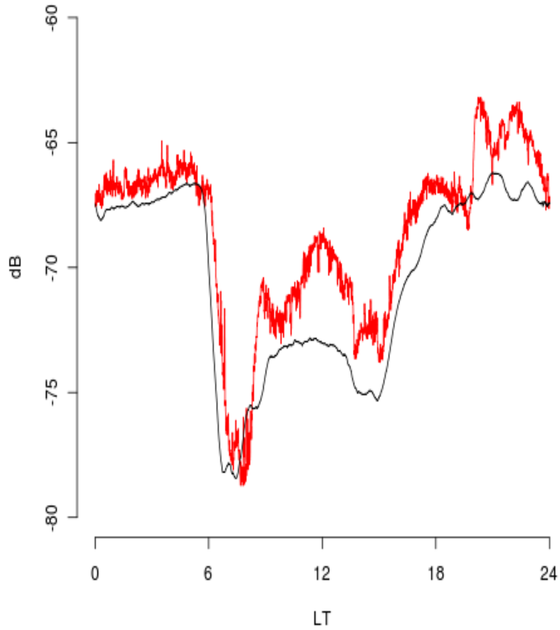

(b) 22/12

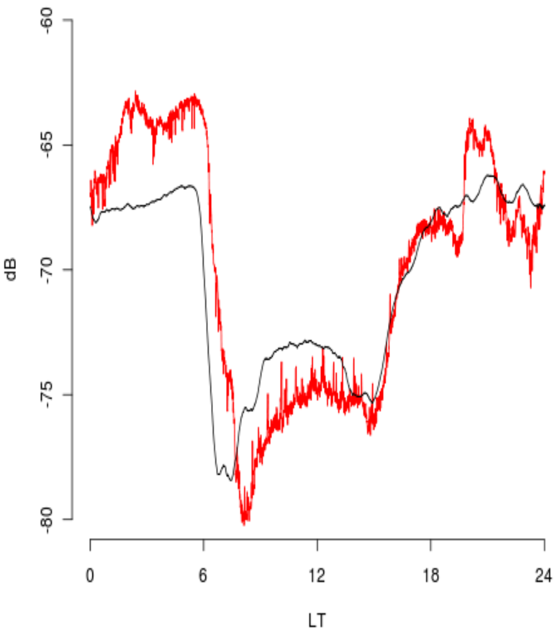

(c) 23/12

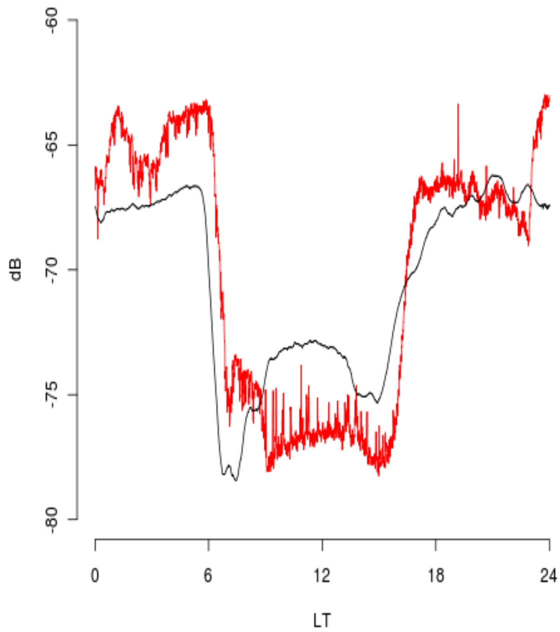

(d) 24/12

Figure 2.25: Anomalous VLF step-like perturbations and enahncements (red) above the quiet-day curve (black) for 21 - 24 December 2007, with the well defined step-like perturbations seen in the late hours, and enhancements during the daytime hours.

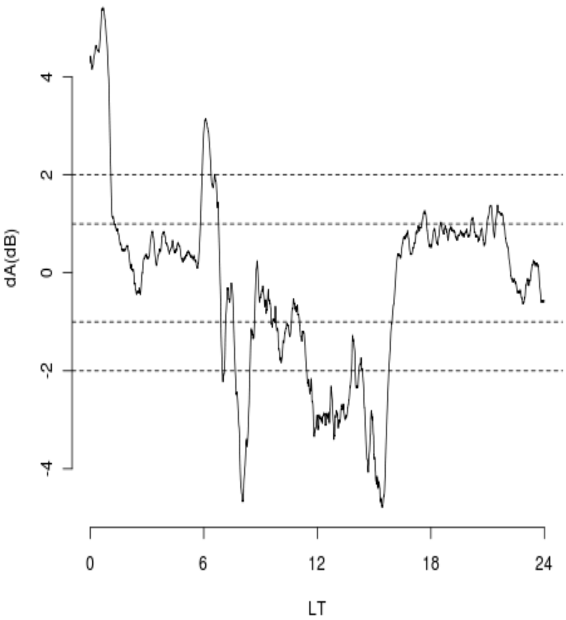

(a) 21/12

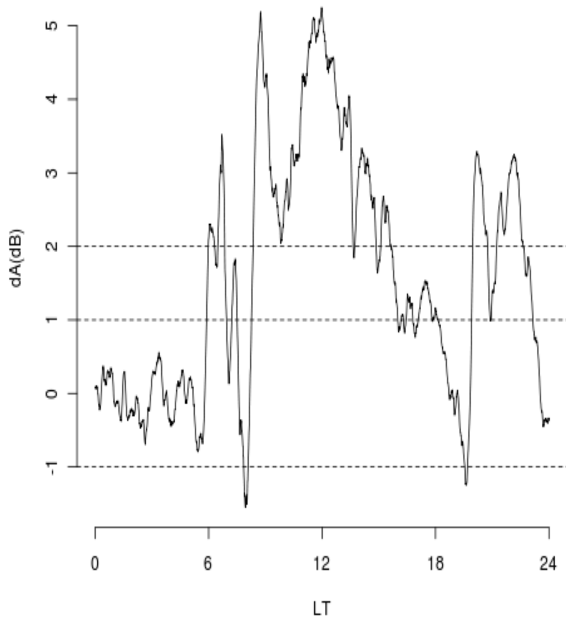

(b) 22/12

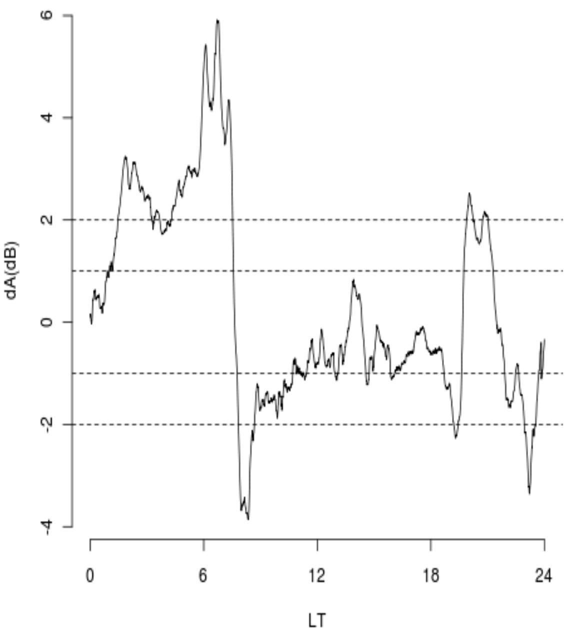

(c) 23/12

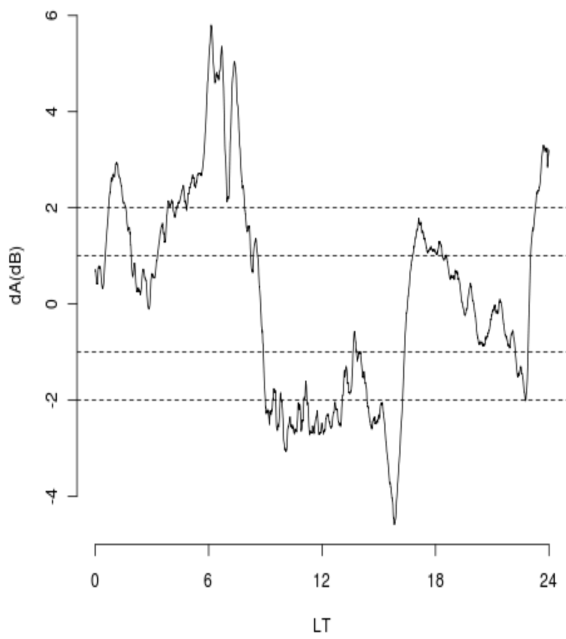

(d) 24/12

Figure 2.26: dA plots for 21- 24 December 2007. Large deviations above $2\sigma = 2$ seen before morning terminator time. Deviations below -$\sigma_2 = -2$ seen only for evening terminator. with large daytime deviations seen for 21 and 22 December 2007 below and above -$2\sigma = 2$ and $2\sigma = -2$, respectively.

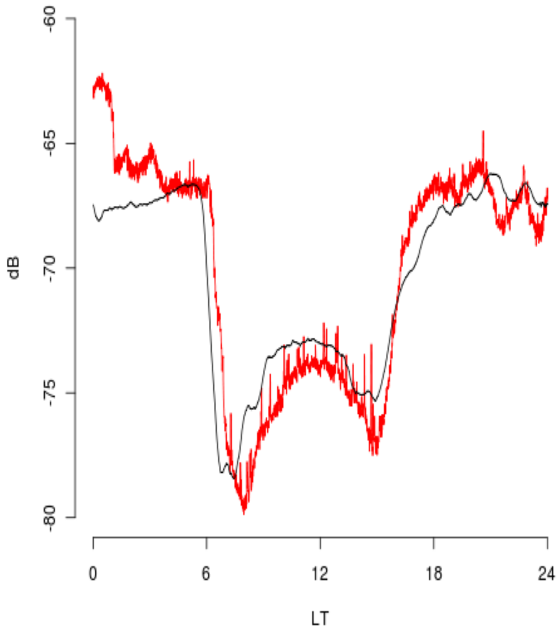

(a) 25/12

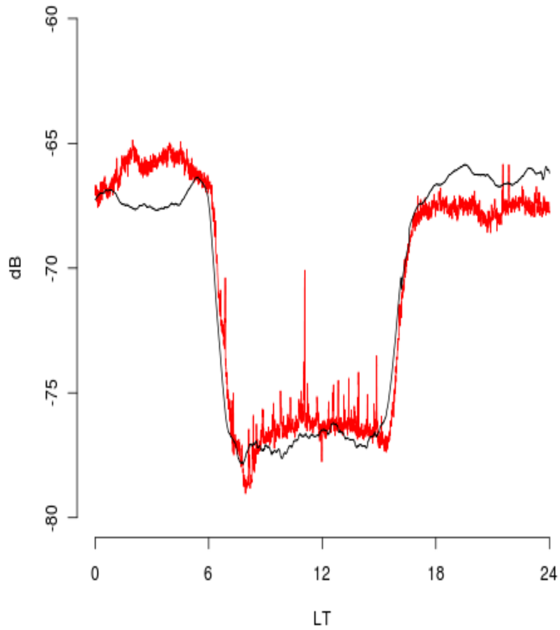

(b) 26/12

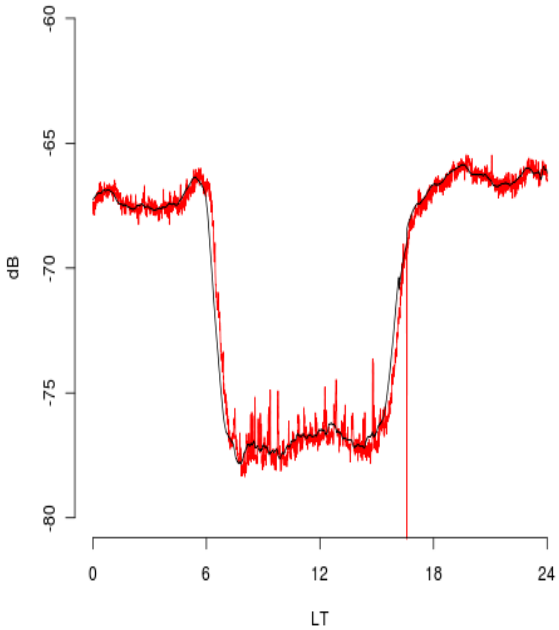

(c) 27/12

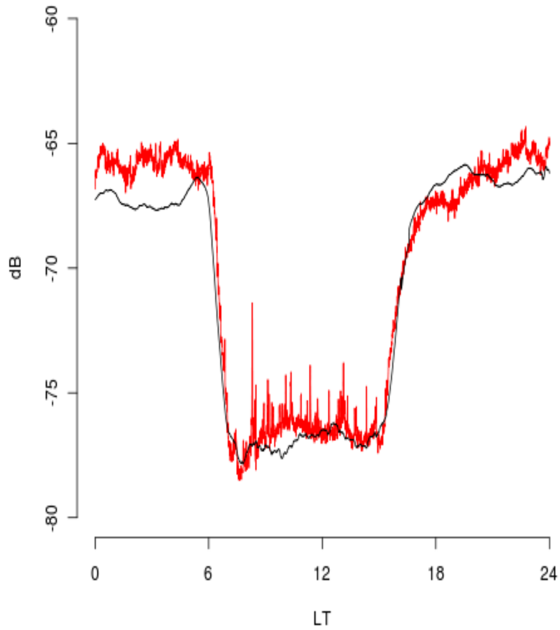

(d) 28/12

Figure 2.27: VLF profiles for 25-26 December 2007 (red), showing relatively quiet period after highly perturbed period seen for 21-24 December 2007.

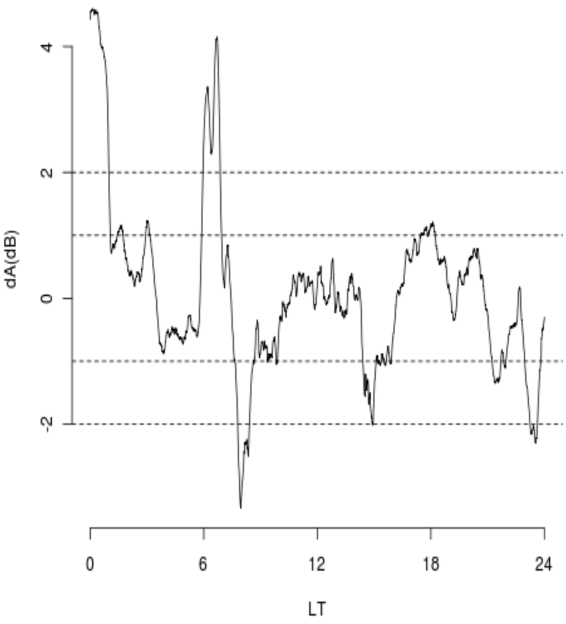

(a) 25/12

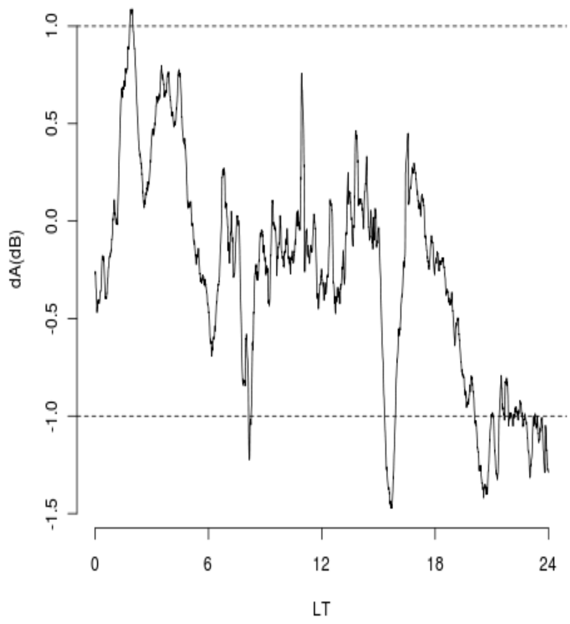

(b) 26/12

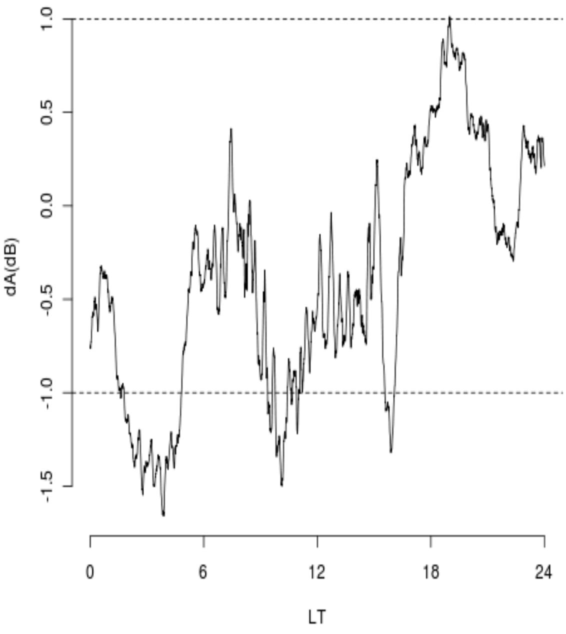

(c) 27/12

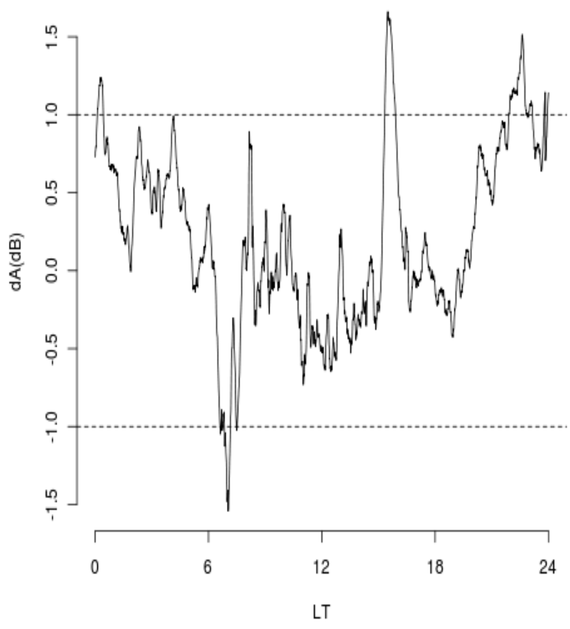

(d) 28/12

Figure 2.28: dA plots for 25-28 December 2007. Only 25/12 profile deviates above $2\sigma = 2$, whereas the other days fluctuate within the standard deviation, 1.5σ to -1.5σ.

Possible associated seismic activity

The seismic activity for December 2007 was very sparse. Three possibly causative earthquakes occurred on 20, 22 and 26 December, with magnitudes 5.7, 6.1 and 5.6 respectively. These can be seen in the December 2007 panel in Figure 2.15. The epicentre of the earthquakes were located at depths of 10km, 23km and 8km, respectively. Individually the epicentres would be too far from the porpagation path to have a good chance of causing any disturbance, based on the Dobrovolsky formula. But because they occured in an area of high seismicity in a very concentrated period, it is possible that the earthquakes could effect signals traversing along the propagation path.

The shallow depths of the epicentres may be the most decisive factor. This may be the case for the earthquakes on 20 and 26 December. Their epicentres occurred at very shallow depths of 10km and 8km respectively. However, the epicentres were located at 39.417°N 33.212°E and 39.446°N 33.162°E, as can be seen in Figure 2.2. An anomalous decrease was recorded for 21 December 2007, one day prior to a magnitude 6.1 earthquake with an epicentral depth of 23km. On the day of the earthquake, the VLF signals were enhanced, almost showing an opposite behaviour to the day before. This could be highly likely due to the influence of the power of the earthquake on the day. But from that day on until 24 December a rapid increase was observed in the late nighttime periods. These step-up deviations persisted, appearring at later times each night until 25 December, where much less but still evident fluctuations occurred around the same time of night.

The anomalous behaviour for 25 December was predominantly an enhancement during the daytime hours above the quiet-day curve. The day after, 26 December, a magnitude 5.6 earthquake occurred at a depth of just 8km. After the range of anomalous days 21 to 25 December 2007 no other earthquakes occurred within reasonable distance, governed by the Dobrovolsky formula, to the propagation path until 4 January 2008.

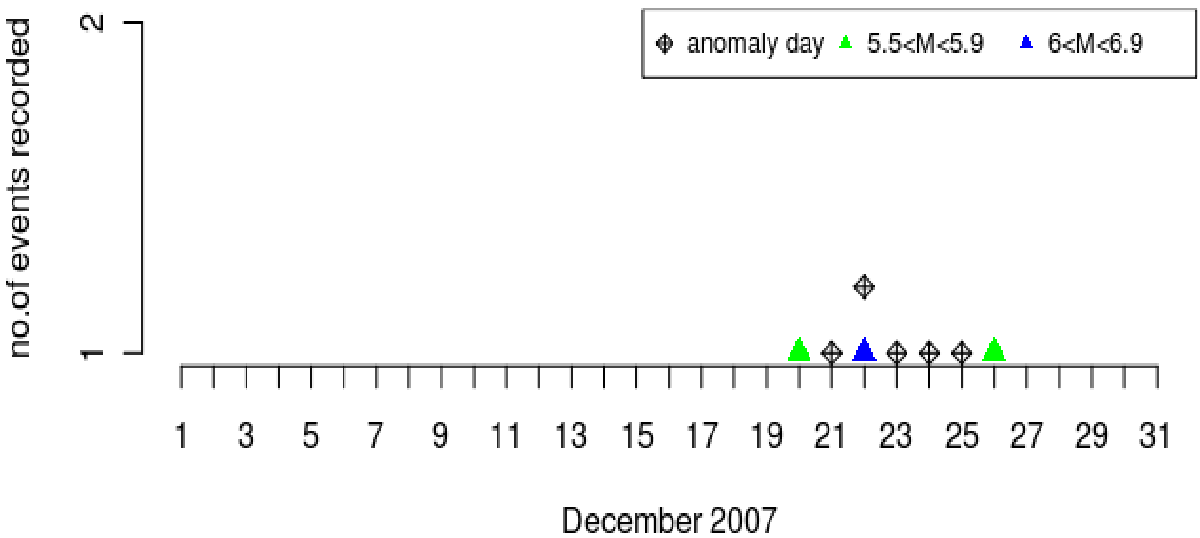

Figure 2.29: Temporal distribution of observed VLF anomalies (♢) in relation to seismic activity for December 2007 and January 2008 (triangles)

Checking for any geomagnetic influences that may bias the anomaly days, the Dst index recorded a strong geomagnetic storm, Figure 2.30a for 16 to 18 December, confirmed by the ΣKp index, where the indices reach -40nT and 30 repsectively. Fortunately none of the anomalies observed fell into the geomagnetic effected range. Eliminating geomagnetic influences it can be concluded that the anomalies observed on 21–25 December 2007 are highly likely possibly due to the effect of the impending earthquakes on 20, 22 and 26 December 2007 respectively.

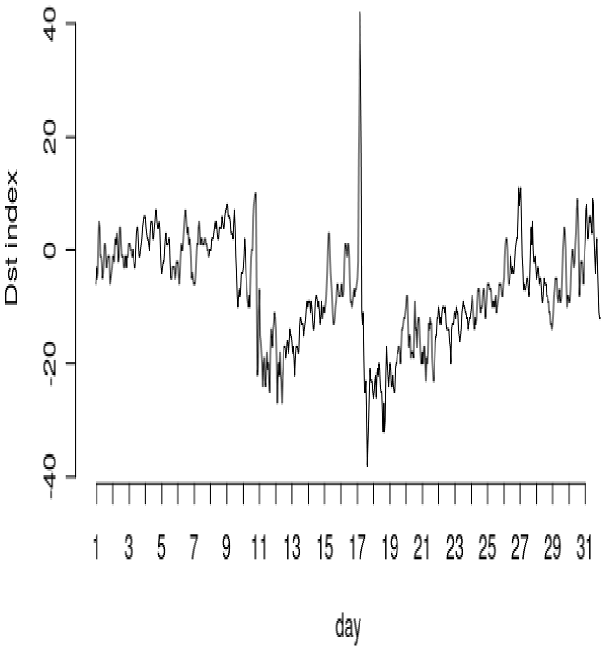

(a) December 2007

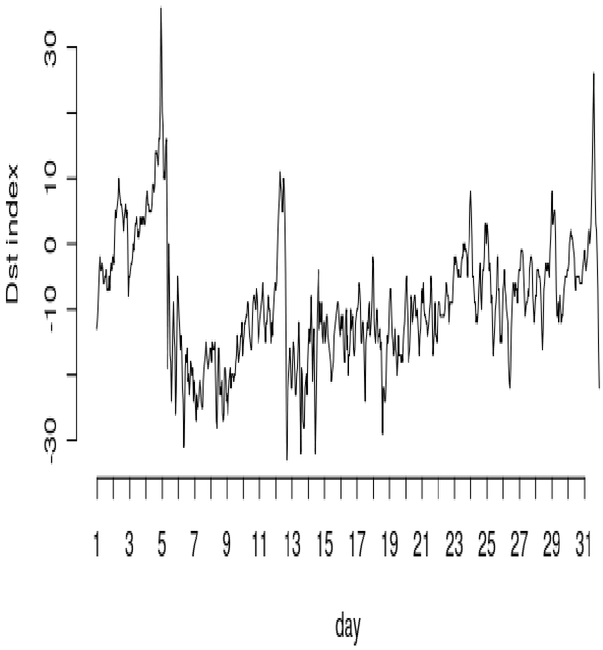

(b) January 2008

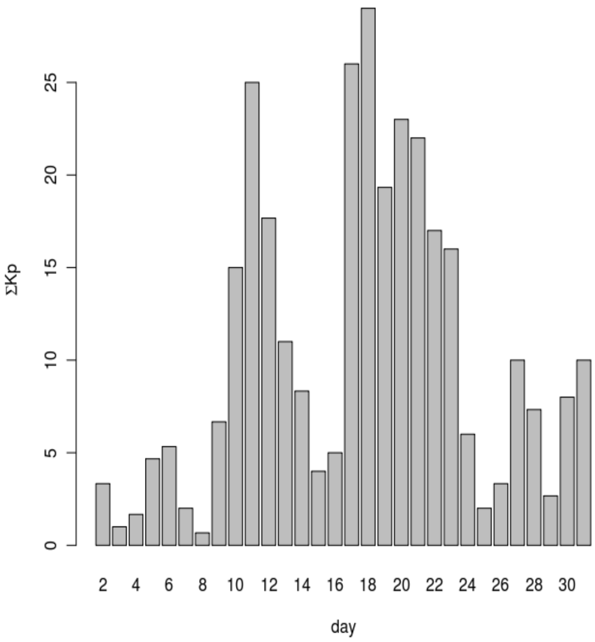

(c) December 2007

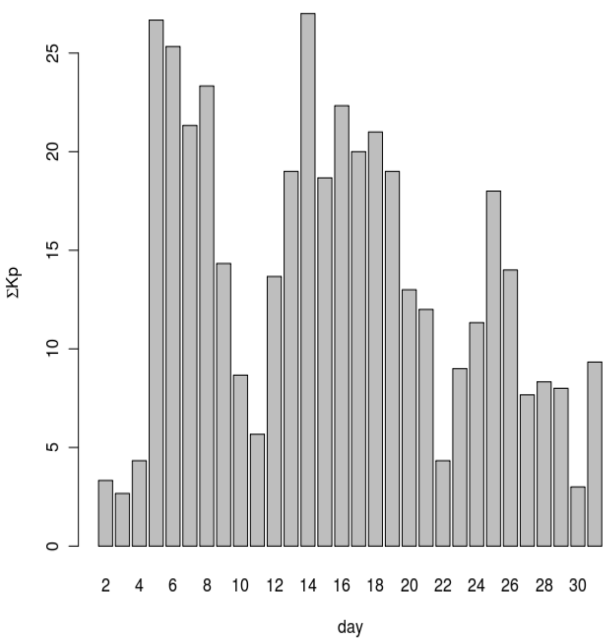

(d) January 2008

Figure 2.30: Dst and ΣKp indices for December 2007 and January 2008.

2.2.6 Anomaly - seismic activity summary

The anomaly dates have been discussed in the previous section. Their structure has been discussed in detail in the previous chapter. This section serves to summarise the VLF anomalies relevence to seismic activity and geomagnetic influences, this information is summarised in table 2.2. The table is broken down into the dates of the anomalies, their shape or form and time of appearance, whether there were any substantial simultaneous geomagnetic influences based on the corresponding Dst and ΣKp indices, and lastly their relation to the surrounding seimic activity.

Describing the meanings of the terms used in the table starting from the anomaly shape and time column, the anomaly forms could be any of step-up (or -down) perturbations, which means that the signal amplitude suddenly increased (or decreased) within a matter of minutes, depicted by a straight vertical line in the VLF profiles. Another form were e-or dBSD forms, which mean enhanced or depressed bay shaped disturbances. Such features are described by the signal amplitude rising or falling sharply, reaching a maximum or minimum, then returning back to the original amplitude before the perturbation after atleast an hour. The $+, -$ in the earthquakes column represent that the anomlay was observed either prior or after the closest earthquake, respectively.

Table 2.2: List of all anomaly days, structures, times of appearances as well as relation to geomagnetic and seismic activity observed from July 2007 to January 2008.

Anomaly date	Anomaly shape & time	Possible geomagnetic geomagnetic influences	days appeared in relation to seismicity
2007			
23 July	step down - 07-08hLT	-	-2
24 July	step down - 07hLT	-	-1
25 July	eBSD - 10-18hLT	-	0
27 July	step down - 14h30LT	-	+1
24 August	eBSD - 11-14hLT	-	-19
25 August	eBSD - 11-18hLT	-	-18
29 August	step-down - 02hLT	-	-14
	eBSD - 10-15hLT	-	-14
30 August	eBSD - 11-14hLT	-	-13
	step-down - 17hLT	-	-13
1 September	step-down - 10 and 15hLT	-	-11
6 September	step-down - 15hLT	-	-6
	eBSD - 22-23hLT	-	-6
9 September	step-up - 21hLT	-	-3
11 September	dBSD - 0-4hLT	-	-1
12 September	dBSD - 20-24hLT	-	0
12 October	step-down - 19, 23hLT	-	-12
13 October	step-down - 19hLT	-	-11
14 October	step-down - 19, 23hLT	-	-10
16 October	step-down - 19LT	-	-9
19 October	dBSD - 19–23hLT	Dst -50nT, ΣKp 22	-5
20 October	step-down - 20hLT	-	-4
22 October	step-up - 20hLT	-	-2
21 December	step-down - 11hLT	-	-1, +1
22 December	eBSD - 10-14hLT	-	0, -4
	step-up - 19hLT	-	0, -4
23 December	step-up - 19hLT	-	-3
24 December	step-up - 23hLT	-	-2
25 December	eBSD - 8-15hLT	-	-1

2.3 Tihany observations

2.3.1 Case study 5: Highly perturbed VLF period observed prior to seismic activity during February 2008

The transmitter-receiver propagation path between the 19.8kHz NWC transmitter in Australia and the narrowband VLF receiver in Tihany, Hungary (46.90890°N, 17.879230°E) was also studied for anomalous VLF amplitude fluctuations. The propagation path follows the same general path as that for the NWC-Budapest path, shown in figure 2.2. The distribution of seismic activity is also shown for the month of February 2008. This overlaps with the sets of VLF data dates available for the Tihany receiver.

The possibly relevant earthquakes vary in magnitude from 5.5–7.2. The two strongest earthquakes, magnitudes 7.2 and 7.4, fortunately were seen to have occurred off the west coast of Indonesia within very close proximity to the propgation path. As seen for the Budapest observations as well, the west coast of Indonesia experienced a high density of seismic activity.The seismic activity is shown in detail in table 2.3 Along with the dense concentration of seismic events, the region also experienced the largest earthquakes. Moderately strong to weak earthquakes were scattered from Dili South of Indonesia, through the Greater Sanda Islands in central Indonesia to the Northern Phillipines. Two more earthquakes of $M = 6.2$ and 6.5 occurred off the South coast of Greece, within reasonable distance of the propagation path. The earthquakes epicentral depths range from the shallowest at 9km to a depth of 47km.

The VLF profiles in Figures 2.31 and 2.33 represent the signals received between 14 - 25 February 2008. This set of dates was chosen as it showed the highest degree of fluctuations. The amount of fluctuations was determined by the difference between the quiet-day curve for February 2008, black curve, and the specific diurnal amplitudes, blue curves, just as was done for the Budapest observations. The shape and time of appearance of the anomalies in the signals will be discussed as well as a comparison to seismic and geomagnetic activity. The geomagnetic influences can be read off the Dst and ΣKp indices for February 2008 in figures 2.36b and 2.36d respectively.

Table 2.3: Earthquake details for February 2008

Year	Month	Day	Longitude(°)	Latitude(°)	Magnitude	Depth(km)
2008	2	5	118.070	-3.517	5.9	13
2008	2	7	122.653	1.228	5.8	35
2008	2	12	101.210	-3.008	5.5	47
2008	2	13	128.644	-8.158	6.2	19
2008	2	14	21.863	36.345	6.5	28
2008	2	14	21.670	36.501	6.9	29
2008	2	20	21.775	36.288	6.2	9
2008	2	20	95.964	2.768	7.4	26
2008	2	21	99.880	-2.323	5.7	24
2008	2	23	99.962	-2.511	5.6	32
2008	2	24	99.931	-2.405	6.5	22
2008	2	25	99.891	-2.332	6.6	25
2008	2	25	99.808	-2.245	6.7	25
2008	2	25	99.972	-2.486	7.2	25
2008	2	26	101.067	-3.852	5.9	20
2008	2	29	93.477	3.931	5.6	35

2.3.2 Diurnal Anomaly Analysis

Anomalous perturbations observed in the VLF signals for 14–25 February were analysed in detail, represented in Figures 2.31 and 2.33. Times of appearance and the forms of the deviations will be discussed. The black curves represent the quiet-day curve for Feruary 2008. The blue profiles represent the VLF signal received on the specific days labelled below each plot.

The quiet-day curve is described by a constant amplitude pre-terminator time period (00h00 - 05h00LT) at -68dB, followed by sharp decrease to -82dB, then a rise to a plateau at 10h00LT bove -76dB. The rise in amplitude occurs at 16h00LT to a maximum of approximately -71dB by 19h00LT. In general looking at the profiles in chronological order the obvious feature that stands out is the deviation from the relatively quiet day on 14 February, followed by days of enhanced succesively greater fluctuations, until 25 February when the quiet conditions are again reached.

Figure 2.31 shows the diurnal amplitudes for 14–20 February 2008. It is clear that the only major deviations occur during the late night, where the amplitudes either fall below $-2\sigma = -2$, such as for 14 and 17 February,as seen in Figure 2.32. Or spike above or close to $2\sigma = 2$, as for 15 and 16 February. The first was seen on 14 February, between 19h00 to 21h00LT a depression in the signal amplitude occurred. For the same period an enhancement in the signal occurred on 15 February, also with amplitude of approximately 1dB. A step-up in the amplitude of the 16 Febrary signal was observed between 19h00 and 20h00LT. The nighttime signal for 17 February showed two features. First the amplitude of the signal did not reach as high an amplitude as the quiet curve, but rather showed a depressed followed by an enhanced bay shape disturbance between 17h00 to 23h00LT.

From 21 to 25 February, Figure 2.33, the amplitudes are highly perturbed with the pre-terminator time periods all showing lower amplitudes than the quiet conditions dictate. Looking at the profiles as a whole the profiles are highly compressed compared to the quiet curves. The daytime amplitudes are seen to fluctuate between σ and $-\sigma$, Figure 2.34, whereas the night amplitudes dramatically fell below -2σ. The early night amplitudes have a dA value ranging from -4 to -10 for 19–22 February. The amplitude minimum reached at the terminator time is seen to be enhanced from -86dB to a maximum of -81dB on 19 February. This feature again reaches the quiet amplitude next on 25 February. From 06h00 to 17h00LT the amplitudes are enhanced above quesence, with low levels of fluctuation, as seen for 19 and 20 February. February 21, 22 and 23, however, showed step-down and -up deviations between 06h00LT to 09h00LT. Each jump in amplitude is roughly 2dB. Such structures are absent in the VLF profiles for 24 and 25 February. There were depressed bay shaped disturbances seen during the nighttime hours for 19 and 24 February as well, between 18h00 - 22h00LT and 19h00 - 21h00LT, respectively.

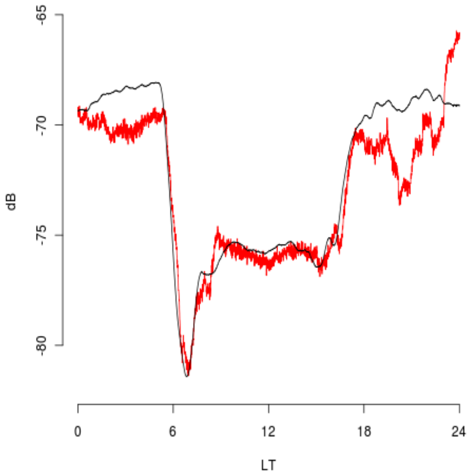

(a) 14/02

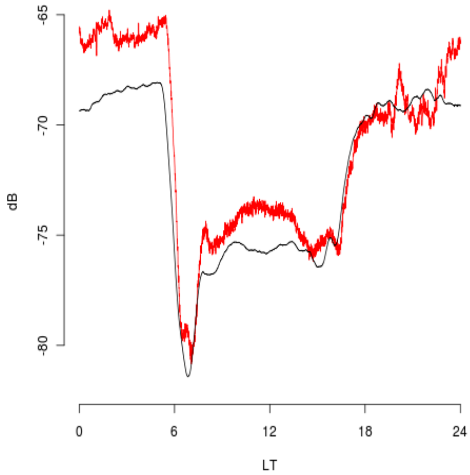

(b) 15/02

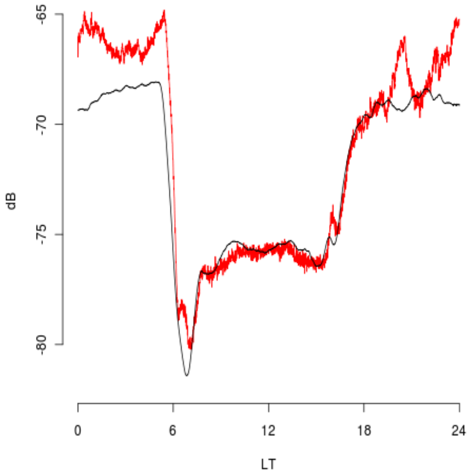

(c) 16/02

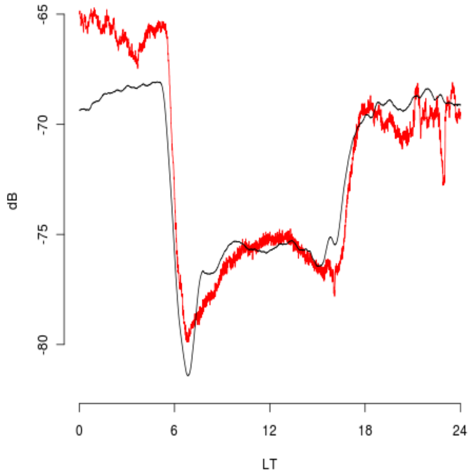

(d) 17/02

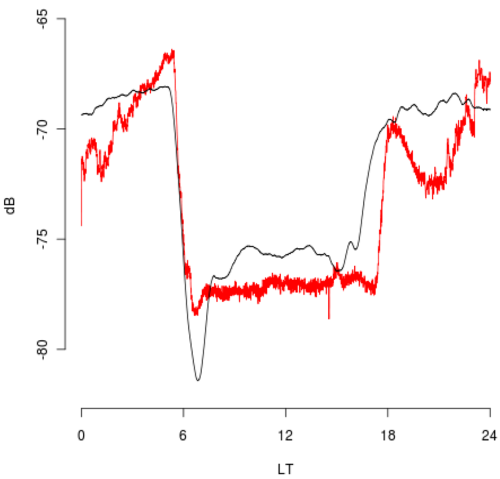

(e) 19/02

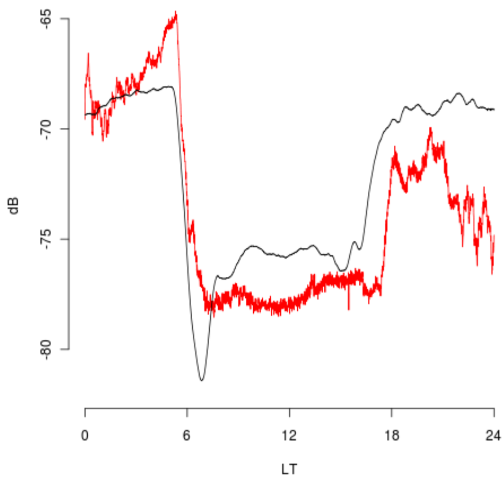

(f) 20/02

Figure 2.31: VLF profiles for 14–19 February 2007. Sharp drops and rises in the signal are seen for each day around 20h00LT. Increase of terminator minimum amplitude evindent, as well as drop in evening and latenight amplitudes.

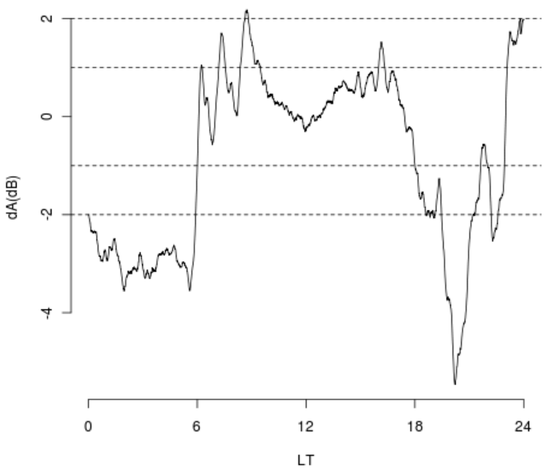

(a) 14/02

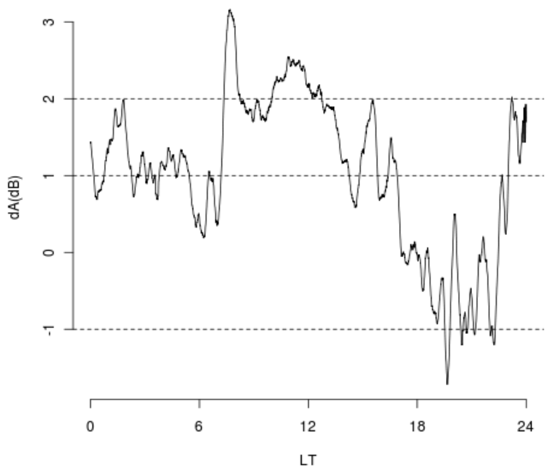

(b) 15/02

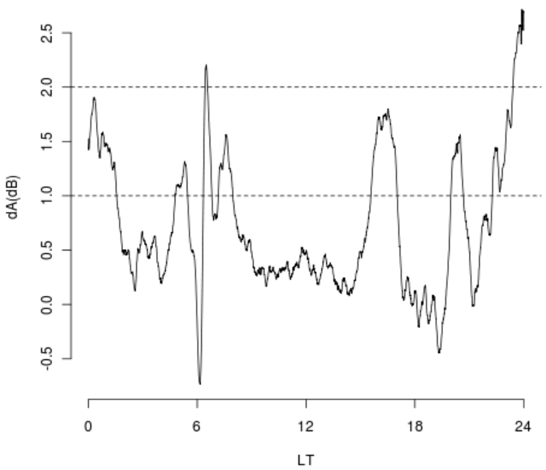

(c) 16/02

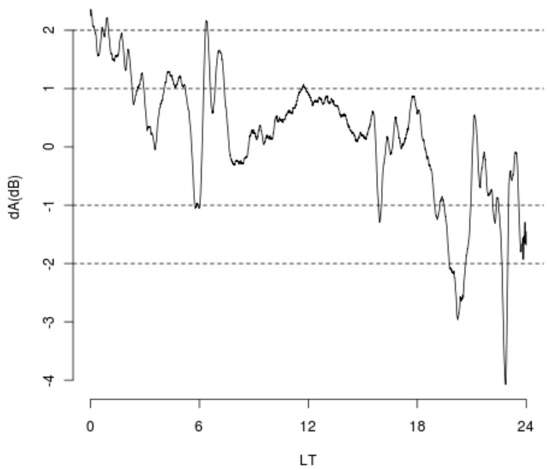

(d) 17/02

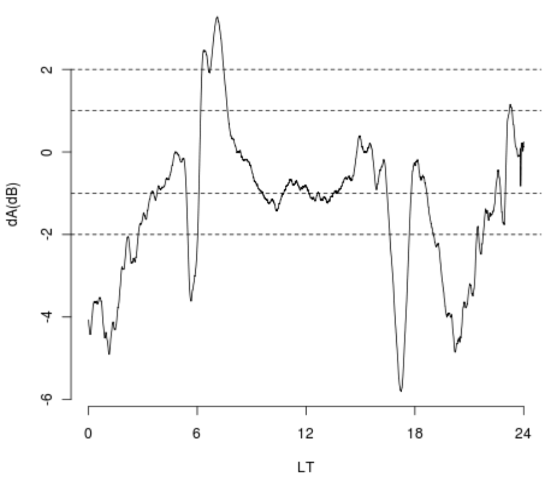

(e) 19/02

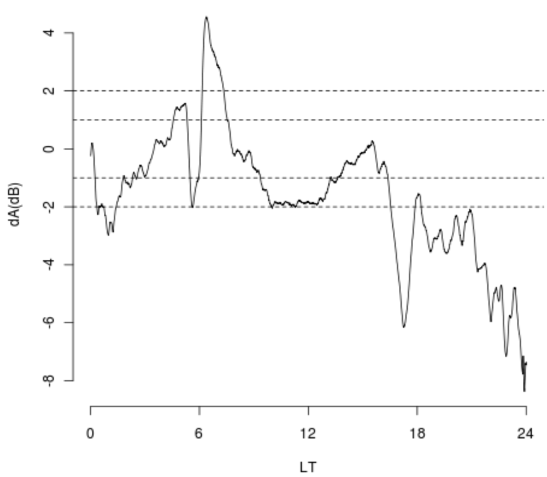

(f) 20/02

Figure 2.32: dA plots for 14-17 February 2007. Large perturbations in nighttime signals seen around terminator times. General quiet daytime activity, but sharp drops below $-\sigma$ ($2\sigma = 2$, $\sigma = 1$, $-\sigma = -1$, $-2\sigma = -2$)

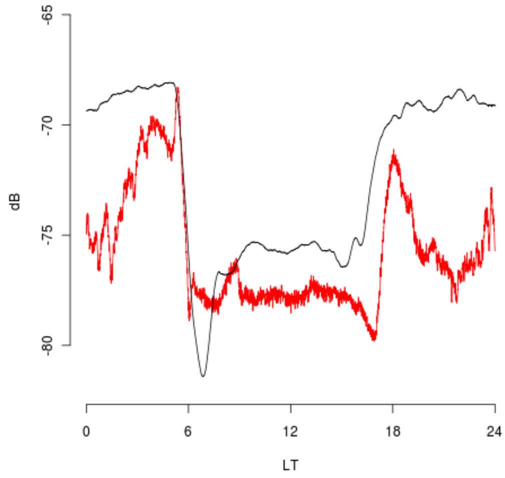

(a) 21/02

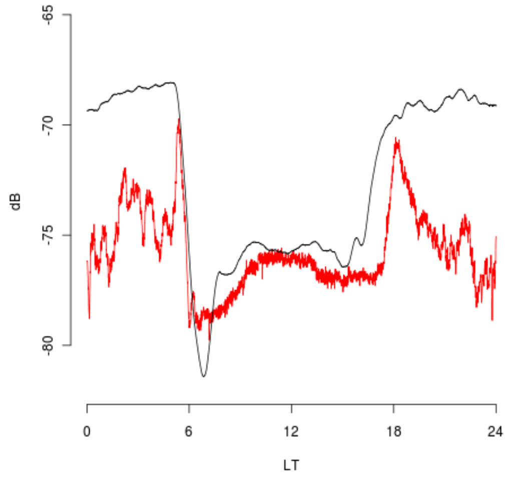

(b) 22/02

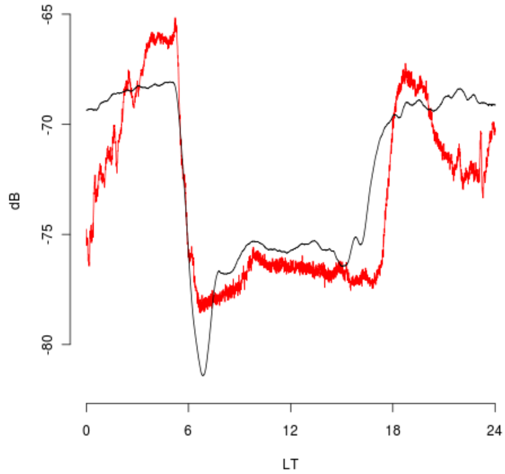

(c) 23/02

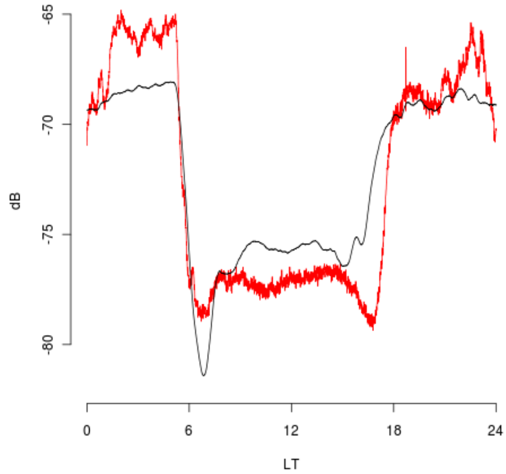

(d) 24/02

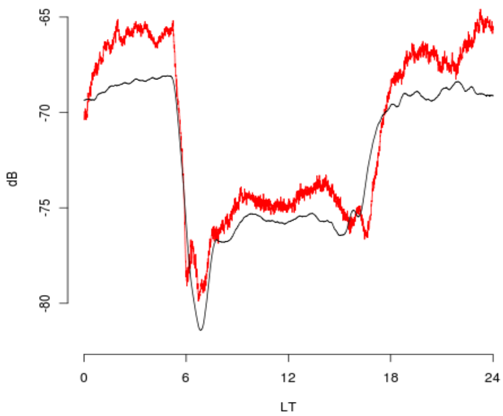

(e) 25/02

Figure 2.33: VLF profiles for 19-22 February 2007 (red). Increase of terminator minimum amplitude evindent, as well as drop in evening and latenight amplitudes. VLF profiles for 23–25 February 2008 showing signal amplitudes reverting back to the quiet-day curve (black) after highly perturbed period, 19–23 February 2008.

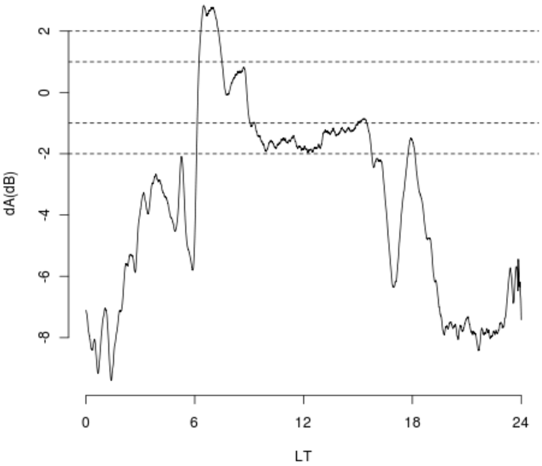

(a) 21/02

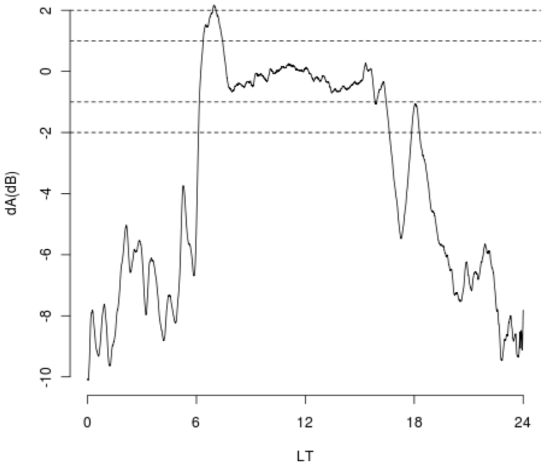

(b) 22/02

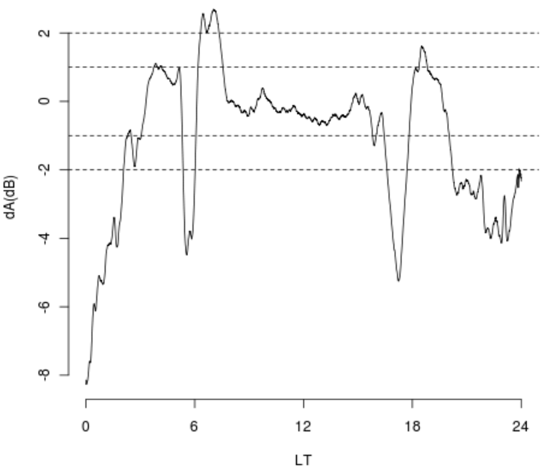

(c) 23/02

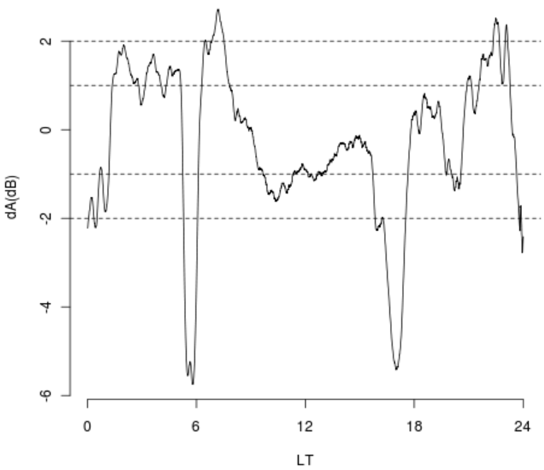

(d) 24/02

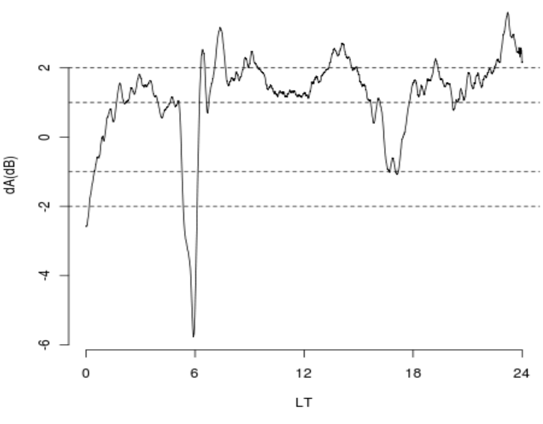

(e) 25/02

Figure 2.34: dA plots for 21–25 February 2008, showing large fluctuations for nighttime readings, well below $-\sigma$. Large terminator drops well below-σ, as well as smaller excursions above σ. ($2\sigma = 2$,$\sigma = 1$, $-\sigma = -1$, $-2\sigma = -2$)

Comparison to seismic activity

During February 2008 twenty earthquakes occurred, shown in Figure 2.2 with details given in table 2.3. However, only ten of these were determined to have epicenters near enough to the propagation path to effect VLF signals propagating along, based on their magnitudes and depths. The location of the epicenters were off the west coast of Indonesia between longitudes 94.477°E and 101.210°E, and latitudes 3.931°N and 3.852°S.

The dense group of earthquakes comprised of five moderately strong shocks $5.5 < M < 6.7$, with epicentral depths ranging from 47–20km. Such a dense group, could possibly be effective enough, collectively, to influence signals traversing along the propagation path, eventhough individually the propagation path would be too far way.

But two much stronger earthquakes occurred in the same region on 20 and 25 February that would overpower the effects, if any, that the weaker earthquakes would have caused. The epicenters of the two earthquakes were located at 2.486°S 99.972°E and 2.768°S 95.964°E. The former was of magnitude 7.2 and occurred at a depth of 25km, whereas the latter was a magnitude 7.4 occurring at a depth of 26km. From the temporal distribution of the anomaly days shown in figure 2.35, it is seen that the anomaly days started on 14 February, 6 days prior to the first earthquake. Although the anomaly days extend from 14–24 February, it must be stated that the anomlies observed before the onset of the seismic activity, 14–19 February, showed predominantly very distinctive latenight fluctuations for a period of a few hours. For the anomalous behaviour during the seismic period, 20–24 February, the amplitudes throughout each day were highly perturbed. see Figures 2.31 and 2.33 This is highly likely due to the direct effect of the earthquakes on the environment. The proximity to the propagation path, as well as the shallow epicentral depth and large magnitudes of the earthquakes are strong evidence that this could be the case.

The week leading up to the earthquake showed nighttime fluctuations in the signal amplitude that became more prominent with every successive day leading up to the earthquake day. From the day after the first earthquake leading up to the next on 25 February the nighttime anomalous structures were absent, but there were more well-defined structures that appeared just after the terminator-time drop.

On 21 February a step-up was observed and step-down deviations on 22 and 23 February all occurring between 06h00 and 09h00LT. Based on the fact that such deviations were so well-defined it may be possible to eliminate the fact they could be caused by large scale effects experienced after an earthquake such as the epicentral zone relaxation stage. The drops and rises were very short lived, matter of minutes, and highly isolated within the signals.

The Dst and ΣKp indices show low levels of geomagnetic activity through the middle of the month of February 2008. See figures 2.36b and 2.36d. The Dst index about -10nT on 14 February to around 0nT around 25 February. The ΣKp index generally decreases from 14 to 25 February from 21 to 7. Such values for the indices are not strong enough to consider that geomagnetic influences could have played a major part in the generation of such strong and well-defined deviations in the signals.

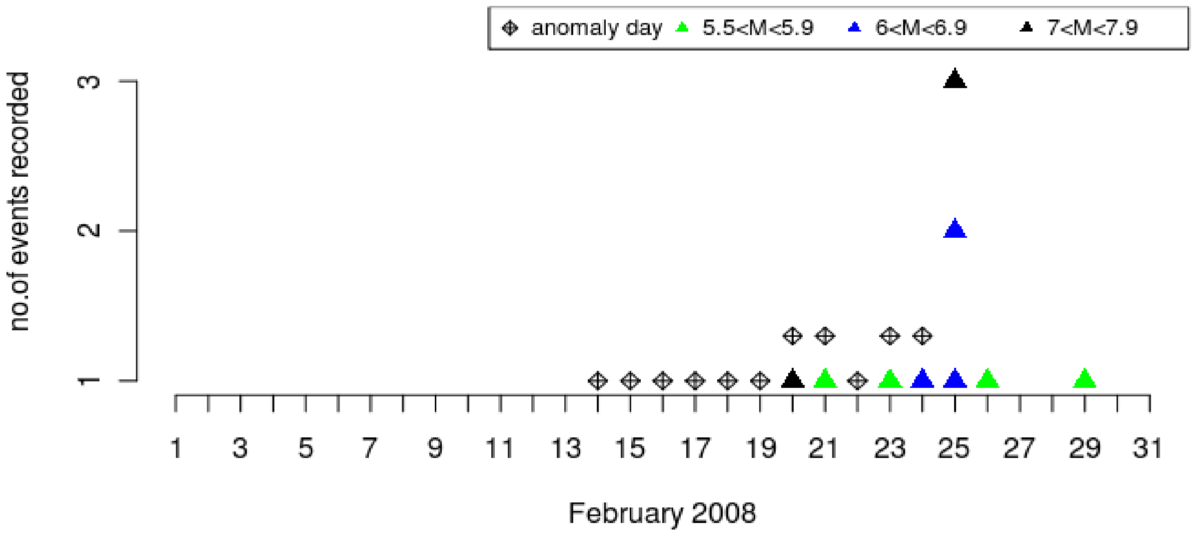

Figure 2.35: Temporal distribution of earthquake activity and anomaly days for February 2008. VLF anomalies observed from 14 February, 6 days prior to the beginning of seismic activity.

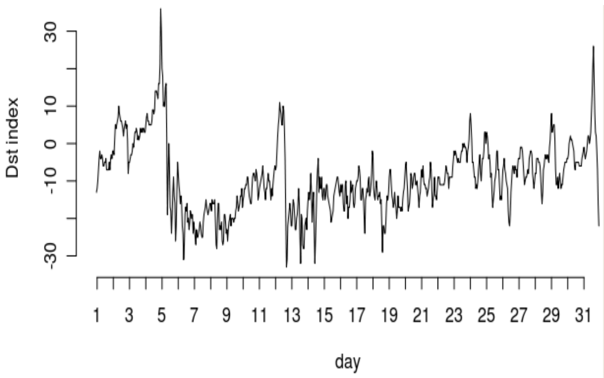

(a) January 2008

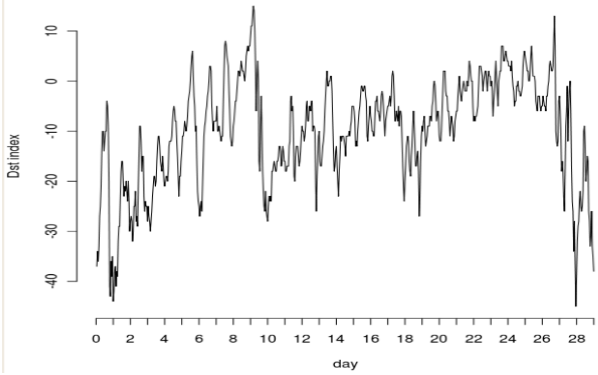

(b) February 2008

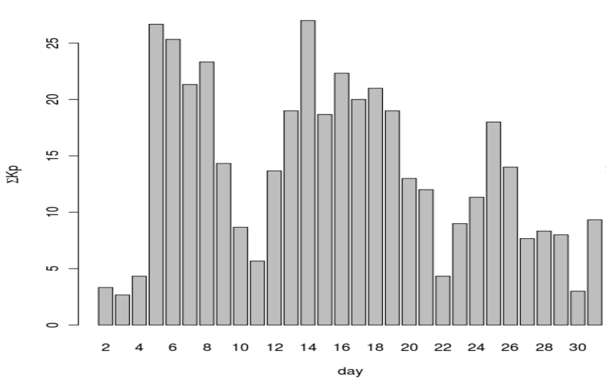

(c) January 2008

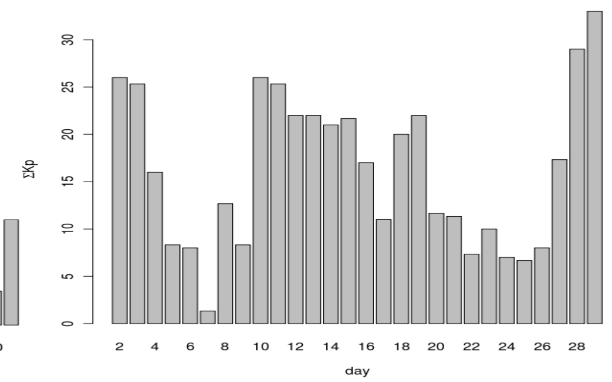

(d) February 2008

Figure 2.36: Dst and ΣKp indices for January and February 2008.

Chapter 3

Discussion

The aim of this thesis is to determine whether anomalous VLF signals observed at receiver stations have some connection with sesimic activity occurring near enough to the transmitter path propagating between the 19.8kHz NWC transmitter situated in Australia and the receiver in Budapest, Hungary. In so doing, ultimately aiming towards being able to definitively isolate earthquake ionospheric precursors and aid prediction. The procedure for searching for possible anomalies in the received signals has been laid out and now can be compared to the relevant seismic activity.

VLF perturbations observed prior to seismic activity were investigated. The 19.8kHz NWC transmitter was chosen from the global set of transmitters due to the high density of seismic events off the west coast of Indonesia, which occurred in relatively close proximity to the transmitter-receiver paths.

For each month the earthquakes have been categorised by magnitude, and every day that had some form of disturbance in the VLF profile had been investigated in relation to seismic and geomagnetic activity. The earthquake magnitudes and quantity per day are compared to the days of anomalies being present. Figures 2.9, 2.15 and 2.29 show the temporal comparison of earthquake occurrence and anomaly presence. Each month is analysed in detail now comparing earthquake occurrence to anomaly observation and possible biasing of data by geomagnetic events influencing the ionosphere.

Four periods of VLF distortions were studied. The periods occurred either only before or occurred prior to and continued during a sequence of seismic events. The first case study covered events that were possibly caused by the earthqake swarm that commenced on 12 September 2007. The swarm consisted of 16 earthquakes. The largest shock occurred on 12 September 2007 with a magnitude of 8.5. During the first two days seven earthquakes occurred, ranging in magnitudes from 5.5 to 8.5. Figure 2.9 shows the temporal distribution of the seismic activity and VLF anomaly appearance. Possible VLF anomalies were observed on 24, 25, 29 and 30 August 2007. Clear VLF anomalies appeared 11, 6 and 1 day prior to the beginning of the swarm as well. There were also no anomalous deviations observed during the seismically active period along the propagation path.

Using the standard deviations of each of the dA plots anomalous drops were identified. The value of σ, σ, -σ and -σ are given in the caption of their respective figures.
Deviations below -σ were observed for the nights between 24-25 and 29-30 August 2007, as well as 1-2, 6-7, 8-9 September 2007. The morning of 4 and 6 September 2007 also deviateed well below $-\sigma$. The morning and late night hours for 11 and 12 September were well below -σ. However the anomalous behaviour on 12 September could be due to the direct effect of the earthquakes on the ionosphere.

The geomagnetic influences at the time were also studied, to make sure there was no bias in the data. The geomagnetic indicators were the Dst and ΣKp indices. Both indices showed very low levels of geomagnetic activity being imposed on the Earth. Thus geomagnetic events influencing the ionosphere to cause the VLF perturbations were ruled out. Leaving the fact that the VLF anomalies observed at the end of August 2007 and on 1, 6 and 11 September 2007 could be seismogenic as a valid argument.

The second case study was for the perturbations observed prior to the 25 July 2007 earthquake. The earthquake was characterised by a magnitude 6.1 and epicentral depth of 15km. VLF anomalous behaviour was noticed from 22 July to 27 July 2007. The anomalies were general enhancements in the afternoon hours as well as very well defined short-lived drops in amplitude. However, such drops were seen on 23, 24 and 27 July 2007. The drops for 23 and 24 July 2007 had a dA amplitude from 2σ to $-\sigma$. Compared to the general daytime fluctuations these seem to be significant. The drop on the former day occurred before midday, whereas the latter day drop occurred after midday. The drop on 27 July may be either caused by much smaller magnitude aftershocks or possibly a precursor to the earthquake couplet occurring on 8 August 2007. In this way it has been eliminated as related to the earthquake on 25 July 2007. The geomagnetic indices showed no significant readings to be considered as the cause of the perturbations.

Latenight deviations were observed for 12–23 October 2007. These were all of the same form and occurred on days with no earthquake activity. The anomaly days preceded the earthquake series onset by seven days. Sharp, sudden short-lived drops in the amplitudes were seen. These all occurred after 19h00LT. The causative earthquake seems to have occurred on 24 October 2007. This was a fairly strong earthquake, $M = 6.8$ and occurred at a shallow depth of 21km. This is highly likely the biggest contributor to the generation of the anomalies based on its depth to magnitudes parameters. There was ageomagnetic storm during 25–27 October hence leading to any anomalies on such days to be neglected. An anomlay was seen on 19 October, however, the ΣKp index spiked on this day leading to this deviation to also be looked over.
The series of earthquakes that occurred at the end of December 2007 were found to be preceded by anomalous VLF behaviour. The earthquakes occurred on 20, 22 and 26 December. A period of anomalous VLF signal behaviour was observed during this range of dates. The well defined breaks in the evening terminator rises were considered as anomalous, as seen in Figures 2.25 and 2.27 . Enhancements in the daytime signals on the days of the earthquakes were considered to be the direct result of the power of the earthquake on the ionosphere, such as for 22 December 2007. However, clear increases in the latenight amplitudes on 22, 23 and 24 December are of similar magnitude as well as time. The late night drops for all three days protrude higher than the 2σ level. Thus they could be seen as precursors to the 26 December earthquake.

The nighttime fluctuations were much more structured, especially in the days leading up to the 26 December earthquake. As can be seen from Figure 2.29 the anomalies appeared from 21 December and lasted through to 26 December. The Dst and ΣKp indices reveal no major geomagnetic events effecting the ionosphere. Thus the anomalous signals may be seismogenic.

The final case study focused on unusual disturbances in the VLF profiles observed by the Tihany receiver for February 2008. An earthquake swarm occurred, commencing on 20 February 2008 with a magnitude 7.2 shock. Another stronger magnitude 7.4 earthquake occurred on 25 February. The large scale of the earthquakes coupled with their very shallow depths of 25 and 26km, respectively make them highly likely to be associated with ionospheric features. VLF signal anomalies were observed from 14 to 24 February, see Figure 2.35. Predominantly late night features were observed up to 17 February. Then onwards from 18 to 24 February the signal fluctuates drastically, before reverting back to the quiet-day curve on 25 February.

The Dst and ΣKp indices show periods of low geomagnetic activity being imposed on the Earth. For the period of VLF anomaly presence the Dst index fluctuates just below zero, and the ΣKp index simultaneously drops, see figures 2.36b and 2.36d. Thus again geomagnetic influences can be ruled out in the generation of these anomalous observations. Leaving the possibilty that the signals may very well be seismogenic.

Results of this thesis compare well with those of *Kushida and Kushida* [2002], where anomalies observed in the VHF band were found to precede seismic activity of magnitude 5 and greater by 4–8 days.

Chapter 4

Conclusion

In this thesis VLF waves from the 19.8kHz NWC Australian transmitter received at the Hungarian VLF narrowband receiving stations were investigated for anomalous perturbations possibly due to seismic activity in an effort to aid in earthquake prediction.

Five cases studies were considered. Three used data obtained from the Budapest station and the fourth from the Tihany station. Nighttime fluctuations were observed well below -2σ, used as a reference point for anomaly identification. The earliest precursors occurred for the earthquake swarm on 12 September 2007. Anomalous deviations were found from the end of August 2007. Short lived drops in VLF signal amplitude were recorded for 1 and 6 September as well. Similar daytime drops were seen for 23 and 24 July 2007, however, these were in relation to the earthquake on 25 July 2007. No anomalies were recorded during the period of seismic activity and geomagnetic influences have been ruled out based on the corresponding.

The latenight drops in VLF amplitude seen for 12–23 October have been concluded to be possibly due to the earthquake on 24 October 2007, with the omission of the anomalies on 19 and 23 October due to a geomagnetic storm and the possible direct effect of the earthquake on the day respectively.

Latenight deviations observed prior to the earthquake on 26 December 2007 were considered to be possibly precursory. The VLF profiles fluctuated greatly but a consistent shaped perturbation during the late night hours was observed leading up to 16 December 2007. Such structures were considered precursory.

The results for the Tihany receiver showed significant late night deviations as well leading up to a highly active seismic period starting on 20 February 2008. The nighttime step up structures continued through to 25 February 2008

All possible precursory deviations were compared to the Dst and ΣKp indices to eliminate any anomalous events that may have been caused by a geomagnetic event. All the perturbations mentioned here that may be precursors to their respective seismic events have been found in periods of low geomagnetic activity.

Future studies should include investigating Radon emanations below the region studied. Being able to conduct a thorough investigation on the effect of Radon emanation from epicentral zones as well as the effect on the ion distribution in the lower ionosphere will go a long way in using this type of possible precursory study to aid earthquake VLF precursor identification. Investigation into the possible mechanisms that occur below the surface within the area of an impending earthquake may be the best way to resolve this kind of phenomenon. As discussed Radon leakage out of cracks and fissures in the expanding and contracting lithology of the epicentral zone causes electric fields to be generated at the epicentre. Such fields are passed into the atmosphere up to the ionosphere, which influences the ion distribution within the D-region. This seems to be the most agreed major mechanism suggested as the generator of seismogenic ionospheric disturbances.

Bibliography

Barr, R., D. L. Jones, and C. J. Rodger (2000), ELF and VLF radio waves, *Journal of Atmospheric and Solar-Terrestrial Physics*, *62*, 1689–1718.

Cheng, Z., S. A. Cummer, D. N. Baker, and S. G. Kanekal (2006), Nighttime D region electron density profiles and variabilities inferred from broadband measurements using VLF radio emissions from lightning, *Journal of Geophysical Research*, *111*, 1–9, doi:10.1029/2005JA011308.

Cummer, S. (2000), Modeling Electromagnetic Propagation in the Earth-Ionosphere Waveguide, *IEEE transactions on antennas and propagation*, *48*(9), 2–12.

Cummer, S. A., U. S. Inan, and T. F. Bell (1998), Ionospheric D region remote sensing using VLF radio atmospherics, *Radio Science*, (December), 1781—-1792.

Dutta, H. N., R. S. Dabas, R. M. Das, K. Sharma, and B. Singh (2007), Ionospheric perturbations over Delhi caused by the 26 December 2004 Sumatra earthquake, *International Journal of Remote Sensing*, *28*(13), 3141–3151, doi:10.1080/01431160601099590.

Fujiwara, H. (2004), Atmospheric anomalies observed during earthquake occurrences, *Geophysical Research Letters*, *31*(17), 2–5, doi:10.1029/2004GL019865.

Hayakawa, M. (2007), VLF/LF Radio Sounding of Ionospheric Perturbations Associated with Earthquakes, *Sensors*, *7*(7), 1141–1158.

Hayakawa, M. (2008), Subionospheric VLF/LF probing of ionospheric perturbations associated with earthquakes (earthquake prediction), *2008 SICE Annual Conference*, *3*(1), 1668–1671, doi: 10.1109/SICE.2008.4654931.

Ho, C., et al. (1998), Global ionospheric tec variations during january 10, 1997 storm, *Geophysical Research Letters*, *25*, 2589–2592.

Hobara, Y., and M. Parrot (2005), Ionospheric perturbations linked to a very powerful seismic event, *Journal of Atmospheric and Solar-Terrestrial Physics*, *67*(7), 677–685, doi:10.1016/j.jastp.2005.02.006.

Horie, T., S. Maekawa, T. Yamauchi, and M. Hayakawa (2007), A possible effect of ionospheric perturbations associated with the Sumatra earthquake, as revealed from subionospheric very-low-frequency (VLF) propagation (NWC-Japan), *International Journal of Remote Sensing*, *28*(13), 3133–3139, doi: 10.1080/01431160601094476.

Kasahara, Y., F. Muto, Y. Hobara, and M. Hayakawa (2010), The ionospheric perturbations associated with Asian earthquakes as seen from the subionospheric propagation from NWC to Japanese stations, *Natural Hazards and Earth System Science*, *10*(3), 581–588, doi:10.5194/nhess-10-581-2010.

Koen, E. (2009), Ionospheric Signatures of Solar Flares, Msc thesis, Univeristy of KwaZulu-Natal.

Kumar, S. (2009), Waveguide Parameters of 19.8 kHz Signal Propagating over a Long Path, *Reseacrh Letters in Physics*, *2009*, doi:10.1155/2009/216373.

Kumar, S., A. Kishore, and V. Ramachandran (2008), Annales Geophysicae Higher harmonic tweek sferics observed at low latitude : estimation of VLF reflection heights and tweek propagation distance, *Annales Geophysicae*, *26*(March 1991), 1451–1459.

Kushida, Y., and R. Kushida (2002), Possibility of earthquake forecast by radio observations in the vhf band, *Journal of Atmospheric Electricity*, *22*(33), 239–255.

Liu, J. Y., Y. I. Chen, Y. B. Tsai, and S. A. Pulinets (2000), 2 seismo-ionospheric precursors prior to.pdf, *Geophysical Research Letters*, *27*, 3113 – 3116.

Liu, J. Y., Y. I. Chen, Y. J. Chuo, and H. F. Tsai (2001), Variations of ionospheric total electron content during the Chi[U+2010]Chi Earthquake, *Geophysical Research Letters*, *28*(7), 1383, doi:10.1029/2000GL012511.

Liu, J. Y., Y. I. Chen, Y. J. Chuo, and C. S. Chen (2006), A statistical investigation of preearthquake ionospheric anomaly, *Journal of Geophysical Research*, *111*(A5), 1–5, doi:10.1029/2005JA011333.

Maekawa, S., T. Horie, T. Yamauchi, T. Sawaya, M. Ishikawa, M. Hayakawa, and H. Sasaki (2006), A statistical study on the effect of earthquakes on the ionosphere , based on the subionospheric LF propagation data in Japan, *Annales Geophysicae*, *24*(1998), 2219–2225.

Molchanov, O., et al. (2006), Global diagnostics of the ionospheric perturbations related to the seismic activity using the VLF radio signals collected on the DEMETER satellite, *Natural Hazards and Earth System Science*, *6*(5), 745–753, doi:10.5194/nhess-6-745-2006.

Ohya, H., M. Nishino, Y. Murayama, and K. Igarashi (2003), Equivalent electron densities at reflection heights of tweek atmospherics in the low-middle latitude D-region ionosphere, *Earth Planets Space*, *55*, 627–635.

Popov, K. (2004), On ionospheric precursors of earthquakes in scales of 2–3 h, *Physics and Chemistry of the Earth, Parts A/B/C*, *29*(4-9), 529–535, doi:10.1016/j.pce.2003.10.004.

Pulinets, S. (1997), Radon and metallic aerosols emanation before strong earthquakes and their role in atmosphere and ionosphere modification, *Advances in Space Research*, *20*(11), 2173–2176, doi:10.1016/S0273-1177(97)00666-2.

Pulinets, S. (1998), Strong earthquake prediction possibility with the help of topside sounding from satellites, *Advances in Space Research*, *21*(3), 455–458, doi:10.1016/S0273-1177(97)00880-6.

Pulinets, S. (2000), Quasielectrostatic model of atmosphere-thermosphere-ionosphere coupling, *Advances in Space Research*, *26*(8), 1209–1218, doi:10.1016/S0273-1177(99)01223-5.

Pulinets, S. (2003), Main phenomenological features of ionospheric precursors of strong earthquakes, *Journal of Atmospheric and Solar-Terrestrial Physics*, *65*(16-18), 1337–1347, doi:10.1016/j.jastp.2003.07.011.

Rai, J., R. Chand, D. K. Sharma, S. Kamakshi, and M. Israil (1998), Studies on ionospheric perturbation due to seismic activity using Indian SROSS – C2 satellite data, *Physics of the Earth and Planetary Interiors*, pp. 3–6.

Rios, V. H., V. P. Kim, and V. V. Hegai (2004), Abnormal perturbations in the F2 region ionosphere observed prior to the great San Juan earthquake of 23 November 1977, *Advances in Space Research*, *33*, 323–327, doi:10.1016/S0273-1177(03)00480-0.

Shvets, A. (2004), A study of ionospheric response to regional seismic activity by VLF radio sounding, *Physics and Chemistry of the Earth*, *29*(4-9), 627–637, doi:10.1016/j.pce.2003.08.063.

Singh, R. P., P. K. Mishra, and B. Singh (2001), Anomalous VLF electric field perturbations associated with Chamoli earthquakes of March / April 1999, *Current Science*, *80*(11).

Singh, R. P., M. Kumar, O. P. Singh, and B. Singh (2009), Subsurface VLF electric field emissions associated with regional earthquakes, *Journal of Engineering*, *38*(August), 220–226.

Tolstoy, A., T. Rosenberg, and D. Carpenter (1982), The influence of localized precipitation-induced D-region ionozation enhancements on subionospheric VLF propagation.pdf, *Geophysical Research Letters*, *9*(5), 563–566.